Real time computer vision technique for robust plant seedling tracking in field environment

Ph.D. Dissertation

Henrik Skov Midtiby

Faculty of Engineering, University of Southern Denmark

Institute of Chemical Engineering, Biotechnology and Environmental Technology

Odense, Denmark 2012

Preface

This dissertation marks the end of my Ph.D. and is a description of the work I have done at KBM guided by my supervisors Rasmus, SDU and Michael, AU from May 2009 to May 2012.

During the last three years I have worked on three projects *The Intelligent Sprayer Boom*, *BrainWeed* and *Operational spraying of single weed plants*. The goal of the Intelligent Sprayer Boom project is to equip a standard sprayer boom with cameras that can detect the presence of weeds in maize fields and adjust the herbicide dosage according to the observations. Field trials are planned for the summer of 2012. The BrainWeed project will extend the crop recognizing capabilities of the Robovator in–row weeding device. The target is to perform in–row weed control of seeded crops like sugar beets. Field trials are planned for the summer of 2012. Operational spraying of single weed plants showed that individual weeds can be targeted efficiently. The project stopped at the end of 2011.

I would like to thank everyone at KBM and collaborators during this project. First of all I would like to thank Rasmus and Michael for designing this project and their guidance during the experimental part of the project. Thanks to Solvejg, Frank P, Frank L and Andreas for discussions about interpretation of results and information about moving image processing methods to other computational platforms.

The Biosystems Engineering group has created an interesting and enjoyable environment open for new ideas. Thanks to Björn Åstrand for his hospitality and mathematical discussions during my study visit in Halmstad.

In the end a great thank goes to family and friends, who have followed my work with interest and curiosity, especially thanks to Linda who has shown enormous patience and gently pushed me forward in the writing process.

Resume

I det konventionelle landbrug er ukrudtsbekæmpelse i dag i højsæde med det formål at få så højt et udbytte som muligt. Undlades det at bekæmpe ukrudt vil udbyttet fra marken falde betydeligt. Fra midten af sidste århundrede har man bekæmpet ukrudt ved hjælp af selektive sprøjtemidler, der primært skader ukrudtet og lader afgrøden stå tilbage i en mark. Først i de senere år er man blevet opmærksom på de skadelige virkninger fra sprøjtemidlerne og hvordan nogle midler ophobes i fødekæden. Dette har medført et politisk ønske om at minimere brugen af sprøjtemidler. 70% af de anvendte sprøjtemidler i Danmark benyttes til ukrudtsbekæmpelse.

Udgangspunktet for denne afhandling er, at det er muligt at bekæmpe ukrudt effektivt uden at belaste miljøet unødigt ved at benytte robotteknologi og computerbaseret genkendelse af afgrøder og ukrudt. Med et kamera kan der tages billeder af planter i marken og ved at analysere billederne kan det bestemmes hvilke planter, der er i billedet og hvor de står. Vides det præcist hvor ukrudtet står kan det behandles målrettet med et sprøjtemiddel. Et sådant, såkaldt, mikrosprøjte system, som doserer en dråbe Roundup på ukrudtet er udviklet og afprøvet i dette projekt. Ved at undgå at ramme afgrøden og jorden kan forbruget af sprøjtemidler reduceres med mere end 95% til ukrudtsbekæmpelse og stadig bekæmpe ukrudtet effektivt har andre vist.

Hvis afgrødens placering kendes og afgrøden står i en rækkestruktur, er det muligt mekanisk at bekæmpe ukrudt i rækkerne. Dette princip benyttes i dag til dyrkning af salat og andre udplantede afgrøder. Fordelen ved at arbejde med udplantede afgrøder er, at det er let for en computer at se forskel på afgrøder og ukrudt. Ønsker man at gøre

det samme med udsåede afgrøder f.eks. sukkerroer, er det ikke helt så let, idet afgrøde og ukrudt har samme størrelse og der skal benyttes mere avancerede teknikker til at skelne mellem de to typer planter. En lovende mulighed er at så roerne i et fast mønster. Ved hjælp af et kamera kan dette mønster genfindes og planterne, der følger mønstret må være afgrøde. I denne afhandling demonstreres et sådant system der automatisk kan træne en form–baseret plante–genkender ud fra det mønster som afgrøden er sået i.

I de benyttede systemer sidder der et kamera over rækken og ser ned på planterne. Det giver nogle udfordringer når forskellige planters blade overlapper. Ved overlap ser computeren en stor grøn klump. Det beskrives hvordan enkelt blade kan detekteres i en sådan klump. Ud fra detekterede enkeltblade er det muligt at bestemme hvilke planter, der er i klumpen og hvor de står. Ved at basere plantegenkendelse på enkeltblade kan plantegenkendelse gøres mere robust overfor overlap mellem de forskellige planter.

Summary

In conventional farming weed control is of paramount importance with the aim of maximizing the yield. Neglect of weed control can lead to significant yield losses. Since the middle of the last century weeds have been controlled using selective herbicides, which controls the weeds and lets the crop remain in the field. This has lead to a political request for minimizing the pesticide usage. 70% of the used pesticides in Denmark are used for weed control.

The basis for this dissertation is that it is possible to control weed effectively without putting unnecessary load on the environment employing robot technology and computer based recognition of crops and weeds. Images of plant in a field can be captured with a camera. Analysis of these images can identify the plant species and determine the plant locations. If knowledge about the precise location of weed plants is available application of herbicides can be targeted at the weed plants. Such a microsprayer system, which can place a droplet of Roundup on weed plants, has been developed and tested in this project. Other researchers have shown that by avoiding deposition of herbicides on crop and soil the use of herbicides for weed control can be reduced with more than 95% and still control the weeds effectively.

If the position of crop plants are known and the crop is placed in a row structure it is possible to control weeds mechanically inside the rows. This approach is used today for growing lettuce and other transplanted crops. The advantage of working with transplanted crops is that it is easy for a computer to distinguish between crops and weeds. If you want to do the same with seed crops like sugar beets, it is not as easy, given that crops and weeds have similar sizes and more advanced

methods are needed to discriminate between the two plant types. A promising opportunity is to sow crops in a fixed pattern. With the use of a camera, this pattern can be detected and the plants that follow this pattern are likely crops. In this dissertation a system that can train a shape based plant classifier based on the pattern that crop plants are sown in described.

In the utilized systems a camera is placed above the crop row, which looks down on the plants. This raises some challenges when leaves of different plants occlude each other. When several plants occlude each other the computer is seeing a single green blob. Methods for detecting individual leaves in such a blob is described in the dissertation. Based on the detected leaves it is possible to determine which plants that are in the blob and where they are located. By basing plant recognition on individual leaves it can be made more tolerant to occlusion between different plants.

List of publications

This thesis is based on work described in the following publications. The publications can be found in the appendix and in the text they will be referred to by their Roman numerals.

I Statistics based segmentation using a continuous scale Naive Bayes approach. / Midtiby, Henrik Skov; Laursen, Morten Stigaard; Krüger, Norbert; Jørgensen, Rasmus Nyholm. Submitted to Sensors, april 2012.

II Modicovi: Spray boom for selectively spraying a herbicidal composition onto dicots. / Jørgensen, Rasmus Nyholm; Krüger, Norbert; Midtiby, Henrik Skov; Laursen, Morten Stigaard. Patent application, submitted march 2012.

III Estimating plant stem emerging point of beets in early growth stages. / Midtiby, Henrik Skov; Mosgaard Giselsson, Thomas; Jørgensen, Rasmus Nyholm. Biosystems Engineering, Vol. 111, p. 83-90, 2011.

IV Performance evaluation of a crop / weed discriminating microsprayer. / Midtiby, Henrik Skov; Mathiassen, Solvejg K.; Andersson, Kim Johan; Jørgensen, Rasmus Nyholm. Computers and Electronics in Agriculture, Vol. 77, Nr. 1, 2011, p. 35-40.

V Upper limit for context based crop recognition. / Midtiby, Henrik Skov; Åstrand, Björn; Jørgensen, Ole; Jørgensen, Rasmus Nyholm. Submitted to Biosystems Engineering, january 2012.

The following conference papers have been submitted.

- Seedling discrimination using shape features derived from a distance transform. / Giselsson, Thomas M.; Midtiby, Henrik Skov; Jørgensen, Rasmus N. Abstract accepted for International Conference of Agricultural Engineering, july 2012.
- Estimating the plant stem emerging points (PSEPs) of sugar beets at early growth stages. / Midtiby, Henrik Skov; Jørgensen, Rasmus N.; Giselsson, Thomas M. Abstract accepted for Precision Agriculture july 2012.
- Location of individual leaves in images of sugar beets in early growth stages. / Midtiby, Henrik Skov; Giselsson, Thomas M.; Jørgensen, Rasmus N. Abstract accepted for International Conference of Agricultural Engineering, july 2012.
- Validation of Modicovi - MOnocot and DIcot COverage ratio VIsion based method for real time estimation of canopy coverage ratio between cereal crops and dicotyledon weeds. / Laursen, Morten S.; Midtiby, Henrik Skov; Jørgensen, Rasmus N.; Krüger, Norbert. Abstract accepted for Precision Agriculture july 2012.

In addition to the above mentioned papers, the following two papers were published based on work in my master thesis.

- Texture of lipid bilayer domains. / Jensen, Uffe Bernchou; Brewer, Jonathan R.; Midtiby, Henrik Skov; Ipsen, John Hjort; Bagatolli, Luis; Simonsen, Adam Cohen. Journal of the American Chemical Society , Vol. 131, Nr. 40, 14.10.2009, p. 14130-14131.
- Correlation between the ripple phase and stripe domains in membranes. / Bernchou, U., Midtiby, H., Ipsen, J. H., & Simonsen, A. C. (2011). Biochimica et biophysica acta, 1808(12), 2849-58.

Contents

List of abbreviations

This section contains an alphabetic list over the abbreviations used in the dissertation. Units are indicated with [unit] after the abbreviation.

$\simeq$	Similar or equal to
2D	Two dimensional
5D	Five dimensional space. Used to describe relative edge locations and orientations
a_k	Weight related to F_k when estimating weed pressure
B	Blue raw colour value
b	Blue chromaticity
BBCH	Biologische Bundesanstalt, Bundessortenamt and CHemical industry, scale for growth stages of plants
$\mathbb{C}$	Object class, either $\mathbb{S}$ or $\mathbb{V}$
CMOS	Complementary metal–oxide–semiconductor
$dF_k(l)$	Increment in F_k by comparing the edge l with all its neighbours
dst	Distance between two edges
D_x, D_y	Image gradient in x and y direction.
ECDF	Empirical Cumulative Density Function

ExG	Excess Green
$\hat{f}_h(x)$	Estimate of probability density
F_k	k^{th} Gaussian feature value
$f_k(l, m)$	increment in F_k by comparing the edges m and l
G	Green raw colour value
g	Green chromaticity
g/L	Concentration: Grams per litre
$\Gamma^{\{p,\sigma^2\}}$	First order symmetry derivative kernel
GPS	Global Positioning System
h	Smoothing bandwidth
$h(\vec{x}_l, \vec{x}_m)$	5D vector that describes the position and orientation of $\vec{x}_m$ relative to $\vec{x}_l$
k	Index variable
$K(x)$	Smoothing kernel
L	Number of observations used for estimating a probability distribution
LUT	Look up table
L	Litre
λ	Normalized weed pressure
L_p	Length of perimeter
L_s	Stem width
LED	Light Emitting Diode
m	Number of Gaussian features
m	Counting element

mm	Milimeter, 10×10^{-3} m
Modivoci	MOnocot and DIcot Coverage ratio VIsion
μ_k	Centre of the Gaussian feature F_k
N	Near infrared raw colour value
n	Near infrared chromaticity
NDVI	Normalized Difference Vegetation Index
NIR	Near Infrared
nm	Nanometer
P	Symmetry order
$P(\mathbb{C})$	Prior probability of class $\mathbb{C}$
$P(F_k\|\mathbb{C})$	Conditional probability distribution of feature F_k when class is $\mathbb{C}$
$p(\vec{x})$	Probability density function describing the probability of finding the PSEP at location $\vec{x}$
PSEP	Plant Stem Emerging Point
R	Red raw colour value
r	Red chromaticity
R^2	Coefficient of determination
RMS	Root Mean Square
RTK GPS	Real Time Kinematics Global Positioning System
$S(\mathbb{C})$	Support for observation belonging to class $\mathbb{C}$
ρ	Weed density, $[\mathrm{m}^{-2}]$
σ	Kernel size
σ_k	Deviation around centre of the Gaussian feature F_k

σ_x, σ_y	Crop position uncertainty, [m]
Σ_{lc}	Covariance matrix of PSEP location
$\mathbb{S}$	Soil class
θ_A, θ_B	Orientation of edges A and B
θ_{BA}	Orientation of edge B relative to edge A
$\mathbb{V}$	Vegetation class
W	Watt
w	Weed coverage percentage, defined by the ratio of weed pixels over all vegetation pixels
x	Plant position along the crop row
$\vec{x}_A$, $\vec{x}_B$	Position vectors of edges A and B
$\vec{x}_{BA}$	Position of edge B in the coordinate system centred on edge A
$\vec{x}_l$, $\vec{x}_m$	Edges that should be compared
$\vec{x}_{\text{lc}}$	Most likely position of PSEP in leaf coordinates
y	Plant position perpendicular to the crop row
Z	Counting variable

General introduction

Chapter 1

Introduction

Major interest in the development of weed control methods is due to the potential of reducing the use of herbicides in modern agriculture. Modern agriculture has developed a high requirement for weed control, as this ensures a high yield from crop plants (Oerke, 2005)

There are several methods of weed control, that can be applied in agriculture. See figure 1.1. Chemical weed control is based on applying a spray liquid to the entire field. The spray liquid contains a herbicide which is intended to harm weeds more than crops. With the available herbicides typical weed infestations can be controlled effectively. Some weed species can only be controlled with a few herbicides and due to new regulations the set of available herbicides in the European Union will be reduced in the coming years (Weis et al., 2012). Mechanical weed control in the form of a harrow can control weeds between crop rows effective, but is unable to control in–row weeds without damaging the crop plants (Weide et al., 2008). Mechanical weed control in the form of fingerweeders assume that crop plants can tolerate more mechanical stress than weeds in the row. For crops like sugar beets the seedlings are very fragile (Kurstjens et al., 2000) and there exist no mechanical weed control method suitable of handling in–row weeds at the time of writing. A detailed description of mechanical weed control methods are described in (Griepentrog et al., 2010) and (Rueda-Ayala et al., 2010). Weed control based on thermal treatment of fields are used for organic

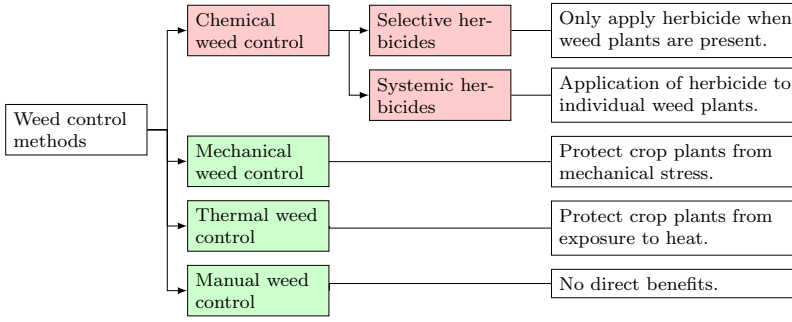

Figure 1.1: *Overview of weed control methods. Weed control methods can be divided into four groups: chemical, mechanical, thermal and manual. Chemical weed control is subdivided into selective and systemic herbicides. For each method a description of how the method can benefit of knowledge about plant positions and types is given in white boxes. Organic weed control methods are marked in green. Methods based on herbicides are marked in red.*

maize. If the treatment is conducted at an early growth stage, the maize is nearly unharmed while the weeds are controlled (Fontanelli et al., 2011). Manual weeding where weeds are removed by hands or hoe, is the most expensive method and it can be difficult to find employees for this task (Åstrand et al., 2002). Organic farms are not allowed to apply chemical methods of weed control and therefore relies on certain crop rotations, mechanical weed control, thermal weed control and manual weeding.

Weed control with herbicides has been the *default* solution in the last few decades (Kurstjens, 2007). Pesticide residues have been found in almost 40% of samples from the Danish underground water reservoirs (Thorling, 2010). Such observations leads to concerns about the environmental impact of pesticides and especially how to minimize the emission. A method of limiting the environmental impact is to reduce the usage of pesticides. To gain significant reductions in the pesticide usage, the usage of herbicides must be decreased significantly as 70% of the used pesticides in Denmark are herbicides (Danish Ministry of the Environment, 2010).

In precision agriculture the main goal is to examine in field variations and respond to these variations by adjusting the amount of herbicide or fertilizer such that the crops are given the best possible growth conditions. Numbers from Jørgensen et al., 2007 show that the amount of used herbicide can be reduced with approximately 40% if the weed population is known for the field. This reduction can be reached by using a herbicide mixture adjusted to the weed population in the field. If the weed population is known on a smaller length scale the reduction potential is even larger (Lund et al., 2008). At the plant scale level reductions higher than 95% is within reach using microspraying (Graglia, 2004). To realize these reductions detailed information about weed infestations is required.

Information about the location of individual crop and weed plants can be utilized in some new weed control methods. How different weed control methods can benefit from this information is presented in figure 1.1. Chemical weed control can benefit from computer vision systems in two ways depending on the used type of herbicide. Selective herbicides are effective at controlling growth of certain plant species but has a limited effect on other species. Systemic herbicides target central parts of the metabolism of all plants and will harm all plant species significantly. When using a selective herbicide a computer vision system can trigger the spray system when weeds are nearby and thus reduce the herbicide usage. This works on larger areas (Sökefeld et al., 2012 mentions patches with an area of $81\,\mathrm{m}^2$) as the crop plants can tolerate the selective herbicide (Christensen et al., 2009). It is much more difficult to develop a full scale sprayer system that uses systemic herbicides, as the system must target individual weed plants or at least ensure that none of the crop plants are exposed to the herbicide. Mechanical weeding systems can use knowledge about the precise location of crop plants to protect them from mechanical stress. Thermal weed control systems can use a similar approach (Poulsen, 2005).

These methods can only be put to effect with access to detailed information about location of crop and weed plants. On the patch scale level this information can be generated by manual sampling at several locations in the field, but this is not economic feasible. Systems based on machine vision for weed monitoring are under development. Acquisition of high resolution images for weed recognition is already

functional but one of the current limitations is the lack of methods for processing and analyzing the acquired information (Christensen et al., 2009).

1.1 Scope and strategy

This dissertation presents methods on how to process and analyse images from machine vision systems for quantification of weed infestations on different length scales. Methods for dealing with the following tasks are described:

- Detection of vegetation based on multispectral images.
- Estimation of the average weed pressure in images of maize seedlings where weeds and crops can occlude each other.
- Detection of the plant stem emerging point in sugar beet seedlings at the sub–centimeter scale.
- Microsprayer control for targeting of individual weeds based on position and current velocity.
- Localized training of a shape based classifier using context features.

The main objective in this project was to gain knowledge about machine vision systems in the context of agriculture and enable extraction of relevant information, like plant species and position, from images.

Six strategies were used to acquire information about the position and type of plants. The strategies were: 1) shape based recognition of plants, 2) estimation of plant centre position using individual leaves, 3) leaf shape based recognition of plants, 4) analysis of neighbour edges for locating dicot weeds, 5) crop recognition based on positions of neighbour plants and 6) use of context features to train a localized shape based classifier. An overview is given in figure 1.2 on the next page.

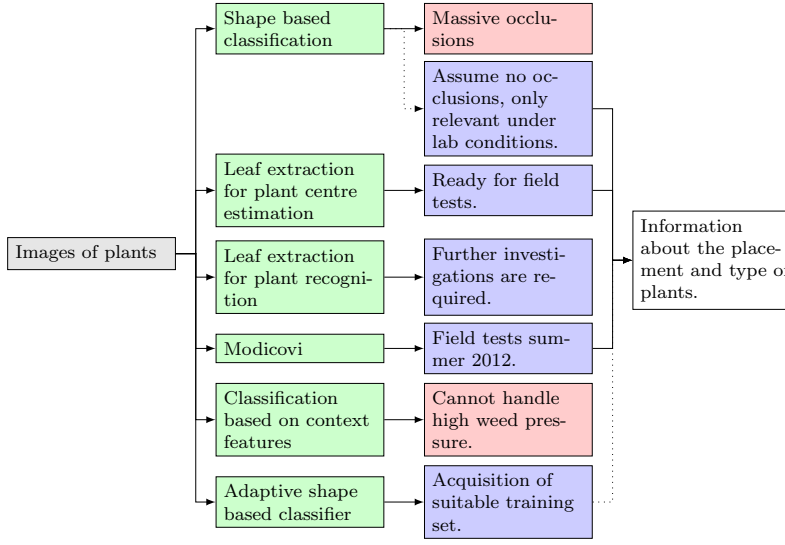

Figure 1.2: *Approaches to acquire information about the placement and type of plants from images of fields. Each approach is marked in green. Red marks an unsuccessful approach and purple marks a successful approach.*

1.2 Reading guide

The methods described in this thesis can be applied for different weed control methods. How information can flow from one method to another is shown in figure 1.3 on page 8. The figure can be perceived as a graphical table of contents.

The general introduction contains the following main sections: Chapter 2 describes existing technologies that relates to machine vision under field conditions and advanced methods for weed control that either rely on or could benefit from input from computer vision systems. The task of locating vegetation in an image is described in chapter 3, the remaining part of this thesis derives from this processing stage. In chapter 4 a method for estimating the weed pressure in maize fields is described. The system handles occluded scenes where crop and weed plants are

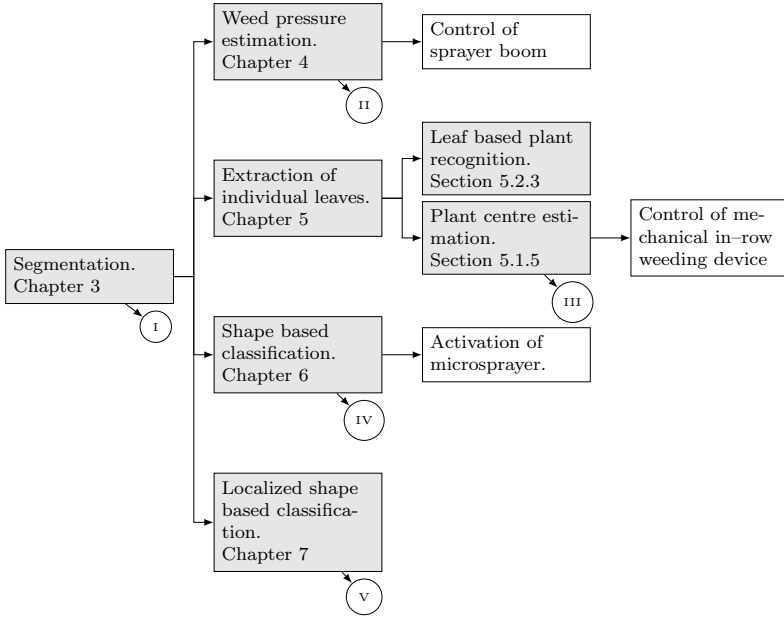

Figure 1.3: *Visualization of information flows for machine vision systems involving parts of this thesis. The shaded regions refer to specific parts of the thesis and the circles represents the publications that are in the appendix. The white boxes are examples of actions that can be controlled using the described methods.*

partly overlapping. Chapter 5 describes two methods for locating individual leaves in images of sugar beet seedlings. Detection of individual leaves can be used to recognize plants in occluded scenes and precise location of the plant stem. A microsprayer system is described in chapter 6. The system distinguishes between crop and weed plants by comparing the observed plant with a set of examples with known classes. The system was tested under different conditions and the results are presented here. Chapter 7 describes how shape based classifiers can use information about the row structure to train themselves such they can adapt to in field variations of the shape.

1.3 Summary of papers

Paper I introduces a robust method for colour based segmentation of multispectral images into regions containing vegetation and soil respectively. Training of the classifier consists of presenting it for a set of annotated images where some regions are marked as vegetation or soil. The pixel values found in the input image is transformed into a set of colour indices which is more suitable for the classifier. The classifier learns the probability density for all combinations of colour indices and segmentation classes. Based on these probability densities new observations can be recognized as either vegetation or soil using Bayes rule.

Paper II introduces a novel machine vision method that can estimate the amount of dicots (weeds) in a Maize field. Maize leaves are characterized by long straight edges while dicot leaves are more round. The method searches for these characteristics by pairing nearby edges and examine how they are positioned and oriented relative to each other. The distribution of these relative coordinates and orientations is a kind of fingerprint of the vegetation present in the image. The fingerprint is invariant to rotation of the input image and is only weakly affected by overlapping leaves in the image. The ratio of dicot leaf area to total area of vegetation can be approximated from this fingerprint.

Paper III presents a method for detecting individual leaves on sugar beet seedlings. The location and orientation of the detected leaves is then used to estimate the location of the plant stem emerging point.

Mechanical weeding devices must protect this point, as the crop would otherwise be harmed. If the position of this point is known with high accuracy, mechanical weeding devices can get closer to the crop plant without the risk of harming it. The error in the estimated plant stem emerging points were on average 3mm, which is an order of magnitude better than what can be delivered by seed tracking RTK–GPS systems.

Paper IV describes a machine vision controlled microsprayer setup and how it was tested. Three different plant species were placed in 1L pots. The pots were moved at a steady pace of 0.5 m/s below the microsprayer setup. The vision system could recognize the weed plants and treat them with the herbicide glyphosate. Two weeks after the experiment the growth stage of the plants were determined visually. Oilseed rape were used as a weed model and 94% of these plants were significantly limited in their growth.

Paper V discuss the advantage of using context based features for recognizing crop plants. The benefit of using context based features depends directly on the weed pressure and the position uncertainty of the crop plant pattern. These two values can be combined to a *normalized weed pressure* λ. If the true seeding points are known, the normalized weed pressure puts an upper bound on the achievable crop recognition rate given by $\frac{1}{1+\lambda}$. The implemented context based crop recognition methods were evaluated in a simulated environment. In the simulation environment the methods were tested under different weed densities and crop position uncertainties. The two best performing methods followed a curve similar to the predicted upper bound, with the curve shifted in direction of a lower normalized weed pressure.

Chapter 2

Existing technologies

The term *precision agriculture* have been used for a long time to describe a set of methods that allow the farmer to monitor in–field variations and act upon them. Prior and ongoing research projects provide access to methods for locating weed and crop plants and also selective target weed plants or protect crop plants. This chapter is divided in three sections. Section 2.1 describes general methods that can give information about the location of crop plants and the presence of weeds. Section 2.2 describes camera technologies which are used for image acquisition. Section 2.3 describe seven systems based on GPS located plants and vision based plant recognition. The systems are either research platforms or available commercially.

2.1 Crop and weed detection methods

If the position of crop and weed plants are known, it is possible to protect crop plants from weed control or direct weed control against the weeds. Reliable information about crop and weed plant positions will allow development of new types of methods for selective weed control. In this section two examples are provided.

2.1.1 Mapping location of seeds and transplanted plants

With RTK GPS systems it is possible to map specific locations with a few centimetres in accuracy, this can be used to mark the location of all seeds sown in a field or all transplanted crop plants. Several research groups have reported results on the accuracy of such systems. Ehsani et al., 2004 measured seed locations with a modified seeder and found distances between actual plant locations and measure seed locations in the range 30 mm – 38 mm. Sun et al., 2010 mapped transplanted plants and found that the position uncertainty in the movement direction is significantly higher than in the transversal direction, the average position error were (20 ± 31) mm.

Nørremark et al., 2007 used optical detection of sowing locations of sugar beets. They found that 95% of the plants appeared within 37.3 mm from the measured seed location. Figure 2.1 visualizes the true plant locations and the mapped seed locations. Furthermore the sources for this variation were investigated. Taking care of GPS drift over time ($\rho_{\text{GPS}} = 9.5\,\text{mm}$) and measured deviations between seed location and plant location ($\rho_{\text{seed–plant}} = 12.4\,\text{mm}$) a minimal RMS error along both axes of $15.6\,\text{mm} = \sqrt{\rho^2_{\text{GPS}} + \rho^2_{\text{seed–plant}}}$ should be expected.

The main flaw of methods that rely on knowing the location of crop plants at one point in time, is that external forces might move the plant in the time between transplanting or seeding and weed control. A tractor wheel can push soil aside and thus move a few plants out of the protected area. On a larger scale an earthquake could move the entire field in the few weeks between seeding and when the seed locations is used for weed control. A more likely scenario is data loss due to corrupted files, failing hard drives.

2.1.2 Vision based detection and classification

Visual detection of crop plants is an alternative to storing all crop plant positions. Given an input image, the method locates vegetation objects and based on the shape of these objects recognizes them as either crop or weeds. The advantages of vision based detection and classification

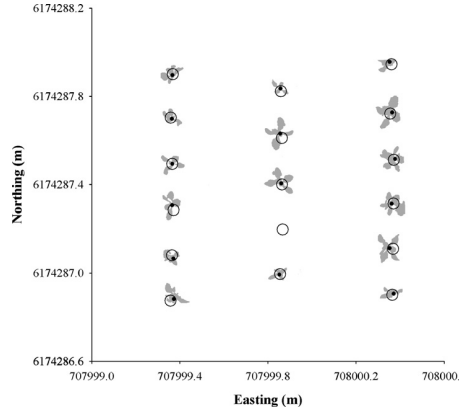

Figure 2.1: *Visual representation of precision using RTK GPS for tracking seed locations. Seed locations are marked by circles (○) with a radius of* 25 mm *and visual location of plant centres are marked with dots (●). From Nørremark et al., 2007.*

of plants are a low uncertainty in plant position and that information about the weed infestation can be extracted from the images. A severe problem is to handle occlusion between multiple plants and many systems for plant recognition ignores this problem, which can lead to inferior classification results.

Guyer et al. (1986) presented the central idea used for much work within the field of plant recognition. Given an input image, the method locates vegetation objects and describes the shape of each object with features like area, length of perimeter, moment of inertia and elongation. Feature descriptors based on the convex hull and the skeleton of the plant shape were introduced by Hemming et al. (2001) and Weis et al. (2009). One method for dealing with the occlusion problem is to model the average shape and typical shape variations of a set of known plants. Active shape models, which are able to model these shape variations, were used for plant recognition by Søgaard (2005) and Persson et al. (2008). They both found that active shape models could locate and recognize occluded plants, but it required a good initial guess on the plant location and orientation.

The first generation of camera based weed monitoring systems were offline systems, meaning that the system acquired images in the field and analysed them at home. This was required as the processing power for analysing the images while driving were not available (Sökefeld et al., 2012). After the analysis proper actions can be taken leading to two passes across the field. The second pass would increase the cost of treatment significantly compared to a single pass solution where the images are analysed and action is taken instantaneous (Oebel et al., 2009).

2.2 Camera technologies

In the literature there is a large variety of technologies for capturing images of plants. In this section different camera technologies are described. The delivery of most of these systems is a map of where vegetation has been observed. This map is then used to analyse the shape of detected plants.

The subsections about spectral properties and camera types describes methods that are used by the systems described in section 2.3. Chlorophyll fluorescence and multiple camera setups are interesting techniques that can be used to deal with the occlusion problem and maybe derive new features for plant recognition. No references to demonstration systems using these methods were found.

2.2.1 Spectral properties of soil and vegetation

How objects appear in a vision system depends on their spectral properties. The reflection spectra of soil and three different plant species are shown in figure 2.2. The reflection intensity of soil increases slowly with the wavelength whereas the reflection of vegetation varies much faster. The bump near 540 nm derives from chlorophyll which is used in photosynthesis (Loomis, 1965). The steep increase in reflectivity in the range [700 nm; 750 nm] is denoted the red edge inflection point, at wavelengths above $750nm$ the vegetation will try to reflect as much of the light as possible to reduce heating, below this threshold the light is used in photosynthesis which is maximized by the vegetation (Atwell

et al., 1999; Scotford et al., 2005).

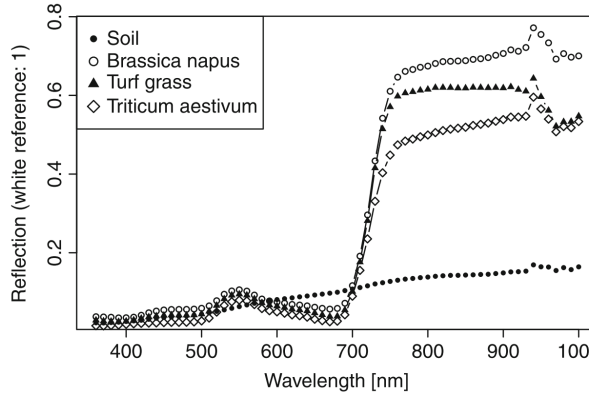

Figure 2.2: *Typical spectra from vegetation and soil. The large difference in reflection between soil and vegetation in the range* $[700\,\text{nm}; 800\,\text{nm}]$ *is used to detect vegetation with the Normalized Difference Vegetation Index. From Weis et al., 2010.*

Spectral information from the visible region can be acquired with RGB cameras and used for detecting vegetation (Bossu et al., 2009). Such a system measures the amount of reflected light near three wavelengths corresponding to red (R), green (G) and blue (B). Each measurement is then quantized to an integer, often in the range $[0, 255]$. Detection of vegetation relies often on thresholding of different colour indices, including the Excess Green (ExG) (Woebbecke et al., 1995; Meyer et al., 2008). ExG is defined as:

$$\text{ExG} = 2G - R - B \tag{2.1}$$

It is not always possible to detect all vegetation with the ExG colour index, as an example see the image in figure 2.3 where parts of the vegetation has a brown shading similar to the soil. The maize leaf in the image have yellow areas while the pineapple–weed plants have brown perimeters. Such variations makes it difficult to recognize areas with vegetation using ExG.

A more stable indicator of the presence of vegetation can be found by looking at figure 2.2 and note the large variation between reflectivi-

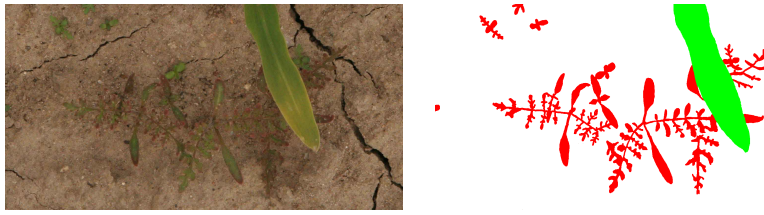

Figure 2.3: *Ilustration of how it is not always possible to detect all vegetation with the ExG colour index. The original image is shown to the left and a manual segmented is shown to the right. The image contains Maize (Zea mays L., shown in green) and pineapple-weed (Chamomilla suaveolens, shown in red). Picture taken at Flakkebjerg in 2010.*

ties of soil and vegetation for wavelengths in the near infrared (NIR) range [750 nm; 950 nm]. If both near infrared and red intensities are measured, the normalized difference vegetation index (NDVI) is an effective way of locating vegetation (Rouse et al., 1973).

$$\text{NDVI} = \frac{N - R}{N + R} \tag{2.2}$$

2.2.2 Matrix and line scan cameras

Matrix cameras are used to capture information about a larger area. The acquired image consists of a 2D array with pixel values. Each pixel can have a few values attached, such as intensity of red, green, blue or near infrared radiation. The line scanning camera takes images of a narrow region, usually with a $1 \times m$ pixel array, and the camera type is often used for hyperspectral image acquisitions (Zhang et al., 2011). The use of line scanning cameras in real time weed control systems requires the camera to capture frames at a very high rate, but the advantage is that the amount of information from each exposure is limited and only a small area needs to be illuminated.

2.2.3 Chlorophyll fluorescence

An other method of characterising the radiation emitted from vegetation is to examine the fluorescent properties of chlorophyll. Tyystjärvi et al. (2011) examined the intensity of fluorescence over time after exposing plants to strong pulses of light. Before the measurements where the plants shielded from illumination for 1 second. Analysis of the variation in fluorescent intensity over time were used to classify vegetation into crop and weed classes with a correct classification rate in the range 86.7–96.1%. The time where plants need to be in shadow will put certain constraints on machinery utilizing this method.

2.2.4 Single or multiple camera setups

Some of the issues related to analysing images from a single camera can be reduced by getting some kind of depth information. To determine which pixels belong to a certain plant, when the image contains overlapping leaves, is one example. Jin et al. (2009) uses a real time stereo setup to extract individual corn plants under conditions where leaves from several plants overlap. The disadvantages of using stereo rigs are increased cost of the image acquisition system and a much larger requirement for data processing power.

2.3 Demonstration and commercial systems

Several demonstration systems exist and a few commercial systems which can control in–row weeds are available. A lot of the mentioned systems have inspired the work in this dissertation. A short overview of the systems, used plant detection methods and weed control systems are given in table 2.1. Two of the systems, the Robocrop and the Robovator, are used commercially for mechanical weed control in transplanted crops like lettuce and cabbage. As a part of the Brainweed project, images acquired by the Robovator were used for evaluation of different image analysis methods.

2.3.1 H sensor

The H sensor is a vision based plant recognition system that recognizes plants based on their shape. A central assumption is that plants to not occlude each other. The camera is a bispectral matrix camera that operates in the red and near infrared spectral regions. The acquired images are analysed by locating individual plants and extracting their shape descriptors Piotraschke, 2010. The sensor has been used for simulated online weed control in fields with winter wheat and maize Sökefeld et al., 2012.

2.3.2 Volunteer potatoes

Sugar beet farmers in the Netherlands have to remove volunteer potato plants from their fields. Volunteer potatoes can be a spreading vector for the potato disease late blight (*Phytophthora infestans*). No selective herbicides are available which targets potatoes while avoid harming sugar beets, so there is a need for alternative solutions, because manual weeding is too costly (Nieuwenhuizen et al., 2007).

Nieuwenhuizen (2009) developed a system using machine vision that can apply glyphosate to volunteer potatoes and avoid hitting the sugar beets. An image of the system is shown in figure 2.5 and an illustration of the image analysis is shown in figure 2.6. The colour information from RGB images is first used to locate vegetation using the excess

System	Plant location technology	Weeding tool	State	Main idea
H sensor	Bispectral matrix camera	Patch sprayer	Demonstration	Shape based plant recognition
Volunteer potato	RGB and NIR matrix camera	Microsprayer	Demonstration	Adaptive classifier based on row structure
GeoSeed			Demonstration	Place crop plants in 2D structures
Cycliod hoe	(GPS based)	Mechanical	Demonstration	GPS based mechanical in–row weed control
Mech weed	RGB matrix camera	Mechanical	Demonstration	Crop recognition based on context features
Robocrop	RGB matrix camera	Mechanical	Commercially	Vision based mechanical in–row weed control
Robovator	Bispectral line scanning camera	Mechanical	Commercially	Vision based mechanical in–row weed control

Table 2.1: *Overview of the described systems containing details about the methods used for plant location and weed control. Ideas that have inspired work in this dissertation are listed in the* Main idea *column.*

Figure 2.4: *Image of the H–sensor. An active illumination system based on LEDs are placed around the bispectral camera. From Piotraschke (2010).*

green colour index, then is the colour information used to distinguish between between crop and weed plants. The system adapts to variations in plant appearance by recognizing the row location, applying the rule that plants close to the crop row most likely will be crops and plants far away from the row will probably be volunteer potatoes. These examples of likely crop and weed plants is then used to train a Bayesian classifier (Nieuwenhuizen et al., 2010a). Performance of this volunteer potato control system was evaluated, 77% of the volunteer potatoes were successfully controlled while 1% of the sugar beets were killed (Nieuwenhuizen et al., 2010b).

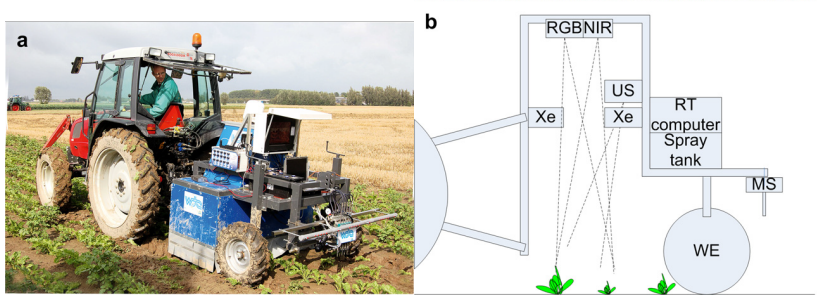

Figure 2.5: *Volunteer potato control machinery image and sketch. Under the blue hood cameras (RGB and NIR), illumination (Xe) and ultrasonic sensors (US) are mounted. Microsprayer (MS), computer equipment and wheel encoder (WE) are placed behind the cover. From Nieuwenhuizen et al., 2010b.*

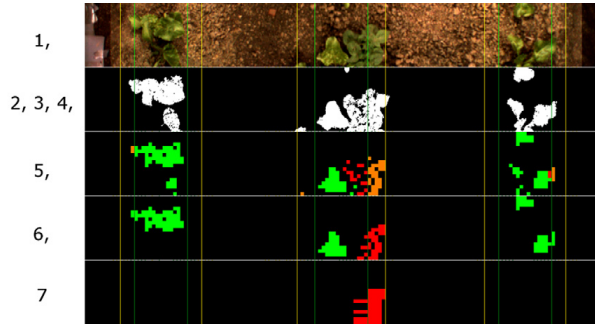

Figure 2.6: *Location of volunteer potatoes in three sugar beet rows. 1) colour image is recorded; 2, 3, 4) vegetation and crop rows are detected, colour features extracted, and classifier is trained; 5) vegetation is classified; 6) small plants are filtered; 7) spraying decisions are made within crop row. Image and caption is modified from Nieuwenhuizen et al., 2010b.*

2.3.3 GeoSeed

In 2011 presented Kverneland the GeoSeed seeder. The machine places seeds at specified GPS coordinates (Kverneland, 2011). With the system it is possible to place crops in well defined 2D patterns, as shown in figure 2.7. When plants are placed in a rectangular grid it is possible to use cross hoeing for mechanical weed control (Rothmund, 2007).

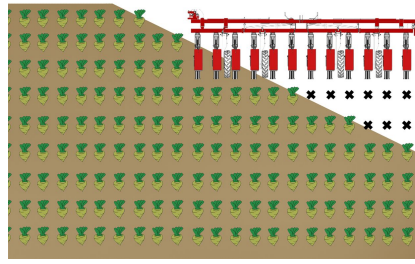

Figure 2.7: *Seeding pattern generated with Geoseed. The rectangular crop placing allows the use of cross hoeing, a technique that can remove part of the in–row weeds. From pressebureauet.dk.*

2.3.4 Cycloid hoe

The cycloid hoe is a mechanical weeding device developed by Griepentrog et al., 2006. It consists of eight fingers mounted on a horizontal platform which rotates around the vertical axis. Each finger on the platform can be moved in the radial direction independently of the other fingers. An example of a movement pattern is shown in figure 2.8. Under normal operation are the fingers spread out such that they cover a large area, including the row in which weeds should be controlled. When a crop plant should be protected, the fingers, that otherwise would harm the crop, are moved out of the crop row.

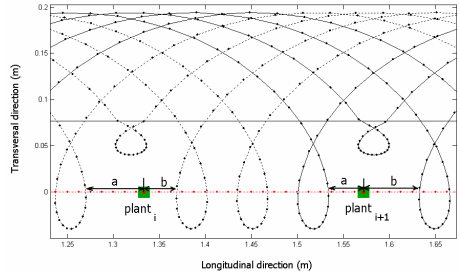

Figure 2.8: *Cycloid hoe tine trajectories. Tines are allowed to move into the row when no crop plants would interfere with the tine trajectory. From Griepentrog et al., 2006.*

2.3.5 Mechanical weed control based on GPS locations

Perez-Ruiz et al., 2012 describes a mechanical weed control system. The system works in transplanted tomatoes, where the position of each crop plan is known from the transplantation process. Two knives are moved through the soil in the row, when a crop plant gets the knives they are moved out of the row. This process is visualized in figure 2.9.

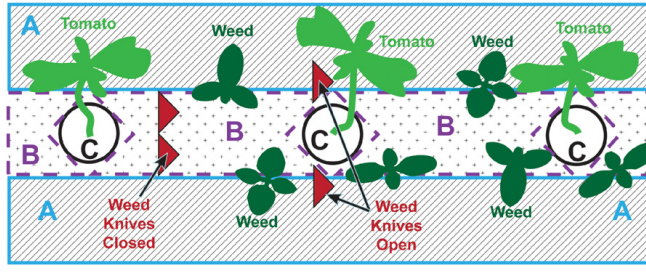

Figure 2.9: *Principle of intra row weeding. Weeds in area A can be controlled by traditional hoeing. Area B can be targeted by in–row hoeing, but mechanical weeding in area C (close to crop region) would harm the crop plant. From Perez-Ruiz et al., 2012.*

2.3.6 The Mech Weed project

A mechanized weeding robot for controlling weeds in sugar beets was described in Åstrand et al. (2002). A sketch of the system is shown in figure 2.10. The robot can drive along crop rows autonomously and distinguishes between crop and weeds using information about plant positions. The software could protect crop plants from the mechanical tool, but the weed control effect was not sufficient for use in agriculture (Åstrand et al., 2002). The robot was equipped with a mechanical weeding tool described as

> *The mechanical weeding tool is a rotating wheel that is rotated perpendicular to the row line. The tool processes only the area between crops in the seedline. If a crop appears, the tool is quickly lifted by a pneumatic cylinder and lowered directly after the crop has been passed.* Åstrand et al., 2002

Field tests showed that 198 of 200 crops and 125 of 236 weeds survived a mechanical weed control treatment with the system (Åstrand et al., 2004).

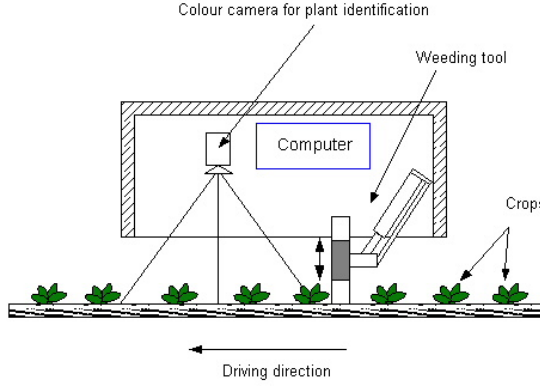

Figure 2.10: *Principle sketch of the MechWeed project. The colour camera recognizes crop plants and controls the weeding tool such that crop plants are not harmed. From www2.hh.se.*

2.3.7 Robocrop

The British company Garford Farm Machinery Ltd produces the Robocrop mechanical intrarow weeder (Garford, 2011). The robocrop is used commercially for weed control in transplanted crops like lettuce and cabbage. A *half moon* shaped plate is moved through the soil in the row. When a crop plant gets close, the weeding device is rotated such that the incision is moved with the crop plant and the plant is thus protected from the weeding, this process is shown in figure 2.11.

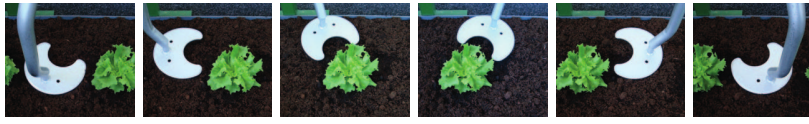

Figure 2.11: *The Robocrop mechanical weeding device. The incision in the weeding device is moved such that the crop plant is protected. From Garford, 2011.*

An image of the weeding device is shown in figure 2.12. Crop detection and localization is based on a colour camera. The image analysis software looks for large green regions utilizing a two dimensional Mexican hat wavelet (Tillett et al., 2008).

2.3.8 Robovator

The Robovator is a precision weeding platform for in–row weed control. A bispectral line scanning camera is mounted over each crop row. Vegetation is detected using NDVI. Detected plants are classified as either crop or weed based on the size and shape. The platform can be equipped with either a mechanical or a thermal weeding device. The mechanical weeding device consists of two knives that are dragged through the soil inside the row. When a crop plant is detected, the knives are removed from the row. An image of the Robovator using the mechanical weeding device is shown in figure 2.13. The thermal weeding device is a linear array of gas burners mounted along the crop row. Burners are enabled during normal operation. When a crop plant moves along the row of gas burners, the burners are turned off while the

Figure 2.12: *Robocrop in action. A camera locates crop plants and controls the weeding device such that crop plants are protected from mechanical in–row weeding. From Garford (2011).*

Figure 2.13: *The Robovator in action. Halogen lamps were used to provide controlled illumination for the vision system. From visionweeding.com.*

crop passes by. The Robovator is used commercially in transplanted crops like lettuce, cabbage and chives.

2.4 Summary of existing technologies

There is a massive development in the field of precision agriculture and weed control on the individual plant level. The volunteer potato control device can apply glyphosate to individual potato plants. Systems for mechanical control of weeds in the in–row area of transplanted crops are available from Garford and F. Poulsen Engineering. At this moment the limiting factor is the vision based recognition of crop plants. The commercial systems all rely on the assumption that crop plants are larger than weeds, which is the case in transplanted crops. This thesis investigates methods that does not depend on this assumption and are suitable for recognition of seeded crops in occluded areas.

Results

Chapter 3

Segmentation

In computer vision, segmentation is the process of partitioning digital images into regions containing certain elements. The goal of segmentation is to simplify the image into something that is easy to analyse. All techniques described in this dissertation use image segmentation to locate vegetation regions and boundaries in images.

Segmentation into vegetation and soil regions is usually performed by thresholding of either the excess green colour index or the normalized difference vegetation index in real time applications due to their simplicity and low requirement for computations (Nieuwenhuizen et al., 2010b; Langner et al., 2006).

In this chapter a method that can locate vegetation in multispectral images is described, the method is also described in paper I. The method is based on the framework of Bayesian classifiers and is trained by an example image where a few regions of soil and vegetation are marked as examples of these classes. From this input, the system learns the distribution of colour values in the two classes. This knowledge can then be used to estimate which class a new observation belongs to. With this method, and a suitable training set, it is possible to get better segmentations than thresholding of either excess green or the normalized difference vegetation index.

3.1 Materials and methods

The statistical framework behind the classifier is presented in section 3.1.1. Kernel density estimation is used to estimate the colour distributions in the soil and vegetation class, this is described in section 3.1.2. Section 3.1.3 lists some colour features which can be derived from images. Training of the classifier consists of presenting it for some pixels in soil and vegetation regions, how these training samples are marked is described in section 3.1.4.

3.1.1 Naive Bayes classifier

The purpose of a classifier is to predict which class, $\mathbb{C}$, a new observation, $\vec{F}$ belongs to. The classifier is trained by showing it a set of observations and associated class labels.

A Naive Bayes classifier is a simple classifier based on applying Bayes' theorem using a strong assumption about independent input variables and the classifier belongs to the group of Bayesian classifiers (Pérez et al., 2009). This group of classifiers model the joint probability distribution, $P(\mathbb{C}, \vec{F})$, of the discrete class variable $\mathbb{C}$ and the continuous input variables $\vec{F}$. Based on the joint probability function, the classifier calculates the probability that a new observation belongs to class $\mathbb{V}$ and not class $\mathbb{S}$ as follows:

$$P(\mathbb{V}|\vec{F}) = \frac{P(\mathbb{V}, \vec{F})}{P(\mathbb{V}, \vec{F}) + P(\mathbb{S}, \vec{F})} \tag{3.1}$$

Training of the Naive Bayes classifier consists of approximating the joint probability function. $P(\mathbb{C}, \vec{F})$ is a function of several variables and to approximate it would require a number of training samples that scales exponentially in the number of variables. This is a prohibitive large number of samples even with a small set of variables. An alternative representation of the joint probability distribution is to express it in terms of conditional probabilities as below

$$P(\mathbb{C}, \vec{F}) = P(\mathbb{C}) \cdot P(F_1|\mathbb{C}) \cdot P(F_2|F_1, \mathbb{C}) \cdot P(F_3|F_1, F_2, \mathbb{C}) \cdot \ldots \tag{3.2}$$

This still requires memory exponential in the number of features which is infeasible for more than a few features. By making the naive assumption that different input features are independent, the representation can be changed to the following product of the prior probability of the class and the conditional probabilities for each of the input variables given that class.

$$P(\mathbb{C}, \vec{F}) \simeq P(\mathbb{C}) \cdot P(F_1|\mathbb{C}) \cdot P(F_2|\mathbb{C}) \cdot P(F_3|\mathbb{C}) \cdot \ldots \tag{3.3}$$

Now $P(\mathbb{C}, \vec{F})$ can be approximated with a much smaller training set. Even if the assumption about independent input features is seldom valid, the Naive Bayes classifier seems often to perform surprisingly well (Hand et al., 2001). The advantage of the Naive Bayes classifier is that it only requires a small amount of data to be trained.

3.1.2 Estimation of conditional probability densities

The conditional probability density for each input variable is estimated using Kernel density estimation (Silverman, 1986; John et al., 1995). The estimated probability density $\hat{f}_h(x)$ can then be expressed as:

$$\hat{f}_h(x) = \frac{1}{L \cdot h} \sum_{i=1}^{L} K\left(\frac{x - x_i}{h}\right) \tag{3.4}$$

$$K(x) = \frac{1}{\sqrt{2\pi}} e^{\frac{-x^2}{2}} \tag{3.5}$$

where L is the number of training samples and h is the bandwidth of the Gaussian kernel. The bandwidth is chosen manually for each input variable.

3.1.3 Colour features

The set of colour features used for segmentation is described in paper I and consists of

- Four raw colour values (R, G, B, N).

- Four colour chromaticities (r, g, b, n).
- The excess green colour index (ExG).
- The normalized difference vegetation index (NDVI).

Both RGB and RGBN images (Images with red, green, blue and near infrared colour values) can be used. If the near infrared colour value is not present in the image, the value is fixed to zero, and the normal classification process can continue.

3.1.4 Defining the training set

Before the Naive Bayes classifier can segment images, it needs to be trained. Training of the classifier consists of presenting two image to it; a reference image and a masking image. The reference image is a raw image as acquired by the camera system. The masking image contains information about which regions in the reference image that are vegetation or soil, regions with vegetation is marked by white while soil is marked by black, see examples in figure 3.1. The masking image is generated manually and can either be sparse or complete. In a sparse masking image some regions are marked as vegetation, other regions marked as soil, and the remaining part of the image is ignored in the training process. In a complete masking image all pixels are marked as either vegetation or soil.

Training of the classifier consisted of locating a training image, creating a masking image by duplicating the training image and marking a few regions in the masking image as either vegetation, marked by white, or soil, marked by black. These two images were then used for training the classifier. After training, the classifier was applied to the training image and the segmentation result was inspected. If regions were misclassified, the masking image was updated to contain more examples from these regions and the process was repeated until the segmentation of the training image was satisfactory.

Figure 3.1: *Examples of the segmentation process. The first row contains the raw input image. The second row contains the nir channel of the input image. The third row are annotated images that mark example regions of soil and vegetation. The fourth row are the produced segmentation.*

3.2 Results and discussions

This section describes how a Naive Bayes classifier is trained and tested. The training is described and the result of the training, the estimated probability distributions are investigated. Classification using the individual features and the full set of features are discussed and compared. Experiences from working with the system on different datasets are presented.

3.2.1 Training of the classifier

The Naive Bayes classifier was trained twice using the same reference image and with two different masking images, a sparse and a complete. The reduced training set consisted of 14.396 samples of vegetation and 35.763 samples of soil. For the complete masking image the sample sizes were 294.714 and 3.460.246 for vegetation and soil respectively. For estimating the probability densities, the bandwidths listed in table 3.1 were used. The bandwidths were chosen such that the estimated probability densities appeared smooth for the full training set. Figure 3.2 and 3.3 show the estimated probability densities and the overlapping coefficient for each of the features. The probability densities for the reduced training set is not as smooth as the probability densities for the full training set, this is caused by the difference in number of training samples, a high number of training samples results in a more smooth distribution. The overlap coefficients for n, ExG and NDVI in the reduced training set is significantly smaller than in the full training set. The larger overlap in the full training set might be caused by faulty annotation of pixels near the boundary between vegetation and soil regions.

Feature	R	G	B	N	r	g	b	n	ExG	NDVI
Bandwidth	150	150	150	100	0.01	0.005	0.005	0.005	100	0.005

Table 3.1: *Bandwidths used for density estimation. The bandwidths were chosen such that the estimated conditional probabilities shown in figure 3.2 appeared smooth.*

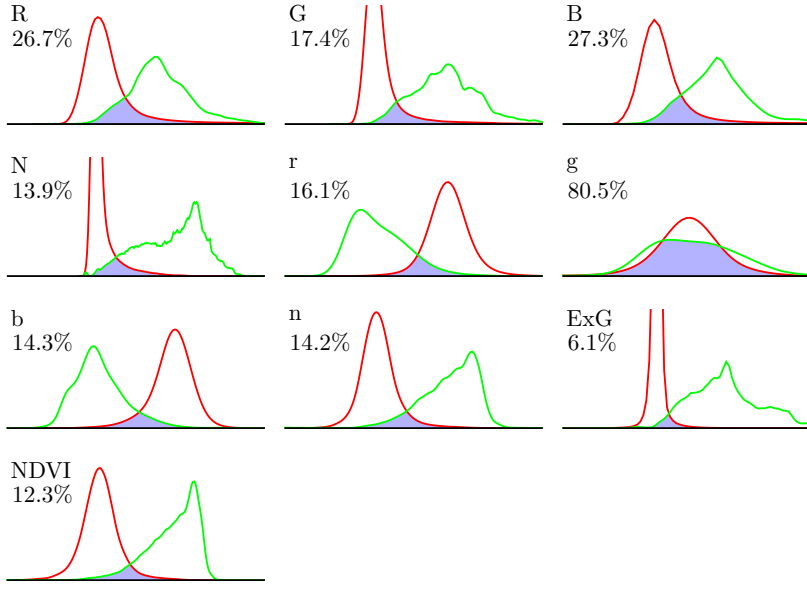

Figure 3.2: *Conditional probabilities for the full training set. Feature distribution for the soil class is shown in red while the distributions for the vegetation class is shown in green. The distributions are normalized to zero mean and equal standard deviation.*

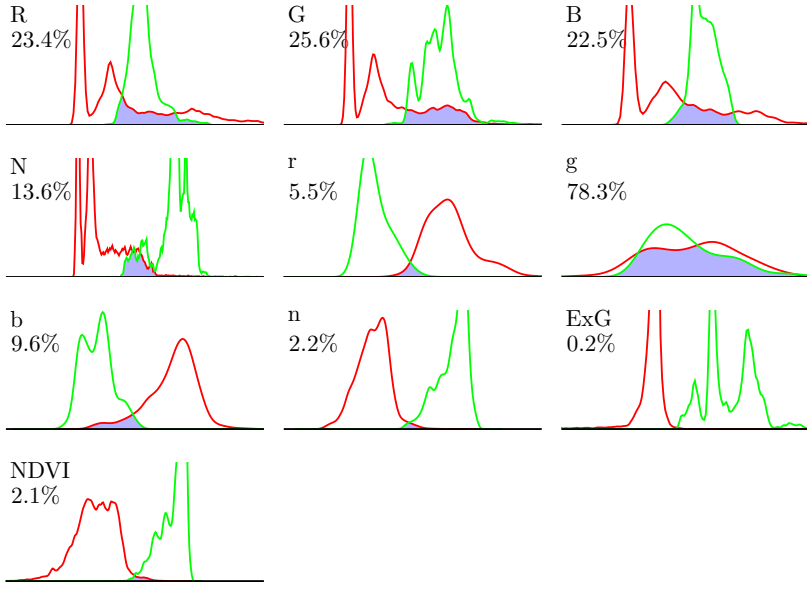

Figure 3.3: *Conditional probabilities for the reduced training set. For symbol definitions see figure 3.2.*

3.2.2 Partial classifications

Classification results based on individual features are shown in figure 3.4 and 3.5. The classifications in figure 3.4 is based on the full training set while the reduced training set is used to generate figure 3.5. In both figures the segmentations based on either the R, G, B or g features are not very good, all segmentations based on these features misclassify a large fraction of the pixels. This was expected due to the large overlaps of the probability distributions in figure 3.2 and 3.3. The remaining features (N, r, b, n, ExG and NDVI) all results in decent segmentations, although the boundary between soil and vegetation regions are much sharper when the reduced training set is used.

3.2.3 Segmentation of different image types

An informal testing of the segmentation have been conducted by using the system for locating vegetation in several image collections. With a new set of images that the classifier should segment, the training process took only a few minutes, which were spent on two tasks: 1) marking regions in the masking image and 2) testing the classifier trained using the masking image.

In the examined image sets it were possible to achieve satisfying segmentations. High levels of salt and pepper noise were often seen in segmentations based on images stored in lossy formats like *JPEG*, an example is shown in the left column in figure 3.1 and in figure 3.6. In segmentations based on uncompressed images this was not observed, see right column in figure 3.1.

3.3 Summary of segmentation with naive Bayes

A system for segmenting multispectral images into soil and vegetation regions has been developed. The system is based on the naive Bayes classifier but modified to handle continuous input values. It was found that training the system on a relatively small training set lead to better

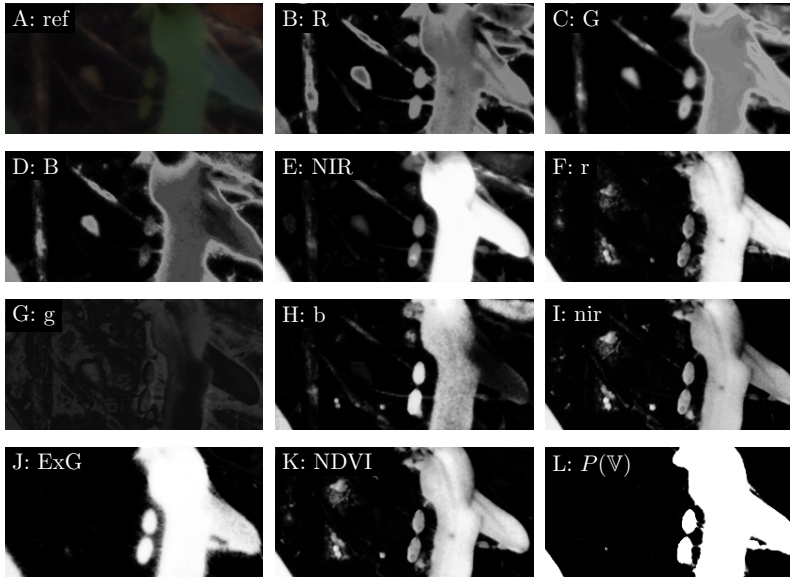

Figure 3.4: *Partial classifications for the full training set. The original RGB image is shown in tile A.*

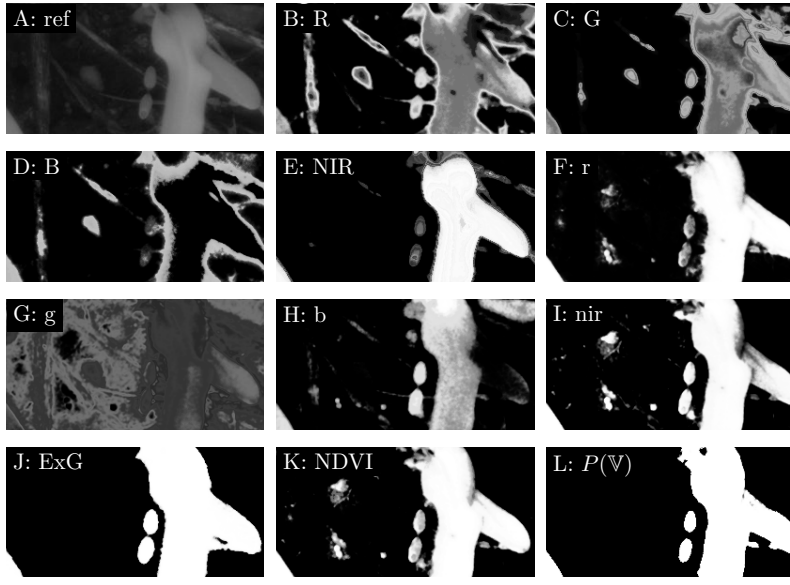

Figure 3.5: *Partial classifications for the reduced training set. The original NIR image is shown in tile A.*

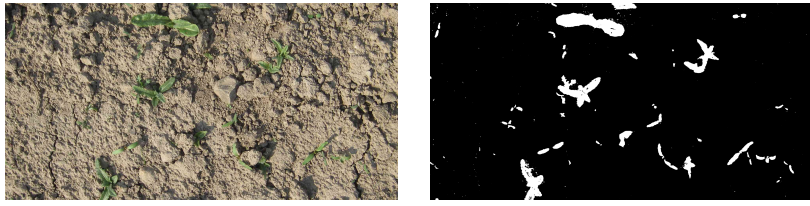

Figure 3.6: *An example of the classifier in action. The input image was stored with a lossy encoding, compression artefacts in the image can cause some salt and pepper noise in the segmented image.*

segmentations than using a full training set. The inclusion of borderline pixels[1] in the training set seemed to confuse the classifier.

The system was tested on different image types and under different illumination conditions. By training of the classifier, fast and satisfactory segmentations were achieved. Images stored in a lossy format contained compression artefacts which were seen as salt and pepper noise in the segmentation results.

[1] pixels not clearly belonging to either class

Chapter 4

Estimation of weed pressure in maize

A lot of the described systems for weed recognition relies on the assumption that plants do not occlude each other. This assumption is often violated in crops like maize, barley and winter wheat. This group of crops share the property that their leaves are elongated with almost parallel edges. Weeds present in these fields are often dicots which tend to have a more curved structure. In this chapter a method for estimating the dicot weed pressure in a monocot crop population is described.

The method is based on the position and orientation of edges relative to nearby edges. Relations between nearby edges are described using two Cartesian coordinates and an orientation. These relations are described as points in a five dimensional space and the density of points in this space is estimated near some interest points. The estimated densities are then used to predict the weed pixel percentage. The weed pixel percentage is the percentage of vegetation pixels in the image that originate from weed plants.

The algorithm will be referred to as Modicovi which is an abbreviation of *MOnocot and DIcot Coverage ratio VIsion*. Modicovi is covered by the patent application P1174DK00 with the title *Spray boom for selec-*

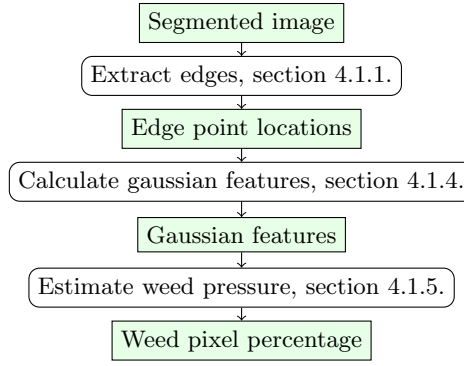

Figure 4.1: *Dataflow in the Modocovi algorithm.*

tively spraying a herbicidal composition onto dicots, which is attached as paper II.

4.1 Materials and methods

Modivoci is based on the general steps shown in figure 4.1. First is the location of edges and their orientation in the image determined, this is described in section 4.1.1. All pairs of nearby edges are then examined. The position and orientation of one element in a pair of edges is expressed relatively to the other element in the pair, see section 4.1.2. The distribution of relative coordinates of nearby edges is a kind of rotation invariant fingerprint of the vegetation population in the image. 2D projections of this fingerprint are described in section 4.1.3. This fingerprint is described in terms of a small set of features, calculation of these features are covered in section 4.1.4.

4.1.1 Detection of edges

To create edges with a single pixel width, the following procedure is used: 1) calculation of edge strength, 2) thresholding the edge strength image and 3) morphological thinning of the detected edge structures.

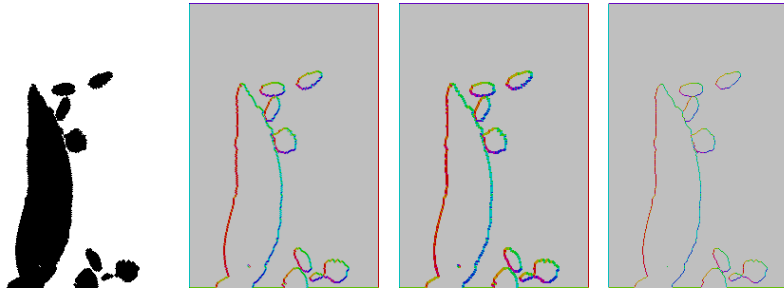

(a) (b) (c) (d)

Figure 4.2: *Steps in the Modicovi algorithm: a) Input image, b) edge strength and orientation, c) thresholded edge image and d) thinned edge image.*

The process is shown in figure 4.2.

The edge strength is calculated by a convolution of the input image with the first order symmetry derivative kernel $\Gamma^{\{p,\sigma^2\}}$ as defined in Bigun et al. (2004).

$$\Gamma^{\{p,\sigma^2\}} = (D_x + iD_y)^p \frac{1}{2\pi\sigma^2} \exp\left(\frac{-x^2 - y^2}{2\sigma^2}\right) \tag{4.1}$$

where D_x is the image gradient in the x direction, D_y is the image gradient in the y direction, $p = 1$ is the symmetry order and $\sigma = 1/4$ defines the effective size of the kernel. Convolution with this complex kernel generates a complex output image. The magnitude of the output image is the edge strength while the phase describes the edge orientation. The magnitude image is thresholded and the resulting image is then thinned (morphological thinning (Ji et al., 1992)) until the edges have a width of a single pixel. The image is divided into 8×8 pixel bins. For each bin is a representative edge located. This reduces the computational requirements in the following steps significantly.

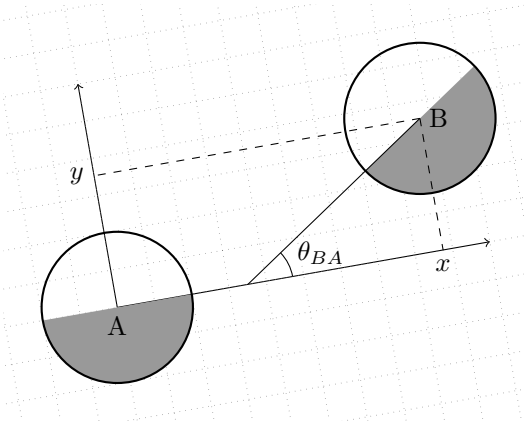

Figure 4.3: *How the location and orientation of edge B described relative to edge A. A coordinate system is placed on edge A and oriented such that the x axis follows the direction of the edge. The location of edge B is described using this coordinate system and the difference in orientation is described by θ_{BA}.*

4.1.2 Relative edge descriptors

To describe the location of B relative to A, a coordinate system is positioned with origin at A and direction of the x axis parallel to the detected edge with the y axis pointing in the direction of highest intensity (into the vegetation) in the original image, see figure 4.3. The position of edge segment B relative to edge segment A is calculated as

$$\vec{x}_{BA} = (\vec{x}_B - \vec{x}_A) \begin{bmatrix} \cos\theta_A & \sin\theta_A \\ -\sin\theta_A & \cos\theta_A \end{bmatrix} \tag{4.2}$$

$$\theta_{BA} = \theta_B - \theta_A + z \cdot 2\pi \qquad Z \in -1, 0, 1 \tag{4.3}$$

where $\vec{x}_C$ and θ_C is used to describe the Cartesian coordinates and the orientation of general edge segment C. The integer Z is chosen such that θ_{BA} is in the interval $[0, 2\pi]$. The relative location is then defined by three values, the two coordinates from $\vec{x}_{BA}$ and the orientation θ_{BA}. For calculating the feature descriptors the following additional descriptors are added: the distance between edge segments *dst* and the magnitude of the direction change $|\theta_{BA}|$.

4.1.3 Projected density plots

To get a rough idea of the relative edge positions of some test images, the observed relative edge orientations were projected to different 2D spaces where methods from kernel density estimation (Silverman, 1986) were used to visualize the densities. Projections of the relative edge orientations for three test images are shown in figure 4.4. The axis limits are shown in table 4.1. Notice how the long straight edges of monocots are visible in the distance vs. angle plot (last row in the figure).

Variable	Lower bound	Upper bound
x	-125	125
y	-125	125
dst	0	125
θ	-180	180
$\|\theta\|$	0	180

Table 4.1: *The Gaussian features are all centred within these limits in the 5D space.*

4.1.4 Gaussian features

The 2D density plots contains information about the structure of vegetation in the image. To condense this information into feature values suitable for use in a weed pressure predicting model, the following Gaussian features were applied. Each of the Gaussian features are defined in terms of a location $\vec{\mu}_k$ in the 5D vector space defined in section 4.1.2 and a set of acceptable deviations σ_k (one for each dimension) of the coordinates. For the edge segment pair $\vec{x}_l$ and $\vec{x}_m$ the function $f(\ldots)$ calculates the increment of the k'th Gaussian feature.

$$f(\vec{x}_l, \vec{x}_m, \vec{\mu}_k, \sigma_k) = \exp\left(-\left|\frac{\vec{h}(\vec{x}_l, \vec{x}_m) - \vec{\mu}_k}{\sigma_k}\right|^2\right) \tag{4.4}$$

where σ_k is a diagonal matrix with coordinate weights along the diagonal and $\vec{h}(\vec{x}_l, \vec{x}_m)$ is a description of position and orientation of the m'th edge in relation to the l'th edge.

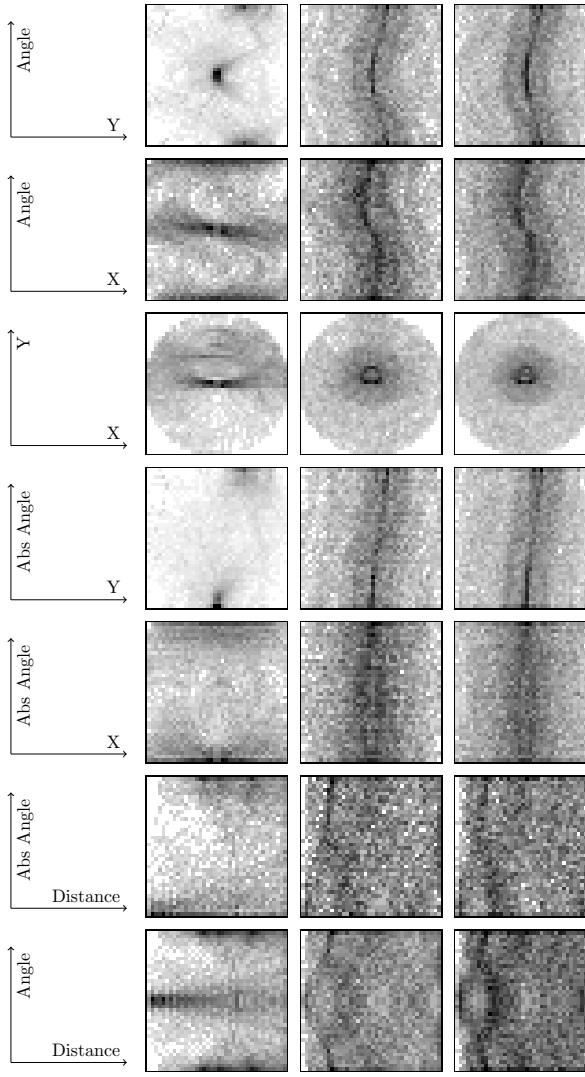

Figure 4.4: *Projected density plots. Each row consists of a description of the used axes and three density plots based on images of crop only, both crop and weed and weed only. The analyzed images are shown in figure 4.5. Axis limits are given in table 4.1.*

The edge segment l, is compared to all edge segments within a threshold distance (in $neigh(l)$). The contribution of the l'th edge segment to the Gaussian feature is given by.

$$dF(l, \vec{\mu}_k, \sigma_k) = \sum_{m \in neigh(l)} f(x_l, x_m, \vec{\mu}_k, \sigma_k) \tag{4.5}$$

The full Gaussian feature value is then defined using the sum

$$F_k = \frac{1}{n} \sum_{l \in E} dF(l, \vec{\mu}_k, \sigma_k) \tag{4.6}$$

where n is the number of edge pairs with a distance less than 125 pixels.

4.1.5 Estimation of weed pixel percentage

Given the Gaussian features calculated in section 4.1.4 the weed pixel percentage is estimated with the linear model

$$w = \sum_{k=0}^{5} a_k \cdot F_k \tag{4.7}$$

The value of F_0 does not depend on the analysed image and is set to one.

4.1.6 Generation of test images

To train the system a large set of training images with known weed coverages are required. It is not feasible to annotate enough images by hand, so a set of constructed test images with known weed densities were generated. Each image was generated by placing random examples of crop and weed plants in the image. Some examples are shown in figure 4.5. The random plant examples were taken from a set of manually segmented images. By tracking the number of vegetation pixels from crop and weed templates the true weed density was determined.

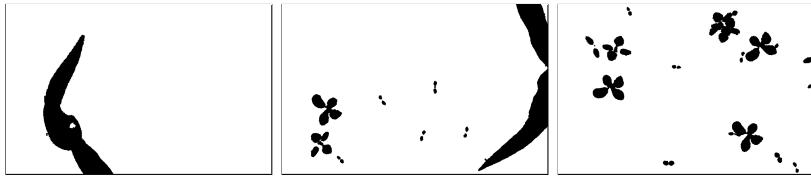

Figure 4.5: *Examples of test images with weed coverage percentages of 0%, 19% and 100%.*

4.1.7 Training of the system

Training of the system consists of choosing a set of Gaussian features and a linear relation between the Gaussian features and the weed coverage percentage. Each Gaussian feature is described by a vector $\vec{\mu}_k$ and position uncertainties $\vec{\sigma}_k$ in the 5D space spanned by x, y, $dist$, θ and $|\theta|$. Instead of selecting the Gaussian features by hand, a brute force approach were chosen. A large set of Gaussian features were sampled from from a uniform distribution of points within the limits given in table 4.1 and with position uncertainties in the range $[5, 1000]$.

Feature values for the set of sampled features were calculated for all the test images. The five best Gaussian features for predicting the weed pressure in the training set were selected using a heuristic hill climbing method.

4.2 Results and discussions

This section presents results based on training Modicovi on a set of test images and testing the algorithm on the same set of images.

4.2.1 Feature selection

A set of 1000 test images were generated. For each test image the weed density is known. Similarly a set of 1000 Gaussian features were generated by sampling. For every test image all Gaussian features were calculated and stored as intermediate results. The five best Gaussian

features for estimating the weed density were found using a heuristic method. The position and uncertainty describing the Gaussian features are listed in table 4.2 and 4.3 and the related feature weightings α_k are listed in table 4.4.

The relation between estimated and true weed coverage is visualized in figure 4.6. R^2 values for the training and the validation set are 0.7623 and 0.7843 respectively.

k	θ	dst	x	y	$\lvert\theta\rvert$
1	118.4331	46.6759	48.9991	39.9160	7.3202
2	-95.6296	18.9219	13.7717	102.8588	21.2321
3	-8.2292	8.9513	-30.6901	-0.1807	50.3614
4	-14.9098	44.5021	-34.4460	-57.6941	53.7109
5	-24.1421	104.5940	-65.5361	13.7205	77.9058

Table 4.2: *Locations $\vec{\mu}_k$ of the five selected Gaussian features.*

k	θ	dst	x	y	$\lvert\theta\rvert$
1	665.6258	645.2558	71.9448	655.9676	37.7467
2	24.8503	9.0433	36.6404	97.1721	92.5668
3	117.1818	12.9288	813.1579	17.5869	27.3123
4	6.5739	33.0036	531.1982	89.5006	312.9555
5	133.6098	437.9738	230.6548	760.5225	18.5108

Table 4.3: *Widths $\vec{\sigma}_k$ of the five selected Gaussian features.*

4.2.2 Analysis of test image

The image shown in figure 4.2 was taken through the process described in this chapter. Table 4.4 lists the five Gaussian feature values that were derived from the edge image. By addition of the weighted features, a weed coverage percentage of 31% were found. The image contains 2517 pixels from dicots / weeds and 8770 pixels from maize, which gives a weed percentage of 22.3%.

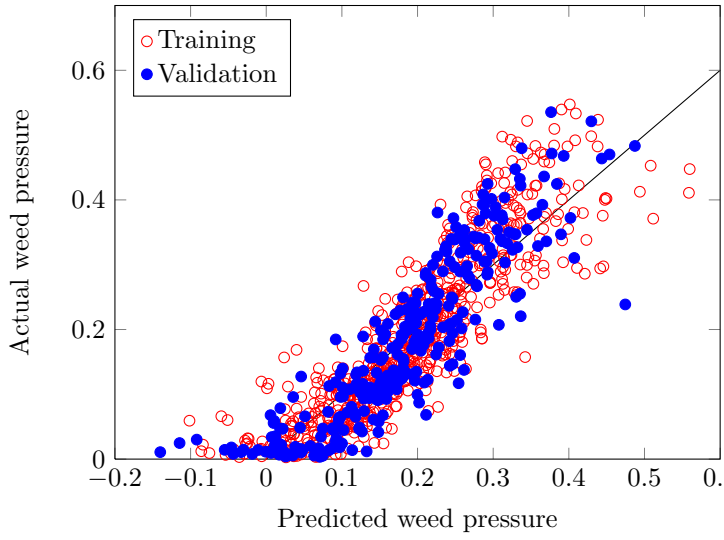

Figure 4.6: *Correlation between actual and predicted weed percentage.*

4.3 Summary of weed pressure estimation

A method, Modicovi, that can estimate the dicot weed coverage in maize fields have been described and tested. The method can handle images with occluded plants which is often seen under real world conditions. Test images are generated by overlaying crop and weed models. The weed pixel percentage is used for quantifying the weed pressure. Modicovi can estimate the weed pixel percentage, the estimate is strongly correlated with the true weed pixel percentage. While the principle of Modicovi seems promising there is still room for significant improvements. Alternative measures derived from the relative edge locations could improve the accuracy of the generated estimates.

k	$1000 \cdot F_k$	a_k	$1000 \cdot F_k \cdot a_k$
0	1000.000	0.5149	514.9
1	141.891	-1.9318	-274.1
2	0.977	180.8226	176.7
3	7.491	1.5482	11.6
4	2.533	-8.6629	-21.9
5	61.112	-1.5241	-93.1
			314.0

Table 4.4: *Gaussian feature values F_k derived from the test image. Feature weights, a_k, are multiplied with the feature values and the resulting numbers are summed op. The sum is the estimated weed percentage.*

Chapter 5

Locating individual leaves

The traditional methods for plant recognition devised by Guyer et al., 1986 and Weis et al., 2007 assumes that plants do not occlude each other. This assumption is seldom valid under real world conditions, where plants often occlude each other. If not compensated for, occlusions will reduce the correct classification rate when recognizing plants and the position of plant centres will be determined with large errors.

The problem of occluded plants can be handled with different methods which are listed below:

1. Models of the plant shape that can be fitted to parts of the boundary. Active shape models described by Persson et al., 2008 is one example of this approach.
2. The individual plants can be ignored and the average weed pressure can be estimated in the entire image, this was covered in chapter 4.
3. Extraction and analysis of plant parts that are not occluded.

A few authors have addressed method 3 from the list above, a summary of their contributions is given here. Franz et al., 1991 extracted leaves

Figure 5.1: *Left image: Bispectral image in false colours used for leaf detection. Right image: Segmented version of the left image.*

from plant boundaries of free standing seedlings of velvetleaf (*Abutilon theophrasti*), ivyleaf morning glory (*Ipomoea hederacea*), giant foxtail (*Setaria faberi*), and soybean (*Glycine max*). When several plants occluded each other this method failed to extract individual leaves. Detection of individual leaves in colour images were addressed by Neto et al. (2006) and Tang et al. (2009). Neto et al., 2006 extracted individual leaves based on their colour and texture using Gustafson–Kessel clustering. Tang et al., 2009 detected individual leaves by combining watershed segmentations based on intensity, hue and saturation.

This chapter describes two methods for extracting individual leaves in a segmented image. The methods were developed for targeting seedling leaves of sugar beets in the early growth stages (up to BBCH14), an example is shown in figure 5.1. When leaves have been detected, their position and shape can then be analysed. This information can be used to recognize the plant species or determine where the plant stem is located. Information about crop plant locations are vital for mechanical weed control methods that operates in the crop row, as they have to stay clear of the plant stem.

5.1 Materials and methods

Image acquisition is described in section 5.1.1. Section 5.1.2 describes a method for locating individual leaves based on leaf boundary curvature and a subsequent search for a leaf stem. A method based on the convex hull concept is presented in section 5.1.3. The leaf cut off points suggested by the two methods can often be improved by local search, section 5.1.4 describes such a method. The last section presents a method that use the position of detected leaves to estimate position of the plant stem emerging point.

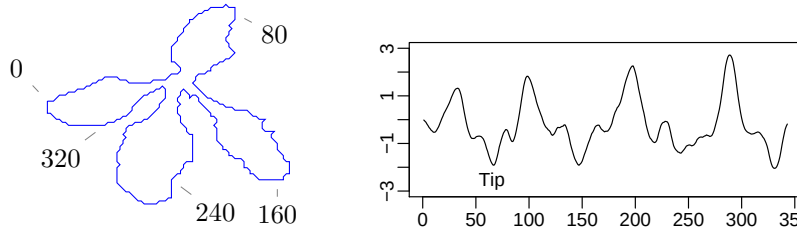

Figure 5.2: *Example input plant shape with markings indicating the clockwise tracking of the boundary and the associated curvature. Minima in the curvature measure indicates leaf tips.*

5.1.1 Image acquisition

Bispectral images of sugar beet seedlings were acquired with the Robovator and segmented by thresholding the resulting NDVI image. Pixel width and height were 1.1 mm. For more information about the image acquisition setup and the curvature based leaf extractor see paper III.

5.1.2 Curvature based leaf detection

The curvature based leaf detector is a two stage algorithm for locating leaves. Each stage is based on one of two characteristic properties of leaves:

- The tip of a leaf is convex with a high curvature.
- The leaf is attached to the remaining part of the plant with a thin stem.

In stage 1 probable locations of leaf tips are found by analysing curvature of the plant boundary. In figure 5.2 an example plant shape is shown together with a measure of the perimeter curvature. Negative values indicate convex regions where the boundary curves towards its interior like a circle, leaf tips candidates are located on local minima in the estimated curvature. Positive values refers to concave regions

which often are found near the plant stem or when leaves occlude each other.

In stage two the probable leaf tip locations are examined individually. From the leaf tip a search for a thin leaf stem is initiated. If a thin stem is located, a leaf is detected.

5.1.3 Convex hull based leaf detection

The convex hull based leaf detector will locate things that stick out from the contour of an object. An example of the process is shown in figure 5.3, references to the subfigures are placed in parenthesis. The first step is to calculate the convex hull of the input contour, this corresponds to placing a rubber band around the plant contour (A). Sticking to this rubber band metaphor, the next step is to make the rubber band follow the perimeter more tightly, as shown in figure (B), this is achieved by pinning the rubber band to certain locations on the contour. These locations are identified by locating the point on the contour that has the largest distance to the corresponding part of the rubber band (C). If this distance is larger than a certain threshold distance the rubber band is pinned to this location. This process of pinning the rubber band at certain locations on the boundary is repeated as long as points with a distance to the nearest rubber band is above the threshold.

Pin locations tend to gather near the plant centre. The boundary between two pin locations will often contain a single leaf. A local search, as described in section 5.1.4, is then used to find the best leaf cut off locations. To detect and remove false leaf detections, the ratio

$$L_s/L_p \tag{5.1}$$

is computed and compared to 0.3. L_s is the distance between leaf cut off points and L_p is the length of the perimeter between the cut off points. If the ratio is above this threshold the leaf is discarded, otherwise a leaf has been detected. The threshold value of 0.3 was chosen empirically.

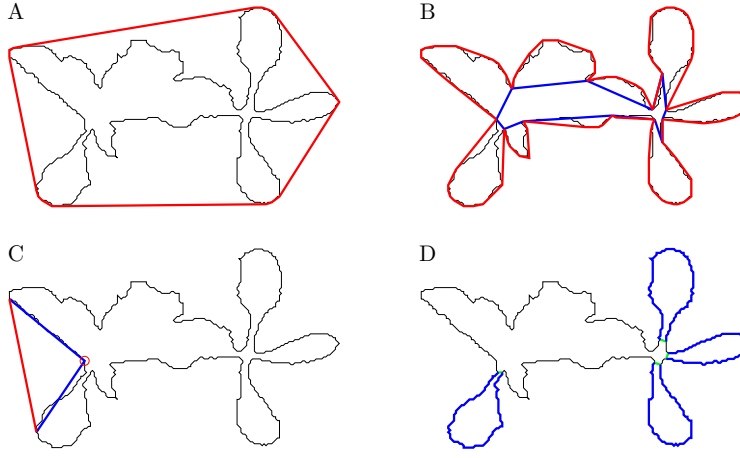

Figure 5.3: *Examples of steps in the convex hull leaf detector. A) Initial configuration of the rubber band with no pinnings to the contour. B) Final state of the rubber band after the rubber band were pinned to the contour at eleven locations. C) Location of one of the pinning points. D) The four detected leaves marked with blue.*

5.1.4 Improving leaf cut off positions by local search

The two described methods produces each a list of two points that describe where a leaf can be cut out of the input boundary. For post analysis it is preferred that the leaves are cut off as close to the plant centre as possible. This makes it easier to recognize leaves based on their shape and to derive accurate information about plant centres. To improve the leaf cut off points for a specific leaf, the the following quantity is maximized using local search.

$$\alpha \cdot L_p - L_s \tag{5.2}$$

The value α is the weight of maximizing the perimeter length compared to minimize the stem width, values near 0.7 were found to give the best results. The examined neighbourhood consists of all combinations of moving both leaf cut off points at most two steps forward or backwards. When the local search reaches a local maxima the search is stopped. Location of leaf cut off points before and after the local search is shown in figure 5.4.

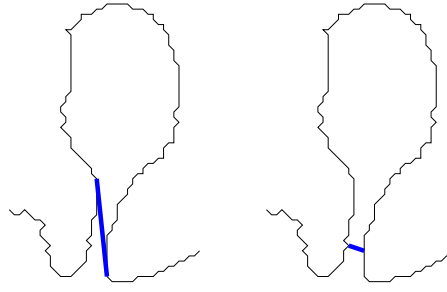

Figure 5.4: *How local search improves the leaf cut off points by minimizing the distance between cut off points and maximizing the perimeter length between cut off points. The initial cut off location is shown on the right and the final location is shown on the left.*

5.1.5 Estimation of plant stem emerging points

The located leaves can be used to estimate the position of the plant stem emerging point (PSEP) as described in paper III. The position and orientation of a detected leaf is described in terms of its centre of mass C and the midpoint S between the two leaf cut off points, this is illustrated in figure 5.5. The true PSEP locations were marked manually and the position of the PSEPs relative to detected leaves were modelled by the multivariate normal distribution described by the parameters $\vec{x}_{lc}$ and Σ_{lc}:

$$p(\vec{x}) = \frac{1}{2\pi\,|\Sigma_{lc}|} \exp\left[-\frac{1}{2}(\vec{x}-\vec{x}_{lc})^T \Sigma_{lc}^{-1}(\vec{x}-\vec{x}_{lc})\right] \tag{5.3}$$

where $\vec{x}_{lc}$ is the average stem location in the leaf coordinate frame and Σ_{lc} is the covariance matrix that describes the uncertainty in the stem location. The ellipses in figure 5.5 are contour lines of $p(\vec{x})$. The probability of finding the PSEP inside the ellipses are 68%, 95% and 99.7% respectively.

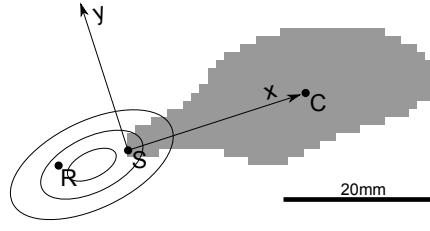

Figure 5.5: *Model for plant stem location in leaf frame. The ellipses are contour lines for the probability density function that contains 68%, 95% and 99.7% of the volume under the probability density function.*

When two leaves were detected on the same plant the position and orientation of both leaves were used to estimate the location of the PSEP. Information from both observations were combined by multiplying the probability distributions:

$$p_C(\vec{x}) \propto p_A(\vec{x}) \cdot p_B(\vec{x}) \tag{5.4}$$

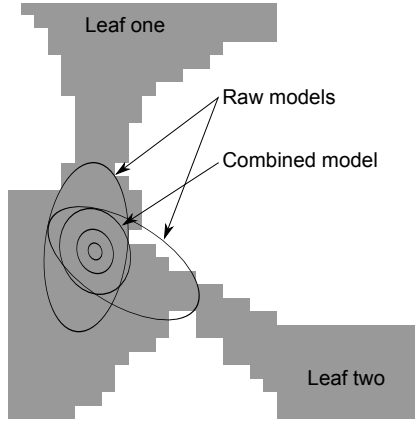

Figure 5.6: *Two root models can be combined by multiplying their underlying probability distributions, this leads to a better estimate of the plant stem emerging point. Contour lines for the involved probability distributions are shown with ellipses. Observe how the probability distribution of the combined root model is more condensed than the two original root models.*

This process is visualized in figure 5.6, the ellipses indicate contour lines as in figure 5.5 where the 68% and 95% contour lines are not shown for the detected leaves. Equation (5.4) can be generalized to an arbitrary number of leaves by increasing the number of probability density functions that are multiplied on the right hand side.

5.2 Results and discussions

The two leaf detectors were tested under varying conditions. Leaf detector performance is evaluated in section 5.2.1. Accuracy of plant centre location based on detected leaves are given in section 5.2.2. Finally are the use of leaf shapes for plant recognition discussed in 5.2.3.

5.2.1 Detection of individual leaves

The methods based on curvature and convex hull for detecting individual leaves were used to locate leaves in a test image. A part of this image is shown in figure 5.1. 200 well defined leaves with no occlusion of other leaves were manually located in the image. The number of detected leaves for both detectors are shown in table 5.1. The two first leaf detectors each found around 40 leaves that were not well defined, this is marked as false positives in the table. More than 82% of the well defined leaves were found by these detectors. To decrease the number of false positives the threshold for accepting leaves according to equation 5.1 were reduced to 0.1. This removed a large fraction of the false positives from the detector but also removed some of the well defined leaves.

Method	# Leaves	Real leaves	False positives	Running time
Curvature	200	165	35	2.9 s
Convex hull (0.3)	230	189	41	1.0 s
Convex hull (0.1)	140	133	7	1.0 s

Table 5.1: *Number of detected leaves, false positives and running time of the leaf detector methods.*

5.2.2 Estimation of plant stem emerging points

The model for root locations relative to the detected leaves were estimated based on 223 observations of detected leaves and the associated plant stem emerging point location. The model parameters for sugar beet seedlings at the BBCH12–14 growth stage were found to be

$$\vec{x}_{lc} = \begin{pmatrix} 5.40 \\ 0.24 \end{pmatrix} mm \qquad \Sigma_{lc} = \begin{pmatrix} 12.65 & 1.28 \\ 1.28 & 2.35 \end{pmatrix} mm^2 \tag{5.5}$$

The detected leaves in three test images were used to estimate the true PSEP locations. By comparing the estimated PSEP locations with the manually marked ground truth values, the estimation error could be investigated. Figure 5.7 shows the fraction of estimates with an error larger than a certain threshold distance. Estimates based on a different number of detected leaves are shown. When two or more leaves of a

plant were detected the plant stem emerging point could be located with an average error less than 1.9 mm. The average error rose to 3.3 mm when information from a single leaf were used to estimate the plant stem emerging point. These errors should be compared to what can be achieved by plant mapping systems based on RTK GPS. Sun et al., 2010 found that 95% of transplanted plants were within 51 mm from the mapped location. The position error of GPS located plants are thus an order of magnitude higher that the error from the leaf detection method.

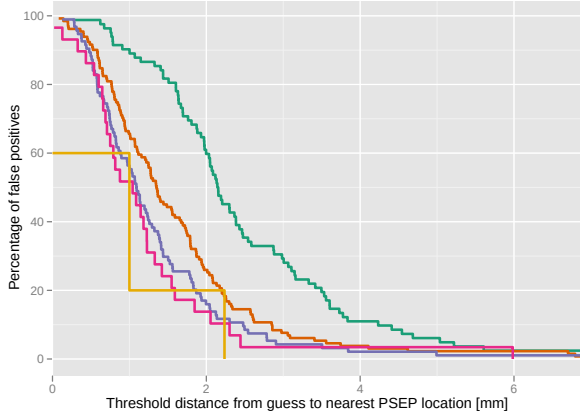

Figure 5.7: *Distance from estimated PSEPs to the nearest real PSEP location. The line colours indicate the source of the PSEP estimates.* ■ *one leaf,* ■ *two leaves,* ■ *three leaves,* ■ *four leaves and* ■ *manual annotation. Estimates based on two or more leaves are almost as accurate as the manual annotation.*

5.2.3 Classification of individual leaves

Detection of individual leaves can be used to recognize plants in occluded scenes. Several researchers have already addressed the task of recognizing plant species based on leaf shapes (Hearn, 2009; Du et al., 2007; Camargo Neto, 2005).

The main advantage of recognizing plants based on their leaf shape compared to the shape of the entire plant is a drastic reduction in shape variations. The shape variations of sugar beet seedlings were investigated with active shape models by Persson et al., 2008. An active shape model consists of a mean shape and a number of *modes of variation*. The five modes of variations that best explains the observed plant shapes are shown in figure 5.8. Four of the five modes are related to variations in leaf positions between cotyledons and true leaves.

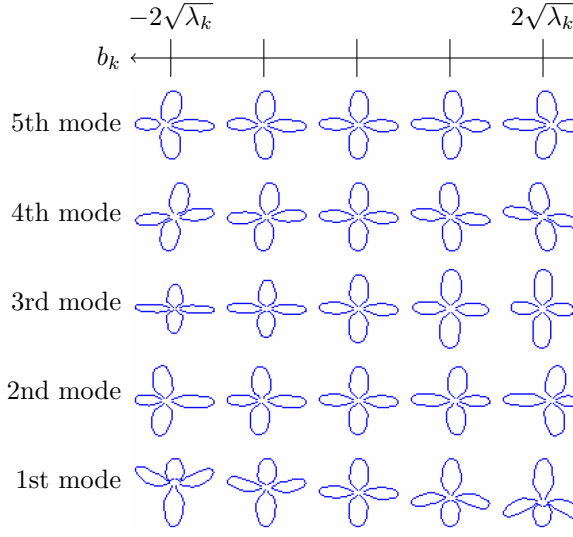

Figure 5.8: *Leaf shape variations of sugar beet seedlings. Notice that a majority of the modes of deformation are related to variations in leaf positions. From Persson et al. (2008).*

5.3 Summary of locating individual leaves

Automatic location of individual leaves in an image containing several plants is one approach to handle occlusion. Two methods for leaf extraction has been described, one based on boundary curvature and the other based on convex hulls. Both methods were able to detect more

than 82% of the non occluded leaves in test images.

Extracted leaves were used to estimate the location of plant stem emerging points. The average error of the estimated positions were 3.3 mm when position and orientation of a a single leaf was used for the prediction. When two or more leaves were used the average error got below 1.9 mm.

The use of extracted leaves for plant recognition seems promising. The variation in shape is significantly smaller for individual leaves than for whole plants. Leaf based recognition would also be a better approach to identify partially occluded plants

Chapter 6

Microsprayer

When the crop and weed plants in an area have been located, it is time to use this knowledge to control the weeds without harming the crops. One approach for control of individual weed plants are microspraying. A microsprayer system that can target individual weed seedlings is described in this chapter. The system utilizes visual tracking of plants to estimate the current speed and relies on shape based classification to distinguish between crop and weed plants. The efficiency of the microsprayer were tested under various conditions and the results are presented at the end of the chapter. The system is described in detail in paper IV which covers the first set of experiments.

Microsprayer systems for in–row weed control were first described by Lee et al. (1999). The system could distinguish between tomato and weeds and target individual plants recognized as weeds. The sprayer moved at a velocity of 0.33 m/s relative to the plants and sprayed 47.6% of the weeds and 24.2% of the tomatoes. Lamm et al., 2002 presented a system for controlling narrow leaved weeds in cotton fields. Søgaard et al., 2007 examined the application accuracy of a microsprayer system. The microsprayer had 20 nozzles placed with a distance between neighbouring nozzles of 5 mm. The system aimed at circular targets with an area of 110 mm^2 and hit on average 2.6 mm from the centre of the target. A system for controlling volunteer potatoes using a coarse microsprayer system were built by Nieuwenhuizen et al., 2010b.

Figure 6.1: *Example image from the vision system. Hard shadows and specular reflections were avoided by the use of indirect illumination.*

6.1 Materials and methods

The materials and methods sections presents the basic components of the microsprayer system and how the system was tested. Additional information about the sprayer system and the small scale testing can be found in paper IV.

6.1.1 Image acquisition and spray system

Image acquisition were performed with a CMOS camera (PixeLINK PL-B742F-R). The field of view covering an area of 140 mm × 105 mm with a resolution of 800 pixels × 600 pixels. The area were illuminated indirectly by 18 3 W white LEDs (ProLight PG1X-3LXS-SD) to avoid specular reflections and hard shadows. An example image from the vision system is shown in figure 6.1.

The spray system was based on a Willett 3150 Si/800 inkjet printer head, which were designed to print text on cardboard boxes in an industrial environment. Six spray nozzles, placed 10.5 mm apart, were used in the experiment. The distance between the spray nozzles and the soil surface was approximately 100 mm.

6.1.2 Motion estimation

The time between a spray command is sent to the spray system and the spray liquid hits the target, is a fixed delay, which has to be taken into account. In practice this means that the vision system needs to predict when a certain object gets below one of the spray nozzles and issue the spray command such that the spray liquid hits the target. Accurate predictions rely on knowing the current motion. The acquired images were scaled down and converted to monochrome images. The motion between two images were determined from the cross correlation between the two images.

6.1.3 Plant recognition

Each green object detected by the vision system had its shape described in terms of its area and the seven Hu moments. The Hu moments are shape descriptors that are invariant to scale, rotation and translation (Hu, 1962). A nearest neighbour classifier (Bishop, 2007) using the shape features were used to distinguish between crop and weed plants. More details about the classifier can be found in paper IV.

6.1.4 Small scale testing

In the first test, the vision and microsprayer system were mounted on top of a conveyor belt. Maize (*Zea mays L.*) were used as a crop model. Oilseed rape (*Brassica napus L.*) and scentless mayweed (*Matricaria inodora L.*) were used as weed models. All plants were at the BBCH10 growth stage and the classifier were trained on a few samples of all plant types. 1 L pots containing both crop and weed plants were placed on the conveyor belt and moved below the active microsprayer with a speed of 0.5 m/s. The spray liquid were water mixed with RoundUp Bio (Monsanto Europe) with a concentration of 5 g/L. The experimental setup and some of the plants used in the experiment is shown in figure 6.2. The growth stage of the treated plants were evaluated visually two weeks after the microsprayer treatment. At the same time the plant fresh weights were measured of the oil seed rape plants.

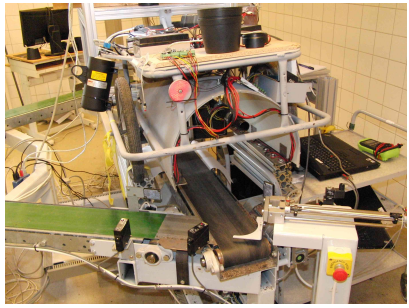


Figure 6.2: *The microsprayer test setup and some of the plants used in the small scale experiment.*

6.1.5 Large scale testing

The goal of the large scale testing were to gain information about how different parameters affected the performance of the microsprayer system. Answers for the following questions were sought. Does the plant density affect the ability of the system to hit the plants? How fast can the sprayer move and still hit the plants reliably? Is a high concentration of glyphosate in the spray liquid required?

The camera and microsprayer were mounted inside a bicycle trailer during the test. The complete system were then dragged over the plants that should be treated, this setup is shown in figure 6.3. Three different velocities (0.25 m/s, 0.5 m/s and 0.7 m/s) were used for the experiments. The spray liquid was water mixed with glyphosate. Two different concentrations, 5 g/L and 20 g/L, of the active compound were used. The spray system was tested on nightshade (*Solanum nigrum*) seedlings at the BBCH12 growth stage. 24 seedlings were placed in the pattern shown in figure 6.4, the first 12 seedlings had an approximate density of 100 plants per square meter and the remaining 12 had a density of 300 plants per square meter.

During the microsprayer treatment, the spray control computer logged all analysed images, all planned spray events and when each spray command were sent to the microsprayer. The idea with the logging system were to investigate cases where the system had failed to deposit

Figure 6.3: *The microsprayer setup used for the large scale experiment. Bicycle trailer equipped with the sprayer system is ready treat the plants in the black plant trays. Three trays with plants in a low density pattern is placed nearest the sprayer while an single tray with high plant density is at the bottom of the image.*

glyphosate on seedlings. It was then possible to investigate whether the system had failed to issue spray commands or had targeted the seedling but not hit it properly.

Immediately after spraying the seedlings were moved to 1L pots and placed in a green house. Three weeks after treatment the plants were harvested and their fresh and dry weight were measured.

6.2 Results and discussions

6.2.1 Small scale testing

163 plants in total were treated by the microsprayer system. The distribution of plants on the different plant types and the number of plants that followed the expected growth is presented in table 6.1. All maize

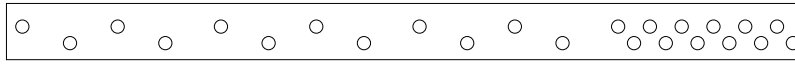

Figure 6.4: *Plant pattern for microsprayer testing. The twelve plants to the left is placed in a low density pattern with* $100\,\mathrm{m}^{-2}$ *while the remaining twelve plants had a density of* $300\,\mathrm{m}^{-2}$.

Plant	k	n	f	95% CI
Maize (crop)	33	33	1.00	[0.92; 1.00]
Scentless mayweed	48	76	0.63	[0.52; 0.73]
Oilseed rape (weed)	3	54	0.06	[0.01; 0.14]

Table 6.1: *Results of visual inspection of treated plants. k is the number of plants following the expected growth, n is the total number of plants, f is the fraction of normal growing plants and 95% CI is the 95% credible interval of f.*

plants followed the expected growth which indicate that the system did classify these plants as crops. The oil seed rape plants were effectively treated by the microsprayer as only 6% of the oilseed rape followed normal growth. The average size of the oilseed rape plant were approximately 11 mm by 14 mm The weight distribution of reference and treated oil seed rape plants are shown in figure 6.5.

The growth of 37% of the scentless mayweed plants were reduced. This reduced efficiency can partly be explained by the size of the plants. Some of the smaller plants cannot be hit by the sprayer as there is an approximate 8 mm wide strip between neighbouring spray nozzles in which no spray liquid is deposited. At the time of the experiment the leaf area of scentless mayweed plants were approximately 3 mm by 8 mm.

The small scale test showed that the system could distinguish between crop and weed plants in real time and effectively target and hit plants larger than 10 mm by 10 mm.

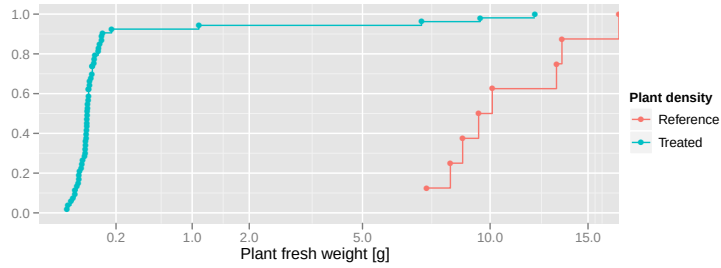

Figure 6.5: *Fresh weights of oil seed rape plants two weeks after microsprayer treatment. Only three plants had weights comparable to the reference population while 51 had weights significantly below.*

6.2.2 Large scale testing

In the second evaluation of the system 672 plant seedlings were treated by the microsprayer . The log files contained information on every activation of the spray system. By comparing the logged spray activations with the plant pattern shown in figure 6.4, the location of each of the plant seedlings were marked. Each location was specified by a time of passage and the nozzle position the seedling passed under. Then the number of spray activations were counted for each plant. The relation between the forward velocity and the number of spray activations is visualized in figure 6.6. The number of spray activations is seen to be inverse proportional to the forward velocity although the individual variations are large for the lowest velocity.

A direct measure of the effect by the microsprayer treatment is the plant fresh weights. The distribution of plant weights under different experimental conditions are shown in figure 6.7. The weight distribution of the reference plants is visualized as the black line. For velocities of $0.25\,\mathrm{m\,s^{-1}}$ all plants had a fresh weight lower than 9 g which is equal to or lower than all the reference plants. A general observation is that the ability to control growth of plants is reduced when the velocity is increased and the glyphosate concentration is reduced.

While figure 6.7 gives information about the average performance of the system it does not explain why some of the plants were not affected

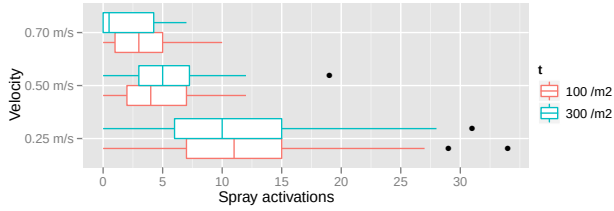

Figure 6.6: *Relation between forward velocity and number of spray activations. When the velocity is increased, the number of spray activations decreases.*

by the microsprayer treatment. Based on information in the log files, the set of plants that activated the spray system was found. The set contained 90% of the treated plants and their weight distributions are shown in figure 6.8. Nearly all the plants that activated the spray system had significantly reduced fresh weights. Why 10% of the plants did not activate the spray system is still not known.

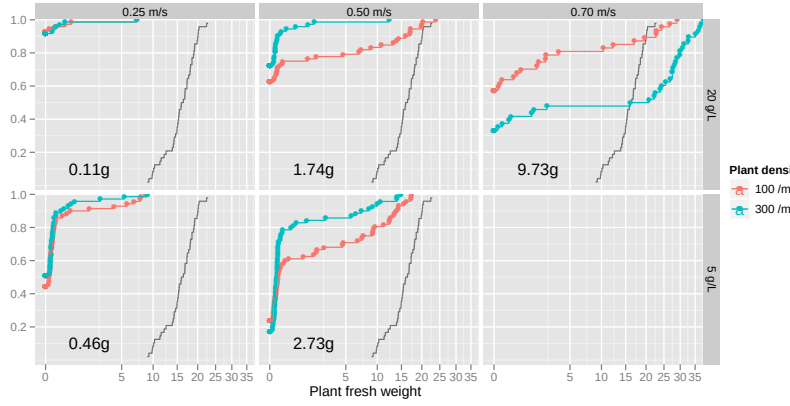

Figure 6.7: *Weight distributions of treated plants shown as Empirical Cumulative Distribution Functions (ECDFs). The reference population is shown in black. The numbers in the lower left corner of each plot is the average plant fresh weight of all plants exposed to this treatment.*

Some images of the plants three weeks after the spray treatment are shown in figure 6.9. All plants in the reference groups had reached growth stage 23-25 according to the BBCH scale (Hess et al., 1997). Only a small set of the treated plants had reached this growth stage. Most of the plants had a size similar to the size at the time of spraying.

6.3 Summary of microsprayer

A microsprayer system have been implemented, it consists of 6 nozzles that can be activated independently of each other. A vision system estimates the motion and plan spray actions based on plant position and shape. First the system was tested on 163 plants of three species, two weed models and one crop model. 1L pots containing examples of all three plant species were moved below the microsprayer system at a velocity of $0.5\,\mathrm{m\ s^{-1}}$. All crop plants were unaffected by the treatment while 94% of the oilseed rape seedlings were killed or had their growth significantly delayed.

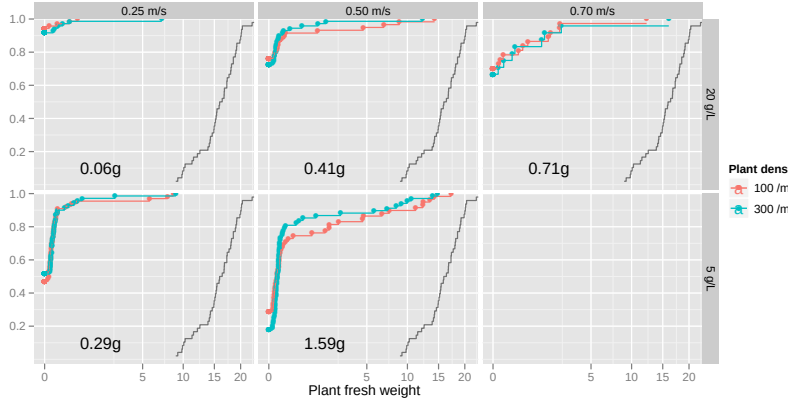

Figure 6.8: *Weight distributions of the plants that activated the spraying system. The plants have a significantly lower weight than the group of treated plants.*

Figure 6.9: *Reference plants (left) and a fraction of the treated plants (right). Most of the treated plants were eradicated, only a few survived the treatment.*

To investigate how the microsprayer system reacted to changes in different system parameters like velocity a more detailed evaluation was conducted. Black nightshade were used in the test where 672 plants were treated by the microsprayer system. Roughly 90% of the plants activated the spray system. The evaluation revealed that when the system was activated it hit the targeted plant.

Chapter 7

Localized feature based classification

Plant recognition can be based on different kinds of information. A system that uses shape or spectral features for crop plant recognition relies on a training set consisting of examples of typical crop and weed plants. The best performance of such a system is when the training set are representative of the group of plants that should be classified. It is not feasible to gather samples from all possible scenarios due to a huge number of combinations of different growth stages, soil conditions, availability of water and others. Even if such an *all circumstances* training set were acquired large in–class variations would lead to low recognition rates (Feyaerts, 1999). This chapter investigates an alternative set of features, context features, which are based on relative plant locations and knowing the structure in which plants are sown.

The idea is to mimic the mental process of a person placed in a random field, like shown in figure 7.1. Even if the person had never seen a field before, he would recognize the row structure and notice that some plants would appear at regular intervals in the row. The plants that follow this row structure are most likely crop plants while plants outside the structure are probably weeds. By looking for a known row structure, a system can automatically generate a training set for shape

based plant recognition based on observations in the field. This training process could be repeated several times during the weed control operation and the shape based plant recognition could then adapt to in–field variations in plant appearance.

Figure 7.1: *Row structure seen in sugar beets. For humans the task of recognizing what is in the row is easy. With some additional information about the row structure a computer can also handle this problem.*

Adaptive classifiers have been described earlier in the literature for crop recognition based on spectral signatures. Feyaerts (1999) used an imaging spectrograph to measure the reflection spectra of crop and weed plants. Spectra recorded in the row were marked as unknown while spectra of plants out of the row were marked as weeds. The spectra were grouped according to their similarity and each group were marked as either crop or weed. These automatically annotated spectra were then used for training a classifier that could distinguish between crop and weed plants.

Training and discrimination between sugar beets and volunteer potatoes using an adaptive classifier were presented by Nieuwenhuizen et al. (2010a). Input features for the classifier were colour indexes and texture descriptors. Objects near the row centre were used as crop examples and objects outside of the row were used as weed examples. Two first–in–first–out (FIFO) queues were used for storing 100 training examples of crop and weed objects respectively. The adaptive classifier was compared to a static classifier and the adaptive classifier performed significantly better than the non–adaptive classifier.

7.1 Shape based crop recognition

Recognizing plants based on their shape were introduced by Guyer et al. (1986). Guyer assumed that each image only contained a single plant

and calculated features describing the moment of inertia, elongation and complexity. With a set of 8 features they were able to distinguish between corn and non–corn with a 9% error rate. This approach to recognizing plants has got a lot attention (Lee et al., 1998; Tian et al., 1999; Hemming et al., 2001; Du et al., 2007; Weis et al., 2007; Weis et al., 2010). The list of suggested features is quite long but some general properties of the suggested features are that they

- Are invariant to translation and rotation.
- Are invariant to scale (not always required).
- Are weakly affected by small deformations (eg. leaf movements).
- Can be used to discriminate between two classes of interest (typical crop and weed).

The idea of training the classifier on a known set of crop and weed examples before entering the field leads to sub optimal plant classification results. The problem is that there is a large variation in the appearance of both crop and weed plants through the whole field. The variations in segments of the field is expected to be significantly lower.

7.2 Context based features

Instead of relying 100% on shape based recognition of crop plants, the shape information might be complemented with a different type of information which is less affected by changes in growth stage, soil conditions and similar. For crops planted in a row with a fixed distance between neighbouring crop plants, features based on the position of nearby plants have shown promising results (Åstrand et al., 2004).

An example of a context based feature is the position score introduced in paper V. The score is constructed such that plants in the row structure will get relative high position values while plants outside the row structure get low values. The position score of plant i when looking for

N neighbour crop plants is given by:

$$c_i = \sum_{m=1}^{N} \left[\max_k \exp\left(\frac{-||\vec{x}_k - \vec{x}_i - m \cdot \vec{d}||^2}{2s^2\sigma_x\sigma_y} \right) \right] \tag{7.1}$$

Where $\vec{x}_i$ is the position of the i'th plant, $\vec{d}$ is the expected distance between neighbouring crop plants and s is a twiddle factor. The position uncertainty of the crop plants along and perpendicular to the crop row is described by σ_x and σ_y.

7.3 Limitations on context based features

There is a direct limitation on the achievable crop recognition rate that can be reached with context features under certain conditions. Paper V introduces the normalized weed pressure λ. The normalized weed pressure depends on the weed density ρ (plants per square metre) and the deviation in crop plant positions from the expected crop pattern. The deviation is modelled with a normal distribution described by the uncertainty along the row σ_x and the uncertainty perpendicular to the row σ_y. Given these measures, the normalized weed pressure is given by

$$\lambda = 2\pi\rho\sigma_x\sigma_y \tag{7.2}$$

If the plant nearest to a known seeding position is classified as a crop, the probability that the classification is correct is described by the positive predictive values (PPV) given by:

$$PPV = \frac{1}{1+\lambda} \tag{7.3}$$

When the normalized weed density increases the accuracy of the context classifier is reduced. In the case were the location of the sowing pattern should be estimated from the data, the recognition rate will be lower. Simulations in paper V show that recognition rates can get close to

$$\frac{1}{1+2\lambda} \tag{7.4}$$

The relation between weed density, crop position uncertainty, normalized weed pressure and the upper limit on the context based crop recognition rate described by equation (7.2) and (7.3) is visualized in the nomogram presented in figure 7.2.

7.4 Local training of shape based classifiers based on context features

Shape based classification and context based crop recognition both have advantages and disadvantages, an overview of these is shown in table 7.1. Shape based classification works on the plant level (or even on the leaf level as suggested in chapter 5) and can thus recognize plants at high weed pressures. Shape based classification is vulnerable to variations in plant shape between the field and the training set. Due to local variations of plant shapes in the field, the use of a single training set for the entire field will lead to inferior performance. The main advantage of context features is that they are robust to variations in soil conditions and growth stage of crop and weed plants. The value of context features is decreased when the normalized weed pressure is increased. If a crop recognition rate above 95% is required, the normalized weed pressure must be below $\lambda \sim 0.05$.

Method	Pros	Cons
Shape	Independent on weed pressure	Shape variations
Context	Stability of features	Requires low weed pressure

Table 7.1: *Overview of advantages and disadvantages of classifiers based on either shape or context features.*

Examination of these properties leads to the conclusion that a combination of shape and context features for crop recognition could be more robust than systems relying on either shape or context features. If the context features could be used to train a shape based classifier given samples of plant shapes acquired a moment ago, the shape based classifier would be able to adapt to in–field variations in shape of crop and weed plants.

In the remaining part of this section two context trained are described.

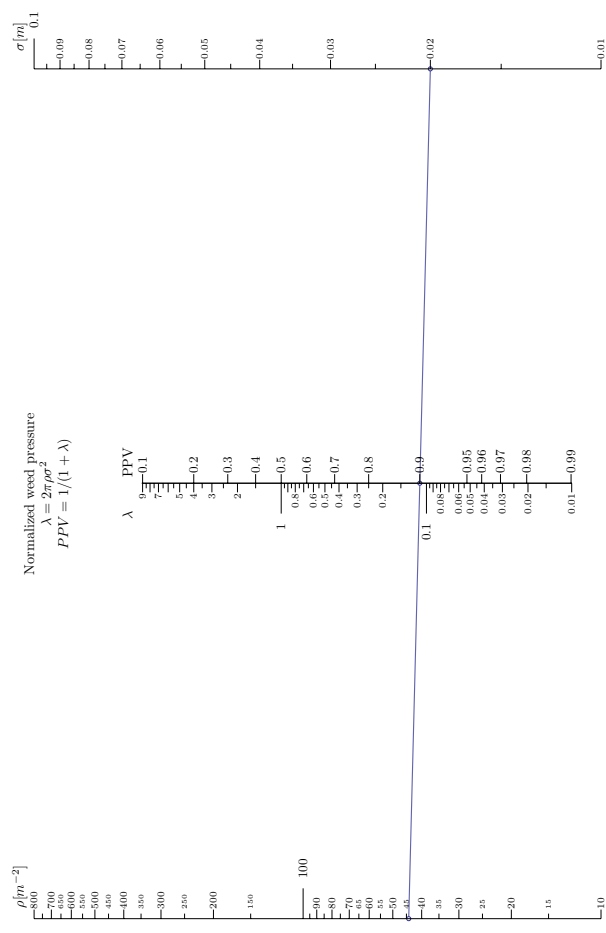

Figure 7.2: *Nomogram showing the relation between weed density ρ, crop position uncertainty σ, normalized weed pressure λ and the upper limit on the context based crop recognition rate. Calculations with the nomogram consists of connecting values on the three scales by straight lines. An example calculation is describe here. What is the highest weed pressure that can be allowed if a PPV higher that 0.9 is required and the crop plant position uncertainty is* 2 cm *(answer* $44.2\,\mathrm{m}^{-2}$*). Example calculation is shown in blue.*

The first is based on shape features and tested on constructed fields based on real plant images. The second classifier demonstrates the advantage of an adaptive classifier that can adjust to local variations.

7.4.1 Construction of training images

Test images were constructed based on samples of different plants. Oilseed rape at the BBCH12–13 growth stage were used as crop plants while cornflower at growth stage BBCH10–12 were used as weeds. 64 images of the crop and weed models were used for constructing the synthetic images. Crop plants were placed in a row structure with a fixed distance between neighbouring plants, this pattern were distorted by displacements sampled from Gaussian distribution with deviation σ in both x and y direction. A number of weed plants were spread uniformly across the simulated field.

7.4.2 Shape descriptors

The shape of plant objects were described with these features: area, elongation, length of major and minor axes derived from image moments and ten features based on a distance transform. The distance features were introduced by Giselsson, 2012 and are determined the following way. The distance from all pixels in the shape to the nearest boundary pixel is determined. All these distances are then sorted by value and 10 equidistant values are extracted as shape descriptors.

7.4.3 Context trained shape based classifier

An example of a shape based classifier is presented below. Given an input image the system locates plant objects and calculates position scores using equation 7.1 for each plant object. The plants with positions scores below the 20% percentile were marked as weed examples while the plants with positions scores above the 80% percentile were used as crop examples. A Naive Bayes classifier (as described in chapter 3) was then trained using shape features derived from these crop and

weed examples. Finally were the classifier applied to all plant object in the input image.

The training process of the classifier is visualized in figure 7.3. The figure contains the input image, the plants recognized as crops and weeds based on context features and classification results from the shape based classifier trained according to the context features. The normalized weed pressure of the test image was 0.2. Notice that both training sets contains elements from both the weed and the crop classes. These faults in the training set seems not to disturb the shape based classifier significantly.

7.4.4 Adaptive feature based classifier

A classifier which can adopt to local variations in weed population and plant growth stages can perform better than a globally trained classifier. A constructed example of this is shown in figure 7.4. The figure contains nine image segments and the segments should be concatenated such that segment A is followed by segment B, segment C and so on. The image contains a set of small rectangles that have different orientations. Each rectangle represents a single plant and the orientation of the rectangle corresponds to a shape feature derived from the plant. Weed plants have a random orientation while the orientation of crop plants is changing slowly. In addition crop plants are placed in a well defined row structure with a fixed distance between neighbour plants.

When the whole field is examined the distribution of orientations for crop and weeds will be identical, as weed orientations are drawn from a uniform distribution covering a half rotation and the crop orientations have gone through a half rotation. If the orientation is examined for each segment the two distributions will be quite different, the crop plants will now have a preferred orientation.

An adaptive classifier using the following training method were implemented. The original image were divided into segments with a width of 2000 pixels and for each segment the succeeding steps were taken. Position scores (as defined in paper V) were calculated for all plants. Plants with high position scores were used as training examples of crop plants and the remaining plants were used as weed examples. A Naive

Figure 7.3: *Example of a context trained shape based classifier working in an image with a normalized weed pressure of 0.2. A: Original image, B: Plants recognized as part of the row structure (high position score), C: Plants recognized as not being part of the row structure (low position score), D: Probability of belonging to the crop class based on shape features (black 100% and white 0%) indicates weed) and E: Thresholded shape based plant recognition.*

Bayes classifier (described in chapter 3) using the orientation as input were trained with these examples. The classifier were then used to recognize crop and weed plants in the next segment. The classification results are shown in figure 7.4 on page 89 where crops are marked by black and weeds by grey.

The test image contains 800 small rectangles of which 200 are crops and the remaining are weeds. The confusion matrix of the adaptive classifier is shown in table 7.2, the classification results from the first segment are not included. The classifier recognizes both crop and weed plants as crops, which is to be expected as some weed plants will point in the same direction as the crops. What is more interesting is the ability of the classifier to correctly recognize weeds. The accuracy of the adaptive classifier is 70.20%, which is significantly higher than the 50% that can be expected from a globally trained classifier.

	Crop	Weed
Crop	148	191
Weed	6	316

Table 7.2: *Confusion matrix for the adaptive classifier. Columns describe the correct class while rows indicate the classification result.*

7.5 Summary of localized shape based classification

Shape based features are often used to distinguish between crop and weed plants. Use of a single training set is not optimal due to in–field variations in plant appearance and growth stages. Features based on context information are less sensitive to variations in plant shapes and growth stages. When only context based information is used for recognizing crop plants, the correct recognition rate is directly related to the normalized weed pressure λ. When the normalized weed pressure increases, the recognition rate will decrease.

The idea behind a context trained shape based classifier was presented. Experiments showed that a shape based classifier can be trained from

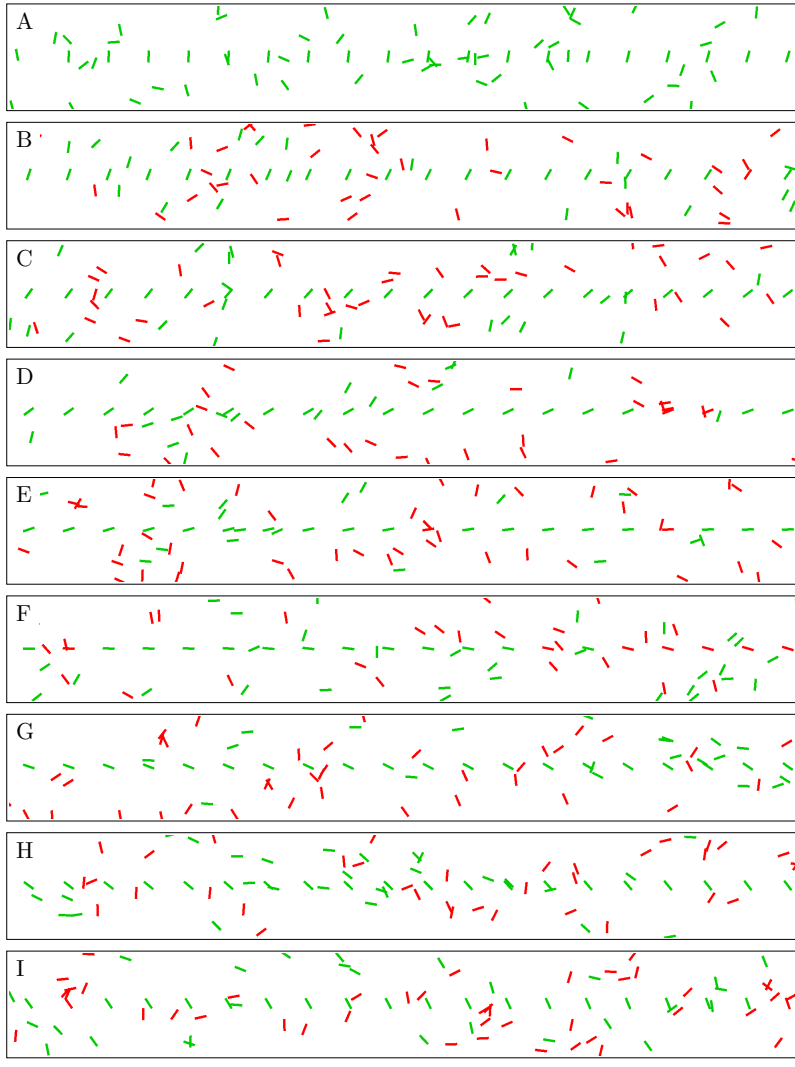

Figure 7.4: *Example of an adaptive classifier. Green indicates plants that are recognized as crops while red indicates weeds. The plants in one segment is used to train the feature based classifier used in the next segment. Notice how accurately the adaptive classifier can detect weeds.*

an example image and knowledge about the crop row structure.

A method for training a local adaptive shape based classifier was described. In the constructed example, the adaptive classifier performed much better than possible of a globally trained classifier. A globally trained classifier can only reach a classification accuracy of 50% on average and the adaptive classifier reached 70%. Although shape variations of plants in a field is probably lower than in the constructed example, an adaptive classifier can output perform a non–adaptive classifier most of the time.

Chapter 8

Discussion

The methods used for plant recognition and weed pressure estimation in this dissertation take segmented images as input, where regions of vegetation and background are clearly marked. There exists several methods that can generate segmented images. Thresholding of colour indices, like excess green and the normalized difference vegetation index, provides computationally cheap segmentations. The quality of these segmentations depend strongly on the used image acquisition system. Segmentation based on the Naive Bayes classifier is computationally a more expensive process than thresholding methods. The benefit is that the system can be trained to generate high quality segmentation under many different conditions. For speeding up the process look up tables (LUTs) is a possibility. This solution will work when the LUT can be stored in random access memory (RAM). The size of a LUT for segmenting RGB images with 8 bit information per colour channel is $2^{8 \cdot 3}$ bits which equals 2 megabytes of memory. This can without problems be stored in standard RAM. If either the number of bits for each colour channel or the number of colour channels are increased, the memory requirements would grow exponentially and make the LUT approach infeasible. Minor modifications of the image acquisition system can, in some cases, simplify the segmentation task significantly. This can be modifications of the illumination system and protection from direct sun light. This is not an option under certain conditions and the

need for robust and adaptable segmentation methods arise.

Information about weed pressure in strongly occluded scenes can be extracted by examining the relative position and orientation of edge pairs in the scene. This process is implemented in the Modicovi algorithm. One measure of the weed pressure is the percentage of pixels in an image that contain weed plants, this is the weed pixel percentage. The weed pressure is not described directly by the weed pixel percentage. If the measure is combined with the number of vegetation in an image, it is straightforward to calculate the number of weed pixels. Computer generated test images were used for training and testing of Modicovi. It is not optimal to train an algorithm like Modicovi on synthetic images, but this approach was chosen due to the need of knowing the weed pixel percentage for each of the training images. A significant correlation between the actual weed pixel percentage and the estimated weed pixel percentage was found. This correlation can be explained by two mechanisms 1) that Modicovi has generalized the crop / weed concept and based on this can generate good estimates or 2) that Modicovi has learned some of the plant shapes in the training set. Based on the low number of Gaussian features used to calculate the estimates, it is unlikely that the system has learned all shapes in the training set. It is more likely that the system has generalised the typical plant shapes and thus can estimate the weed pixel percentage.

One approach for handling scenes with occlusions is to cut regions of vegetation in the basic building blocks, leaves. The two methods for leaf detection, described in chapter 5, are based on some basic assumptions of how typical leaf shapes are formed. The curvature based leaf detector will only detect leaves that have a mainly convex shape near the leaf tip and are attached to the rest of the plant with a thin stem. Similarly will the convex hull based leaf detector only find leaves which *pop out* from the blob of vegetation that is being analysed. An assumption about how a leaf is shaped is needed such that the computer knows what to search for. The large variation in leaf shapes of different plants is difficult to express in terms a computer can work with. The fractal structure of carrot leaves do not follow the assumptions and the leaves will probably not be detected reliably. A problem with the described leaf detectors is that they can only detect leaves which is connected to the rest of the plant in the segmented image. If a leaf is not connected, detection of

the leaf stem fails and the leaf is discarded. Tuning of the segmentation process is one way to reduce this leaf connectivity problem The best possible input for the leaf detector are images where all leaves of one plant are in the same blob of vegetation. If the segmentation process breaks single plants into multiple blobs, the leaf detector is unable to locate the free standing leaves, and information from them is therefore lost in the following analysis.

The task of selectively applying a spray liquid to individual weed plants was tested under lab conditions. In the small scale experiment the microsprayer performed satisfactory weed control of oilseed rape seedlings. This was repeated in the large scale experiment although the system failed to control around 10% of the plants. This is probably an issue related to the vision system but it is difficult to confirm as input data for the vision system was not logged during the experiment. When a plant was located by the vision system the microsprayer hit it reliably. This was observed for all the tested velocities. Velocities above 0.7 m/s was not investigated due to limitations in the test setup, but the accuracy of the system is expected to decrease when the velocity is increased. High amounts of motion blur in the captured images were observed at the larger velocities. Operation at velocities above the tested would probably require an upgrade of the illumination system, such that motion blur in the images can be reduced. The process of scaling up a microsprayer system from using a few nozzles to hundreds or even thousands is bound to be problematic. Vibrations with amplitudes larger than a few centimetres are often seen in farm machinery, such vibrations will disturb the microsprayer system significantly. The benefits of reduced herbicide usage and the possibility of using systemic herbicides might outweigh the problems. In addition it is difficult to control that the system performs as expected by the farmer. Treatment with a microsprayer leaves almost no traces that can be observed a few minutes after the treatment. Droplets of spray liquid are quickly absorbed by the plants and it takes days before the growth inhibiting effect of the herbicide can be observed. This is a problem for the initial adoption as the farmer will only invest in a microsprayer system if he believes that the system will work as expected.

Recognition of plant species based on shape information is a difficult task, that usually requires a large set of training samples. The best

recognition results are achieved when the training set is representative of the field in which the plants grow. The approach of generating a training set manually for each field is not feasible as generation of such a training set would usually require a large amount of human interaction. If the crop plants are placed in a recognisable structure a training set can be generated or updated without human intervention. The quality of the automatically generated training set depends strongly on the number of mislabelled samples in the set. The probability of correctly recognising a crop plant using information about the relative position of nearby plants is limited by the normalized weed pressure. Low values of the normalized weed pressure indicate that crop plants can be identified with a high accuracy based on plant positions and knowledge of the row structure. A context based classifier that is used to train a shape based classifier is an example of an adaptive shape based classifier. Adaptive classifiers can *learn* the local plant population and adjust to local variations in crop plant appearances and weed population. This flexibility lets adaptive classifiers perform better than similar shape based classifiers that are trained with samples representative of the whole field.

Chapter 9

Conclusion

The goal of this thesis was to investigate methods for computer vision tracking of plants under field conditions. The information derived from such computer vision systems can be used to control advanced weed control methods which can control weed growth effectively while reducing the environmental footprint of the weed control process significantly.

The first step in the plant tracking systems developed in this thesis is to distinguish between soil and vegetation. In the literature is this often handled by thresholding the Excess Green image or the Normalized Difference Vegetation Index image which can be derived from RGB images and red–nearinfrared images respectively. Usually is this approach adequate but under certain conditions, like hard shadows and colour saturation, they will often produce wrongly segmented images. A segmentation process based on the Naive Bayes classifier was described. The segmentation process was tested under varying conditions and was found to produce nearly flawless segmentations in all cases. The price for the improved segmentation is that it requires a larger amount of calculations than the segmentations based on thresholding. On some types of input images this can be speed up using look up tables and real time performance can then be reached.

A system for estimating the weed pressure in maize based on leaf shapes

was devised. Existing systems for this task assumes that crop and weed plants do not occlude each other, this assumption is seldom valid as crop and weed plants fight for the limited resources in the field. The system examines the vegetation image and locates plant contours. All edges in the image are examined and the relative location and orientation of nearby edges are calculated. The distribution of relative location and orientation of nearby edges forms a fingerprint of the structures present in the image. This fingerprint is invariant to rotations of the entire image and are only weakly affected by occlusion between crop and weed objects. By examining the fingerprint an estimate of the weed pressure can be derived. The correlation coefficient between the true weed pressure and the estimated weed pressure were 0.76. The method relies on a limited set of image operations that are available on a DSP platform, this allows a relatively easy porting of the method from a standard computer to an embedded platform. The goal of the system is to control a part of a sprayer boom such that the herbicide application is adjusted to the weed presence.

A different strategy for handling occlusion in images is to split the occluded plant objects into parts which are not occluded by other plants. For recognizing plant seedlings in occluded scenes it is obvious to examine individual leaves. Two methods for locating free standing leaves were implemented. They were both able to locate more than 82% of the well defined leaves in test images.

The shape of located leaves can be used to recognize the plant type. The variation in plant shapes is a combination of variations in leaf shapes and leaf positions. By analysing the shape of individual leaves, the variations in plant shapes can be split into the two earlier mentioned types of variations. As shape variations of individual leaves is less than shape variations in the whole plant, it is expected to make classification based on individual leaves more robust, but this was not investigated directly.

Location and orientation of the located leaves can be used to estimate the plant stem emerging point of sugar beet seedlings with a high accuracy. A Gaussian model of the location of plant centres in the leaf coordinate system was made. From information of a single detected leaf the average error of estimated plant centres is 3.3 mm. When two or more leaves are detected it is checked if their estimated plant centres

coincide and if this is the case the plant centre models are combined to get a better estimate of the plant centre. When observations from two or more leaves are used to estimate the plant stem emerging point the average error is less than 1.9 mm. Visual location of plants have thus an average error which is an order of magnitude lower than comparable GPS based systems.

A microsprayer system for controlling weeds at an early growth stage were developed. The microsprayer consists of 6 nozzles placed side by side covering distance of 6cm, each nozzle in the system can be activated independently of the other nozzles. An area in front of the microsprayer is monitored with a camera. When a green object gets into this region, its shape is analysed and is is classified as either crop or weed. If the shape is recognized as a weed, the spray system is activated when the weed passes under the sprayer. In the first test of the system pots with crop and weed models were moved below the microsprayer at a velocity of 0.5 m/s. The system were able to distinguish between oilseed rape and maize seedlings and activate the microsprayer at that velocity. None of the maize seedlings were harmed while 94% of the oilseed rape plants had their growth significantly reduced. A second test of the system where the camera and microsprayer were dragged over a row of weed models, this time the system were tested at velocities in the range 0.25 m/s to 0.7 m/s. This time extensive data logging under the experiment were performed such that the reason why specific plants were not treated under the experiment could be examined afterwards. Fresh weight of the plants three weeks after the treatment were used to measure the effect of the treatment, the group of reference plants had weights around 15 g to 20 g. The average fresh weight of treated plants were 9.73 g when the system moved at 0.7 m/s. Only a part of these plants activated the spray system, the average weight of the plants that activated the sprayer were 0.71 g.

Plant shape is often used as the only input to plant recognition systems. When the task is to distinguish between crop and weed plants a different type of information which is relevant for the classification is present, this is the context information. If the plant is outside of the row structure it must be a weed and if the plant follows the row structure it is likely to be a crop plant. The crop recognition accuracy of context features depends on the normalized weed pressure, as

the weed pressure increases the recognition accuracy decreases. The benefit of context features are their stability. The distance between neighbour crop plants are not affected by differences in soil conditions, plant growth stages, access to water and similar that can affect the shape of both crop and weed plants. Unfortunately context features are insufficient to reach crop recognition rates above 95% under typical field conditions. Shape based classification systems are often trained on a set of images acquired from one field and tested on images from a different field. If the two fields are not similar with respect to crop types, weed population and growth stages of both crop and weed plants, the classifier will not perform as well as possible. Training of a shape based classifier requires labelled examples of both crop and weed plants, these examples could be extracted from the images analysed in the actual field and labelled based on context information. Such a system would be able to adapt to local variations in plant shapes.

Advanced methods for weed control rely on information about crop placement, weed infestation levels and location of individual weed plants. Methods that can extract this information from in field images are described in this thesis. This shows that it is possible to derive a lot of information about crop and weed plants using machine vision.

9.1 Future work

Future work will address some open ended questions that are not addressed in the dissertation. Focus during the Ph.D. were on developing new algorithms for analysing images that can derive information about position and type of the plants from the image. The next step is to test the developed methods under field conditions.

Camera systems can acquire quality images containing many details of plant seedlings. In a lot of systems this information is reduced to a binary map of where vegetation is present in the image. This type of data reduction is usually applied to simplify the following image analysis. Weak edges caused by occlusion, colour and texture information is often discarded in this segmentation process. With access to this information it will be possible to create robust methods for plant recognition in complex scenes. Extraction of leaves in occluded scenes could be im-

proved by tracing weak edges in the original image, as described in (Franz et al., 1995).

Plant recognition based on extracted leaves can either be performed on the individual leaf level or on the group of leaves level. Classification of individual leaves can be performed using known methods like active shape models or shape feature descriptors. On the next level the task is to classify groups of leaves that are likely to origin from the same plant. Plant seedling models should take into account that cotyledons and the first true leaves have different shapes. As long as individual leaf detectors are unable to locate all leaves in an image, the models must be robust to missing leaves. This approach is more like how humans recognise plants.

Bibliography

Åstrand, B and A. J. Baerveldt (2004). "Plant recognition and localization using context information". In: *Proc. of the IEEE Conference Mechatronics and Robotics*, pp. 13–15.

Åstrand, B. and A.-J. Baerveldt (2002). "An Agricultural Mobile Robot with Vision-Based Perception for Mechanical Weed Control". In: *Autonomous Robots* 13.1, pp. 21–35.

Atwell, B. J., P. E. Kriedemann, and C. G. Turnbull (1999). *Plants in action, Adaptation in Nature, Performance in Cultivation.*

Bigun, J, T Bigun, and K Nilsson (2004). "Recognition by symmetry derivatives and the generalized structure tensor". In: *Pattern Analysis and Machine Intelligence, IEEE Transactions on* 26.12, pp. 1590–1605. ISSN: 0162-8828.

Bishop, C. M. (2007). *Pattern Recognition and Machine Learning (Information Science and Statistics)*. 1st ed. Springer. ISBN: 0387310738.

Bossu, J, C. Gée, G Jones, et al. (2009). "Wavelet transform to discriminate between crop and weed in perspective agronomic images". In: *Computers and Electronics in Agriculture* 65.1, pp. 133–143. ISSN: 0168-1699.

Camargo Neto, J. (Nov. 2005). "Crop species identification using machine vision of computer extracted individual leaves". en. In: *Proceedings of SPIE*. Vol. 5996. 1. SPIE, pp. 599608–599608–11.

Christensen, S., H. T. Søgaard, P. Kudsk, et al. (June 2009). "Site-specific weed control technologies". In: *Weed Research* 49.3, pp. 233–241. ISSN: 00431737.

Danish Ministry of the Environment (2010). *Bekæmpelsesmiddelstatistik 2009*. Tech. rep. 8. Danish Ministry of the Environment.

Du, J.-X., X.-F. Wang, and G.-J. Zhang (2007). "Leaf shape based plant species recognition". In: *Applied Mathematics and Computation* 185.2, pp. 883–893. ISSN: 0096-3003.

Ehsani, M. R., S. K. Upadhyaya, and M. L. Mattson (2004). "Seed location mapping using RTK GPS". In: *Transactions of the ASABE* 47.3, pp. 909–914.

Feyaerts, F. (Nov. 1999). "Hyperspectral image sensor for weed-selective spraying". en. In: *Proceedings of SPIE*. Vol. 3897. 1. SPIE, pp. 193–203.

Fontanelli, M., C. Frasconi, L. Martelloni, et al. (2011). "Effect of flaming with different LPG doses on maize plants". In: *Proceedings of the first international workshop on robotics and associated high technologies and equipment for agriculture*. Ed. by P. Gonzalez-de Santos and G. Rabatel, pp. 23–32.

Franz, E, M. R. Gebhardt, and K. B. Unklesbay (1991). "Shape description of completely visible and partially occluded leaves for identifying plants in digital images". In: *Transactions American Society of Agricultural Engineers (ASAE)*. Vol. 34. 2, pp. 673–681.

Franz, E, M. R. Gebhardt, and K. B. Unklesbay (1995). "Algorithms for extracting leaf boundary information from digital images of plant foliage". In: *Transactions American Society of Agricultural Engineers (ASAE)* 38.2, pp. 625–633.

Garford (2011). *Robocrop inrow*.

Giselsson, T. M. (2012). "Seedling Discrimination using Shape Featurse derived from a Distance Transform". In:

Graglia, E. (2004). "Importance of herbicide concentration, number of droplets and droplet size on growth of Solanum nigrum L,

using droplet application of glyphosate". In: *XIIeme Colloque International sur la Biologie des Mauvaises Herbes*, pp. 527–533.

Griepentrog, H. W. and A. P. Dedousis (2010). "Mechanical Weed Control". In: *Soil Biology*. Ed. by A. P. Dedousis and T. Bartzanas. Vol. 20. Springer Berlin Heidelberg. Chap. 11, pp. 171–179.

Griepentrog, H. W., M. Nørremark, and J Nielsen (2006). "Autonomous intra-row rotor weeding based on GPS". In: *Proceedings CIGR World Congress – Agricultural Engineering for a Better World*.

Guyer, D. E., G. E. Miles, M. M. Schreiber, et al. (1986). "Machine vision and image processing for plant identification". In: *Transactions American Society of Agricultural Engineers (ASAE)* 29, pp. 1500–1507.

Hand, D. J. and K. Yu (Dec. 2001). "Idiot's Bayes?Not So Stupid After All?" In: *International Statistical Review* 69.3, pp. 385–398. ISSN: 0306-7734.

Hearn, D. J. (Aug. 2009). "Shape analysis for the automated identification of plants from images of leaves". In: *Taxon* 58.3, pp. 934–954.

Hemming, J and T Rath (2001). "Computer-Vision-based Weed Identification under Field Conditions using Controlled Lighting". In: *Journal of Agricultural Engineering Research* 78.3, pp. 233–243. ISSN: 0021-8634.

Hess, M., G. Barralis, H. Bleiholder, et al. (Nov. 1997). "Use of the extended BBCH scale - general for the descriptions of the growth stages of mono- and dicotyledonous weed species". In: *Weed Research* 37.6, pp. 433–441. ISSN: 0043-1737.

Hu, M.-K. (1962). "Visual pattern recognition by moment invariants". In: *Information Theory, IRE Transactions on* 8.2, pp. 179–187. ISSN: 0096-1000.

Ji, L. and J. Piper (1992). "Fast Homotopy-Preserving Skeletons Using Mathematical Morphology". In: *Pattern Analysis and Machine Intelligence, IEEE Transactions on* 14.6, pp. 653–664. ISSN: 0162-8828.

Jin, J. and L. Tang (June 2009). "Corn plant sensing using real-time stereo vision". In: *Journal of Field Robotics* 26.6-7, pp. 591–608. ISSN: 15564959.

John, G. and P. Langley (1995). "Estimating Continuous Distributions in Bayesian Classifiers". In: *In Proceedings of the Eleventh Conference on Uncertainty in Artificial Intelligence*. Morgan Kaufmann, pp. 338–345.

Jørgensen, L. N., E. Noe, A.-m. Langvad, et al. (2007). "Vurdering af Planteværn Onlines økonomiske og miljømæssige effekt Bekæmpelsesmiddelforskning fra Miljøstyrelsen". In: 115, pp. 1–246.

Kurstjens, D. A. G., U. D. Perdok, and D Goense (Oct. 2000). "Selective uprooting by weed harrowing on sandy soils". In: *Weed Research* 40.5, pp. 431–447. ISSN: 00431737.

Kurstjens, D. A. (Dec. 2007). "Precise tillage systems for enhanced non-chemical weed management". In: *Soil and Tillage Research* 97.2, pp. 293–305. ISSN: 01671987.

Kverneland (2011). *Electric drive GEOseed offers new opportunities*.

Lamm, R. D., D. C. Slaughter, and D. K. Giles (2002). "Precision Weed Control System for Cotton". In: *Transactions American Society of Agricultural Engineers (ASAE)* 45, pp. 231–248. ISSN: 0001-2351.

Langner, H.-R., H. Böttger, and H. Schmidt (June 2006). "A special vegetation index for the weed detection in sensor based precision agriculture". In: *Environmental monitoring and assessment* 117.1-3, pp. 505–18. ISSN: 0167-6369.

Lee, W. S., D. C. Slaughter, and D. K. Giles (1999). "Robotic Weed Control System for Tomatoes". In: *Precision Agriculture* 1, pp. 95–113.

Lee, W. S. and D. C. Slaughter (1998). "Robotic weed control system for tomatoes using machine vision and precision chemical application". In: *Transactions American Society of Agricultural Engineers (ASAE)*.

Loomis, W. E. (Jan. 1965). "Absorption of Radiant Energy by Leaves". In: *Ecology* 46.1/2, pp. 14–17. ISSN: 00129658.

Lund, I., S. Christensen, L. A. Jensen, et al. (2008). *Cellesprøjtning af ukrudt i majs*. Tech. rep. Miljøstyrelsen.

Meyer, G. E. and J. a. C. Neto (2008). "Verification of color vegetation indices for automated crop imaging applications". In: *Computers and Electronics in Agriculture* 63.2, pp. 282–293. ISSN: 0168-1699.

Neto, J. a. C., G. E. Meyer, and D. D. Jones (Apr. 2006). "Individual leaf extractions from young canopy images using Gustafson-Kessel clustering and a genetic algorithm". In: *Computers and Electronics in Agriculture* 51.1-2, pp. 66–85. ISSN: 0168-1699.

Nieuwenhuizen, A. (2009). "Automated detection and control of volunteer potato plants". PhD thesis. Wageningen University.

Nieuwenhuizen, A. T., L Tang, J. W. Hofstee, et al. (Nov. 2007). "Colour based detection of volunteer potatoes as weeds in sugar beet fields using machine vision". In: *Precision Agriculture* 8.6, pp. 267–278. ISSN: 1385-2256.

Nieuwenhuizen, A. T., J. W. Hofstee, and E. J. Henten (Aug. 2010a). "Adaptive detection of volunteer potato plants in sugar beet fields". In: *Precision Agriculture* 11.5, pp. 433–447. ISSN: 1385-2256.

Nieuwenhuizen, A. T., J. Hofstee, and E. van Henten (Sept. 2010b). "Performance evaluation of an automated detection and control system for volunteer potatoes in sugar beet fields". In: *Biosystems Engineering* 107.1, pp. 46–53. ISSN: 15375110.

Nørremark, M, H. T. Søgaard, H. W. Griepentrog, et al. (Apr. 2007). "Instrumentation and method for high accuracy geo-referencing of sugar beet plants". In: *Computers and Electronics in Agriculture* 56.2, pp. 130–146. ISSN: 0168-1699.

Oebel, H., R. Gerhards, L. Weiershäuser, et al. (2009). *Economics of site-specific weed control*.

Oerke, E.-C. (Dec. 2005). "Crop losses to pests". In: *The Journal of Agricultural Science* 144.01, p. 31. ISSN: 0021-8596.

Pérez, A., P. Larrañaga, and I. n. Inza (Feb. 2009). "Bayesian classifiers based on kernel density estimation: Flexible classifiers". In:

International Journal of Approximate Reasoning 50.2, pp. 341–362. ISSN: 0888613X.

Perez-Ruiz, M, D. C. Slaughter, C. J. Gliever, et al. (Jan. 2012). "Automatic GPS-based intra-row weed knife control system for transplanted row crops". In: *Computers and Electronics in Agriculture* 80.0, pp. 41–49. ISSN: 0168-1699.

Persson, M. and B. Åstrand (Aug. 2008). "Classification of crops and weeds extracted by active shape models". In: *Biosystems Engineering* 100.4, pp. 484–497. ISSN: 15375110.

Piotraschke, H. F. (2010). *H-Sensor*.

Poulsen, F. (2005). *System for selective treatment of plants in a row*.

Rothmund, M. (2007). "Das Kreuzhackverfahren". In:

Rouse, J. W., R. H. Haas, J. A. Schell, et al. (1973). "Monitoring vegetation systems in the Great Plains with ERTS". In: *Proceedings of the Third ERTS Symposium*. Ed. by S. C. Freden and M. A. Becker. Vol. 1. SP-351, 3010-317. NASA. NASA. Chap. SP-351, pp. 309–317.

Rueda-Ayala, V., J. Rasmussen, and R. Gerhards (2010). "Mechanical Weed Control". In: *Precision Crop Protection - the Challenge and Use of Heterogeneity*. Ed. by E.-C. Oerke, R. Gerhards, G. Menz, et al. Dordrecht: Springer Netherlands. Chap. 17, pp. 279–294. ISBN: 978-90-481-9276-2.

Scotford, I. M. and P. C. H. Miller (2005). "Applications of Spectral Reflectance Techniques in Northern European Cereal Production: A Review". In: *Biosystems Engineering* 90.3, pp. 235–250. ISSN: 1537-5110.

Silverman, B. W. (1986). *Density Estimation for Statistics and Data Analysis (Chapman & Hall/CRC Monographs on Statistics & Applied Probability)*. Chapman and Hall/CRC, p. 176. ISBN: 0412246201.

Søgaard, H. T. (July 2005). "Weed Classification by Active Shape Models". In: *Biosystems Engineering* 91.3, pp. 271–281. ISSN: 15375110.

Søgaard, H. T. and I. Lund (Mar. 2007). "Application Accuracy of a Machine Vision-controlled Robotic Micro-dosing System". In: *Biosystems Engineering* 96.3, pp. 315–322. ISSN: 15375110.

Sökefeld, M., M. Keller, M. Weis, et al. (2012). "Using bi-spectral imaging technology for simulated online-weed control in winter wheat and maize". In: *Julius-Kühn-Archiv* 434, pp. 183–190.

Sun, H, D. Slaughter, M. P. Ruiz, et al. (Apr. 2010). "RTK GPS mapping of transplanted row crops". In: *Computers and Electronics in Agriculture* 71.1, pp. 32–37. ISSN: 01681699.

Tang, X. D., M. H. Liu, H Zhao, et al. (2009). *Leaf Extraction from Complicated Background*.

Thorling, L. (2010). *Grundvandsovervågning 2009*, p. 102. ISBN: 9788778712745.

Tian, L, J. F. Reid, and J. W. Hummel (1999). "Development of a precision sprayer for site-specific weed management". In: *Transactions American Society of Agricultural Engineers (ASAE)* 42.4, pp. 893–900.

Tillett, N. D., T Hague, A. C. Grundy, et al. (2008). "Mechanical within-row weed control for transplanted crops using computer vision". In: *Biosystems Engineering* 99.2, pp. 171–178. ISSN: 1537-5110.

Tyystjärvi, E., M. Nørremark, H. Mattila, et al. (Oct. 2011). *Automatic identification of crop and weed species with chlorophyll fluorescence induction curves*.

Weide, R. Y. van der, P. O. Bleeker, V. T. J. M. Achten, et al. (June 2008). "Innovation in mechanical weed control in crop rows". In: *Weed Research* 48.3, pp. 215–224. ISSN: 0043-1737.

Weis, M and R Gerhards (2007). "Feature extraction for the identification of weed species in digital images for the purpose of site–specific weed control". In: *Precision Agriculture '07*. Chap. 3, pp. 537–544.

Weis, M., T. Rumpf, R. Gerhards, et al. (2009). "Comparison of different classification algorithms for weed detection from images based on shape parameters". In: *Proceedings of the 1st Inter-*

national Workshop on Computer Image Analysis in Agriculture, pp. 53–64.

Weis, M. and M. Sökefeld (2010). *Detection and Identification of Weeds*. Ed. by E.-C. Oerke, R. Gerhards, G. Menz, et al.

Weis, M., M. Keller, and V. R. Ayala (2012). "Herbicide Reduction Methods". In: *Herbicides - Environmental Impact Studies and Management Approaches*. Ed. by R. Alvarez-Fernandez. Chap. Herbicide, pp. 95–120. ISBN: 978-953-307-892-2.

Woebbecke, D. M., G. E. Meyer, K Von Bargen, et al. (1995). "Color indices for weed identification under various soil, residue, and lighting conditions". In: *Transactions American Society of Agricultural Engineers (ASAE)* 38.1, pp. 259–269.

Zhang, Y and D. C. Slaughter (June 2011). "Hyperspectral species mapping for automatic weed control in tomato under thermal environmental stress". In: *Computers and Electronics in Agriculture* 77.1, pp. 95–104. ISSN: 0168-1699.

Papers

Paper I

Statistics based segmentation using a continuous scale Naive Bayes approach

Statistics based segmentation using a continuous scale Naive Bayes approach. / Midtiby, Henrik Skov; Laursen, Morten Stigaard; Krüger, Norbert; Jørgensen, Rasmus Nyholm.

Submitted to Sensors, april 2012.

Submitted to *Sensors*. Pages 1 - 13.

OPEN ACCESS

Article

Statistics Based Segmentation Using a Continuous Scale Naive Bayes Approach

Henrik Skov Midtiby [1,⋆], **Morten S. Laursen** [1], **Norbert Krüger** [2] **and Rasmus Nyholm Jørgensen** [1]

[1] Institute of Chemical Engineering, Biotechnology and Environmental Technology, University of Southern Denmark, Niels Bohrs Allé 1, 5230 Odense M, Denmark

[2] The Maersk Mc-Kinney Moller Institute, University of Southern Denmark, Niels Bohrs Allé 1, 5230 Odense M, Denmark

⋆ Author to whom correspondence should be addressed; phone +45 21 35 61 05; email: hemi@kbm.sdu.dk

Version March 20, 2012 submitted to Sensors. *Typeset by LaTeX using class file mdpi.cls*

Abstract: In precision agriculture, an often used preprocessing stage in image analysis is to distinguish between living plant material and soil in images with several colour channels. The normalized difference vegetation index and excess green are two cues that often is used in the segmentation process. A Bayesian method were described and used to segment images into regions containing vegetation or soil. The Bayesian method produces an improved segmentation than both normalized vegetation difference index and excess green. The improvement were sharper edges and less false positives.

Keywords: statistics, Bayes, segmentation, crop, weed, discrimination, NDVI, EXG

1. Introduction

A preprocessing stage used in many machine vision applications is segmentation of an input image into different regions based on their pixel content and context. Examples cover background detection[1], detection of moving objects[2], detection of traffic signs[3], ... The problem of segmenting vegetation from background areas in agricultural images has been described by several scholars. Tian [4] made a segmentation based on a Naive Bayes assumption, in which he used chromaticities of the individual colours as the input data. They reported problems with changes in illumination.

Woebbecke et al. [5] and Meyer et al. [6] examined several combinations of red, green and blue pixel values for distinguishing between vegetation and different background types. Excess green were effective at locating vegetation, but had a high rate of false positives. Excess red were good at recognizing some of these false positives. The combination of excess green and red were suitable for detecting vegetation.

In this paper we investigate the problem of distinguishing between vegetation and soil based on input from separate colour channels and indices such as excess green [6] and the normalized difference vegetation index [7]. Information from the different sources are combined using a Naive Bayes approach adapted to work with continuous input values. To handle continuous input values the underlying probability distribution for each input feature is estimated using kernel density estimation methods [8]. This approach to cue combination is not limited to segmentation of vegetation and could be applied to many segmentation problems.

In addition to red, green and blue values, a near infrared colour channel was used. The nir channel is interesting in the context of vegetation segmentation as plant material tend to reflect a large fraction of near infrared light for keeping the plant temperature low. In this paper, we show that the nir channel can also be used in combination with other segmentation cues based on colour chromaticities. This combines the best from excess green classifiers which have a low error rate, but produces fuzzy edges and normalized difference vegetation index based classifiers which has sharp edges but falsely detects some soil regions as vegetation. Segmentations based on multiple cues are more robust to changes in vegetation cover (underlying prior values) and produces sharper boundaries between soil and vegetation regions.

This paper is structured as follows: Section 2 describes the used equipment and applied methods. Results are presented and discussed in section 3 and conclusion is presented in section 4. The used abbreviations and symbols are listed with brief explanations in table 1.

Table 1. Nomenclature

Symbol	Unit	Description
R, G, B, N	1	Red, green, blue and near infrared raw colour values
r, g, b, n	1	Red, green, blue and near infrared chromacities
ExG	1	Excess green
NDVI	1	Normalized differential vegetative index
$\mathbb{S}$		Soil class
$\mathbb{V}$		Vegetation class
$\mathbb{C}$		Object class, either $\mathbb{S}$ or $\mathbb{V}$
$P(\mathbb{C})$	1	Background probability of class $\mathbb{C}$
$S(\mathbb{C})$	1	Support for observation belonging to class $\mathbb{C}$
F_k	1	k^{th} feature value
k	1	Index variable
$P(F_k\|\mathbb{C})$	1	Conditional probability distribution of feature F_k when class is $\mathbb{C}$
$K(x)$		Smoothing kernel
$\hat{f}_h(x)$		Estimate of probability density
h	1	Smoothing bandwidth
L	1	Number of observations used for estimating a probability distribution

2. Materials and methods

In this section, the steps involved in image acquisition, normalization, feature calculation, classifier training and testing are described. For training the classifier, a manual annotation process is used to generate labelled samples. Then these samples are used to estimate the underlying probability distributions.

Image acquisition is described in section 2.1. Section 2.2 explains how the raw image sensor readings are converted to cues / input values for the classifier. Training of the classifier is covered in 2.4 and classifier prediction is described in 2.5.

2.1. Data acquisition

The image acquisition setup is shown in figure 1. Images were acquired with a JAI[1] AD-080CL four colour channel 2–CCD camera. The camera captured images with a resolution of 1024 × 768 pixels and each pixel consists of four colour values red, green, blue and near infrared (NIR). An example image is shown in figure 2. Hard shadows were avoided by shielding sunlight from the imaged area and providing artificial illumination with LEDs. For the visual spectrum 30 Prolight[2] Power LED PG1A-3LWS-SD were used while the near infrared illumination were

[1] www.jai.com
[2] www.prolightopto.com

Figure 1. Image acquisition setup.

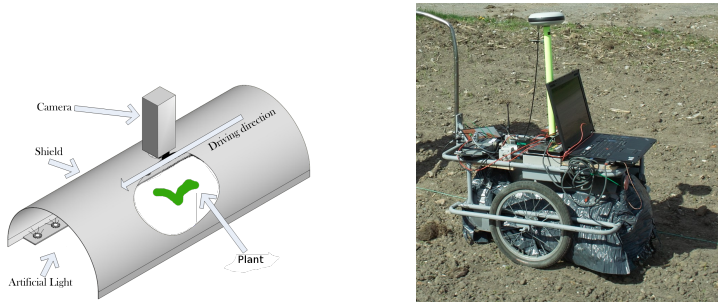

Figure 2. Example image captured by imaging system

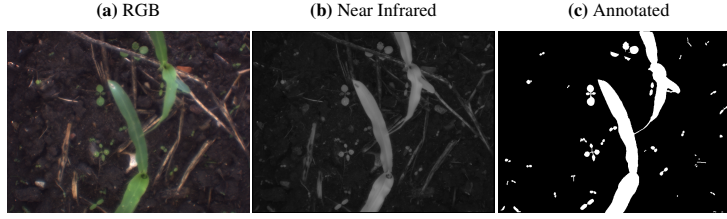

delivered by 150 Vishay[3] TSHG5510 830nm 180mW LEDs. Except the illumination, the setup is similar to the light tunnel described in [9]. White balance was calibrated using a X-rite[4] ColorChecker® Classic[10]. The images were captured in Odense at the University of Southern Denmark the 19th of August 2010.

2.2. *Calculation of colour features*

The raw pixel values associated with the red, green, blue and near infrared colour channels (R, G, B and N respectively) consists of integers in the range $[0; 2^{12} - 1]$. These values are not directly suitable as features for the classification problem as they are highly correlated to, e.g., changes in illumination. Raw colour values can be combined to new values, that are less sensitive to illumination changes but can be used to identify vegetation. Two examples are 1) Excessive green (ExG) [5] and 2) Normalized Difference Vegetation Index (NDVI) [11] which are defined as:

$$\mathrm{ExG} = 2 \cdot G - R - B \tag{1}$$

$$\mathrm{NDVI} = \frac{N - R}{N + R} \tag{2}$$

[3] www.vishay.com
[4] www.xrite.com

The chromaticities (r, g, b and n) are given by the raw colour value divided by the sum of all the colour values.

$$(r, g, b, n)^T = \frac{(R, G, B, N)^T}{R + G + B + N} \tag{3}$$

2.3. *Annotation of training images*

The training images were all annotated manually. The annotation process consisted of marking all pixels in the image that belonged to the vegetation class, the remaining part of the image were then handled as being soil. An example of an annotated image is shown in fig. 2.

2.4. *Classifier training*

We used the Flexible Naive Bayes classifier described by Perez et al.[12]. Training of the classifier consists of learning the probability density distributions of the different input values conditional on the object class (soil or vegetation). The probability densities were determined from annotated images, see example in figure 2, where soil and vegetation regions were marked manually. The four raw colour values, the corresponding chromaticities combined with ExG and NDVI were used as input values for the classifier. To describe the probability density functions $\hat{f}_h(x)$ of the given input variables, kernel density estimation (KDE) was used with a Gaussian kernel $K(x)$, with bandwidth h [8].

$$\hat{f}_h(x) = \frac{1}{L \cdot h} \sum_{i=1}^{L} K\left(\frac{x - x_i}{h}\right) \tag{4}$$

$$K(x) = \frac{1}{\sqrt{2\pi}} e^{\frac{-x^2}{2}} \tag{5}$$

Where L is the number of observations. The bandwidth was chosen manually.

In principle could $f_h(x)$ be calculated for all new values of x using equation (4), but this would require linear time in the number of training samples. Instead the function value were calculated at 255 evenly distributed x values in the interval $[x_{\text{min}} - 3h; x_{\text{max}} + 3h]$, where x_{min} / x_{max} is the minimum / maximum seen value of x in the training set.

The estimated probability density functions are shown in figure 3. The prior probabilities $P(\mathbb{S})$ and $P(\mathbb{V})$ of a pixel being soil and vegetation respectively were also determined from the training set.

2.5. *Classifier prediction*

When the classifier is presented for a new observation, it is calculated how well the observation matches the soil ($\mathbb{S}$) and vegetation ($\mathbb{V}$) classes respectively. The

support for class $\mathbb{C}$ is denoted $P(\mathbb{C}, \vec{F})$. The support is the approximated value of the probability density function given the observations and a test class that could either be soil or vegetation.

$$P(\mathbb{C}, \vec{F}) = P(\mathbb{C}) \cdot P(F_1|\mathbb{C}) \cdot P(F_2|F_1, \mathbb{C}) \cdot P(F_3|F_1, F_2, \mathbb{C}) \cdot \ldots \tag{6}$$

This representation requires a large amount of space $O(d^{\#\text{ features}})$ and to get a usable accuracy an huge number of trainings samples is needed. By assuming independent cues, the probability density function can be estimated by the expression below.

$$P(\mathbb{C}, \vec{F}) \simeq P(\mathbb{C}) \cdot \prod_{k=1}^{10} P(F_k|\mathbb{C}) \tag{7}$$

the input features are named F_k where $k \in \{1, \ldots 10\}$. This representation requires only $O(d \cdot \#\text{ features})$ space and only a fraction of the training samples. After the supports are calculated, the posterior probability that the current observation belongs to the vegetation class is given by:

$$P(\mathbb{V}|\vec{F}) = \frac{P(\mathbb{V}, \vec{F})}{P(\mathbb{V}, \vec{F}) + P(\mathbb{S}, \vec{F})} \tag{8}$$

3. Results and discussion

In this section are results presented and commented. Section 3.1 covers training of the classifier and what can be learned from the observed feature probability density distributions and prior probabilities. Correlation between cues are examined in section 3.2. Section 3.3 investigates the performance of classifiers based on individual cues and all the cues combined.

3.1. Training

4 million annotated pixels in 5 images were used to estimate the probability distributions for each of the 20 combinations of cues and classes[5]. The low number of images used for training could have been problematic if there were a large variety in the images. This was not the case due to the controlled illumination. The background probabilities were found to be $P(\mathbb{V}) = 0.0785$ and $P(\mathbb{S}) = 0.9215$) respectively. The input feature probability distributions are all shown in figure 3. The probability densities are scaled such that the plotting range covers the mean feature value $\pm$ 3 standard deviations. The percentage shown next to the probability distributions is the amount of overlap between the distributions. If two classes have equal

[5] All combinations of 10 cues and 2 classes.

prior probabilities, the overlap percentage divided by two is the upper bound on the expected error rate of the classifier that only uses the analysed input feature. Due to the large overlap (80.5%) the green chromaticity is expected to perform badly in the classification task. The two combined cues ExG and NDVI have a much lower overlaps (6.1% and 12.3%) and will thus produce better results.

3.2. Correlation between cues

The Naive Bayes classifier relies on the assumption that the input values / cues are independent. This is not the case in most applications, including the vegetation / soil classification problem discussed in this paper. Hand and Yu [13] investigated how dependent input values changed the predictions of Naive Bayes classifiers. It was found that the classifier was more confident in decisions compared to independent inputs, but it still made similar classifications. The classifier was more confident in both correct and incorrect classifications than what is expected from the underlying probability density, which makes it more difficult to interpret the strength of the conducted classification.

Figure 4 visualizes the correlation between the input cues. As can be seen the four raw colour values (R, G, B, N) are highly correlated. The four chromaticities are only weakly correlated and the cues NDVI, ExG and n are also correlated.

3.3. Classification

Eleven different classifiers were tested, one classifier for each of the ten cues and a single classifier using all the cues. Classification results of a test image are shown in figure 5 for the eleven classifiers. The four classifiers (B–E) that only used raw colour input values could identify the dark soil, but would also recognize dead plant material as vegetation. The classifier based on green chromaticities (G) produced unusable results as predicted from the large overlap in figure 3. Classifiers based on red, blue, nir chromaticities (F, H, I) performed better than classifiers based on the raw colour values. Edges of vegetation were much sharper but the classifiers had still trouble with soil and dead plant material being recognized as vegetation. The two classifiers based on ExG and NDVI (J, K) had a low rate of recognizing vegetation in regions containing soil and dead plant material, but the located regions of vegetation had blurred edges.

Table 2 lists confusion matrices for the eleven classifiers using equal priors. The column names in the table consists of the true class (determined by annotation) followed by the predicted class. Notice how all classifiers using a single cues as input have a higher probability of classifying soil as vegetation, compared to the classifier using all cues as input. This is to be expected, as classifiers that rely on a single input cue and the priors will be more dependent on the priors, than a classifier

Figure 3. Visualization of probability densities. Two example input images are shown in A and B. C–L contains the probability densities of all the cues. The probabilities are shown for soil in red and vegetation in green. The feature values are scaled such that the area below all curves are identical. The shaded area is a measure of the separability of the two classes and the overlap percentage is shown for each cue.

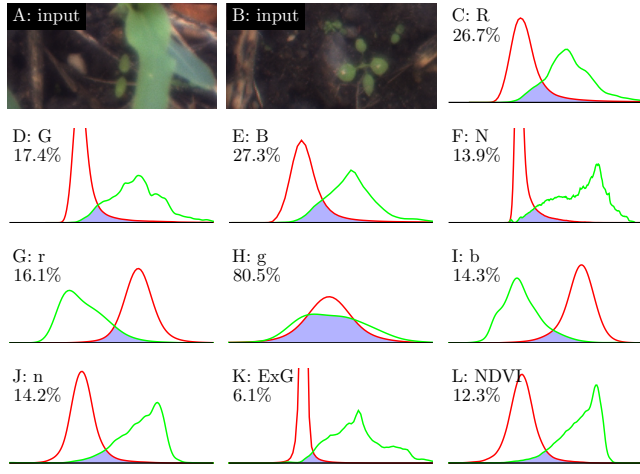

Figure 4. Correlation between the different cues. High correlation is marked by bright squares and low correlation with dark squares.

	R	G	B	N	r	g	b	n	ExG	NDVI
NDVI	0.03	0.25	0.02	0.61	0.95	0.50	0.71	0.97	0.72	1.00
ExG	0.27	0.59	0.30	0.78	0.74	0.13	0.69	0.69	1.00	0.72
n	0.07	0.30	0.06	0.67	0.86	0.55	0.83	1.00	0.69	0.97
b	0.46	0.59	0.33	0.80	0.52	0.21	1.00	0.83	0.69	0.71
g	0.43	0.43	0.48	0.09	0.35	1.00	0.21	0.55	0.13	0.50
r	0.09	0.23	0.03	0.56	1.00	0.35	0.52	0.86	0.74	0.95
N	0.72	0.89	0.73	1.00	0.56	0.09	0.80	0.67	0.78	0.61
B	0.94	0.93	1.00	0.73	0.03	0.48	0.33	0.06	0.30	0.02
G	0.93	1.00	0.93	0.89	0.23	0.43	0.59	0.30	0.59	0.25
R	1.00	0.93	0.94	0.72	0.09	0.43	0.46	0.07	0.27	0.03

which uses input from several cues. The classifier using all ten cues performs much better than the other classifiers.

Table 3 is similar to table 2, except the prior values were set to the values found in section 3.1. The first observation is that the green chromaticity g does not have enough strength to overcome the biased priors and the classifier will thus always classify new observations as soil. The performance boundary between classifiers using a single cue and multiple cues as input has narrowed down. The best performing classifier (according to the confusion matrices) is the one based on ExG, the classifier using all cues is only slightly worse. One thing is the number of misclassified pixels in the test image, a more important aspect is the quality of the detected edges. Examples of the different classifiers in action is shown in figure 5 and 6, the segmentation found using ExG has fuzzy edges while the classifiers using all cues produces much sharper edges and is in general much more confident about its choices.

4. Conclusion

A Naive Bayes classifier using continuous valued inputs was implemented. The classifier showed that several cues could be combined efficiently using this scheme and that the generated results of the combined classifier were equal to or superior to the results of the individual classifiers. Measured by the number of mistakes in the test image, ExG performed slightly better than the classifier using all cues as input. But the combined classifier were more confident in its classifications and produced much sharper edges.

Figure 5. Manually segmented image (A), vegetation probability calculated based on individual cues: raw colour values (B-E), chromaticities (F-I), ExG (J) ands NDVI (G). Vegetation probability calculated using all cues (L).

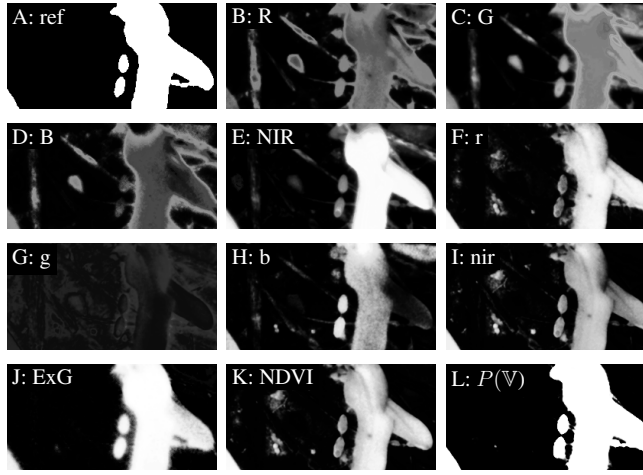

Table 2. Confusion matrices for the different classifiers using identical priors

Classifier	VegVeg	VegSoil	SoilVeg	SoilSoil
R	8.22	0.51	11.07	80.20
G	8.48	0.24	9.62	81.65
B	7.55	1.18	9.88	81.39
N	8.60	0.13	6.75	84.52
r	8.49	0.24	5.83	85.44
g	4.96	3.77	33.24	58.03
b	8.40	0.33	5.91	85.36
n	8.48	0.25	5.79	85.48
ExG	8.71	0.02	4.39	86.88
NDVI	8.55	0.18	6.12	85.15
All	8.63	0.09	2.07	89.20

Table 3. Confusion matrices for the different classifiers using priors estimated from the training data.

Classifier	VegVeg	VegSoil	SoilVeg	SoilSoil
R	3.13	5.59	2.61	88.66
G	6.60	2.13	2.61	88.66
B	2.80	5.93	2.50	88.77
N	7.14	1.59	0.45	90.83
r	7.69	1.04	0.88	90.39
g	0.00	8.73	0.00	91.27
b	7.38	1.35	1.14	90.13
n	7.35	1.38	1.33	89.94
ExG	8.50	0.23	1.20	90.07
NDVI	7.83	0.89	1.29	89.99
All	8.60	0.13	1.43	89.84

Figure 6. Similar to figure 5 but on a different part of the image.

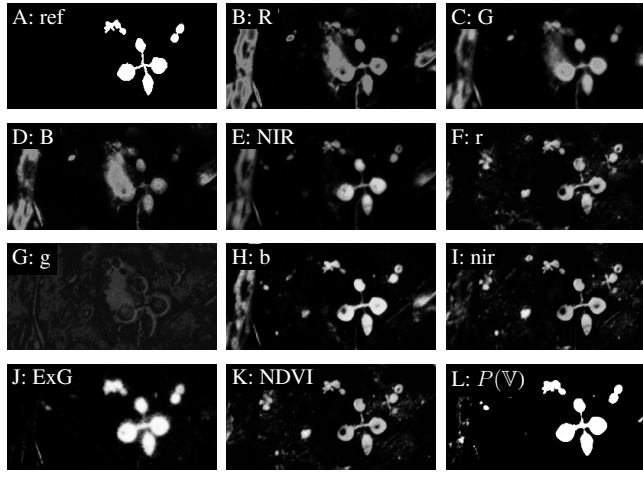

References

1. Andreasen, C.; Rudemo, M.; Sevestre, S. Assessment of weed density at an early stage by use of image processing. *Weed Research* **1997**, *37*, 5–18.
2. *Embedded Smart Camera for High Speed Vision*. IEEE, 2007.
3. de la Escalera, A.; Moreno, L.; Salichs, M.; Armingol, J. Road traffic sign detection and classification. *IEEE Transactions on Industrial Electronics* **1997**, *44*, 848–859.
4. Tian, L. Knowledge-based machine vision system for outdoor plant identification. PhD thesis, University of California Davis, 1995.
5. Woebbecke, D.M.; Meyer, G.E.; Bargen, K.V.; Mortensen, D.A. Color indices for weed identification under various soil, residue, and lighting conditions. *Transactions of the ASAE* **1995**, *38*, 259–269.
6. Meyer, G.E.; Neto, J.a.C. Verification of color vegetation indices for automated crop imaging applications. *Computers and Electronics in Agriculture* **2008**, *63*, 282–293.
7. Thorp, K.; Tian, L. A Review on Remote Sensing of Weeds in Agriculture. *Precision Agriculture* **2004**, *5*, 477–508.
8. Silverman, B.W. Density Estimation for Statistics and Data Analysis. *Applied Statistics* **1986**, *37*, 120.
9. Midtiby, H.S.; Mathiassen, S.K.; Andersson, K.J.; Jø rgensen, R.N. Performance evaluation of a crop/weed discriminating microsprayer. *Computers and Electronics in Agriculture* **2011**, *77*, 35–40.
10. X-Rite. X-Rite ColorChecker Classic.
11. Rouse, J.W.; Haas, R.H.; Schell, J.A.; Deering, D.W. Monitoring vegetation systems in the Great Plains with ERTS. Proceedings of the Third ERTS Symposium, 1973, pp. 309–317.
12. Pérez, A.; Larrañaga, P.; Inza, I.n. Bayesian classifiers based on kernel density estimation: Flexible classifiers. *International Journal of Approximate Reasoning* **2009**, *50*, 341–362.
13. Hand, D.; Yu, K. Idiot's Bayes: Not So Stupid after All? *International Statistical Review* **2001**, *69*, 385–398.

Todo list

© March 20, 2012 by the authors; submitted to *Sensors* for possible open access publication under the terms and conditions of the Creative Commons Attribution license http://creativecommons.org/licenses/by/3.0/.

Paper II

Modicovi: Spray boom for selectively spraying a herbicidal composition onto dicots

Modicovi: Spray boom for selectively spraying a herbicidal composition onto dicots. / Jørgensen, Rasmus Nyholm; Krüger, Norbert; Midtiby, Henrik Skov; Laursen, Morten Stigaard.

Patent application, submitted march 2012.

Spray boom for selectively spraying a herbicidal composition onto dicots

FIELD OF THE INVENTION

The present invention relates to a method and spray boom for discriminating cereal crop (monocot) and weeds (dicots) and relates particularly, but not exclusively, to an agricultural spray boom that incorporates such a spray boom.

BACKGROUND OF THE INVENTION

The most commonly used technique for broad acre spraying of pesticides is the use of a wide sprayer boom, which may be self-propelled or towed behind another vehicle. A typical sprayer boom has a plurality of spray nozzles mounted at spaced locations along a boom, a large tank for containing the spray liquid and a pump system for pumping the liquid to the nozzles.

One of the disadvantages of conventional sprayers is that herbicides are sprayed indiscriminately on the crop, bare ground and weeds. This is of concern in the case of food crops, with consumer groups becoming increasingly vocal about chemical residue in crops and livestock. There is also an economic disincentive since a much greater volume of chemicals must be applied per hectare than is actually required to effectively control the weeds.

Today's conventional agricultural practise is to spray an average herbicide dosage one to several times within a cereal field with no regard to the spatial distribution of crop plants and weeds. Attempts have been made registering or mapping the weed distributions and then apply variable herbicide rates. This procedure has mainly been done manually and recently in an automated and vision based manner. However the current algorithms discriminating the cereal crop (monocot) and weeds (dicots) fails in most cases due to leaf occlusions. Furthermore the present algorithms are computer intensive.

Hence low cost real time discrimination is currently not possible. Furthermore, leaf occlusion between the single plants makes it very difficult to separate the single crop and weed plants, which prohibits any classic discrimination algorithms to be applied with success.

Current real time systems for crop and weed discrimination is mainly capable of operation within crops seeded in rows. After identifying the extent of the crop rows the crop canopy free intra rows area is used to identify areas of living plant material which is then identified as weed. This approach is commercially operational today in real time. The main problem with the latter approach is the dependency of a crop free intra row strip. Within the majority of cereal crops, and especially within autumn sown winter cereals the intra row strip vanish quickly during the tillering stages where multiple planophile cereal leaves enter the intrarow strip between the crop rows 125 mm apart. Hence the occurrence of overlapping or occluded crop and weed leaves makes it highly complex to discriminate cereals and dicotyledon weeds with the methods known today.

Lee *et al* (Precision Agriculture, 1, 95, 113, 1999) disclose a spray boom for selectively spraying a herbicidal composition onto dicots in a living vegetation. The spray boom comprises a plurality of spray nozzles evenly distributed along the spray boom ("valve/nozzle array") and means for activating one or more of the spray nozzles in response to detected dicots so as to selectively apply the herbicidal composition onto the sensed area containing the dicots. Moreover it comprises means for digitally recording an image of the selected area to be treated by a nozzle on the spray boom, whereby the plant material is identified based on a segmentation procedure that transform the raw image data of the image into a measure which describes the likeliness that a given pixel or point of the image is a living vegetation, such as leaves. Meanwhile, Lee *at al* do not disclose any means for detecting dicots by estimating the curvature of the leaves by sampling locally distributed points placed on the edges of the leaves. Especially, Lee *at al* do not disclose any means for estimating the curvature measuring the orientation of the edge at points in a global coordinate frame. Importantly Lee *at al* do not provide any means for estimating the orientation of the leaves and how to extract and interpret relevant features.

It is an object of the present invention to develop new technology with high environmental impact for the agricultural market by reducing the amount of herbicide usage significantly.

Particularly it is an object of the present invention to develop a novel vision based decision system for modified conventional sprayer booms, which is able to detect and apply herbicides on weed plants in real time with a capacity comparable to available sprayers.

It is a further object of the present invention to provide a spray boom that is able to quantify the extent and ratio between cereal crop (monocot) and weeds (dicots), as well as occluded cereal crop (monocot) and weeds (dicots).

SUMMARY OF THE PRESENT INVENTION

The present invention was developed with a view to providing a more efficient method and spray boom for discriminating different types of ground vegetation in agriculture, without the need to change hardware components of the spray boom every time a different type of plant is to be discriminated.

A unique feature of the present invention is automatic estimation of the ratio of weed leaf area relative to the total vegetation leaf area. The computation requirements are relatively low and can to a large extent be paralleled processed (e.g. by a FPGA, a DSP, or potentially a GPU unit) based on standard image processing primitives.

Especially the present invention ensures a proper detection despite occluded leaves. Prior art methods mainly assume that the plants are clearly separated with no overlapping leaves.

So the invention will replace or supplement the algorithms currently used in matrix based images to discriminate and quantify the ratio between cereal and dicotyledon weeds.

The invention utilizes the known difference in appearance between monocots (long narrow leaves) and dicots (shorter and roundish leaves). Despite overlapping leaves the method can be used in a robust and computer efficient manner to estimate the ratio between visible monocot and dicot leaves. The feature that enables this is based on edge detection algorithms used for discriminating the elongated and roundish leaf shapes despite of occluded leaves.

The method and spray boom of the present invention utilize the following basic steps:

1) segmentation of an digitally recorded image in vegetation and soil regions;
2) detection of edges of identified leaves;
3) extraction of statistical features which describe the relative orientation and spatial properties of the detected edges; and
4) Interpretation of the statistical features resulting in a measure of the dicot cover.

According to one aspect of the present invention there is provided a spray boom for selectively spraying a herbicidal composition onto dicots in a living vegetation, the spray boom comprising:

- means for digitally acquiring an image of a selected area to be treated by a nozzle on the spray boom, whereby a plant material is identified based on a segmentation procedure that transforms the raw image data of the image into a measure which describes the likeliness that a given pixel is living vegetation, such as leaves;
- means for detecting dicots by estimating the curvature of the leaves by sampling locally distributed points placed on the edges of the leaves, said means for estimating the curvature measuring the orientation of the edge at the points in a global coordinate frame;
- a plurality of spray nozzles evenly distributed along the spray boom;
- means for activating one or more of the spray nozzles in response to detected dicots so as to selectively apply the herbicidal composition onto the sensed area containing the dicots.

According to another aspect there is provided a method for selectively spraying a herbicidal composition onto dicots in a living vegetation, said method comprising the following steps:

- segmentation of an image into points of a selected area of a field in living vegetation and non-vegetation regions;
- detection of dicots by determining the curvature of the leaves through sampling locally distributed points placed on the edges of the leaves and measuring the orientation of the edge at the points in a global coordinate frame and
- spraying the herbicidal composition to the selected area , wherein dicots have been detected.

BRIEF DESCRIPTION OF THE DRAWINGS

Figure 1 is an illustration of the spray boom.

Figure 2 shows estimations of Dicot ratio, compared to a known reference (Samples sorted by reference ratio).

Figure 3 shows relation between reference and estimated dicot coverage optimized for lowest mean error.

Figure 4 shows distribution of residual errors of the estimated dicot coverage lowest mean error.

Figure 5 shows the relation between points on the edge.

Figure 6 shows the relation between points on the edge for a monocot compared to a dicot.

DETAILED DESCRIPTION OF THE INVENTION

In the following these steps are described in more detailed.

As shown in Figure 1 the spray boom has a set of digital cameras in a vision system that takes images of the field surface immediately in front of the spraying boom. The images are analysed for the occurrence of crop and weed. When one or more weeds are found in the image, the information about their location is saved in a spray map. The image is normally divided into rectangular units (cells) of 200 mm in the driving direction and 250 mm orthogonally to the driving direction. Since the cameras are fixed in relation to the spraying boom, the cells are placed so that the nozzles – with a certain time lapse – pass over the middle of each cell. Under good light conditions the cell sprayer can operate with a forward speed of approximately 3-4 m/s. Commercially available nozzles modified with high speed valves are used to control weeds. The overall conclusions were that it was possible to control weeds with an efficacy comparable to what is achieved with today's broadcast spraying.

Although the invention will be described primarily with reference to the selective spot spraying of weeds, it will be apparent that the method and spray boom for discriminating different types of ground vegetation may also be used to identify weeds for mechanical destruction, mapping of weed infestation coupled with a global positioning system (GPS) or differential global positioning system (dGPS), differentiated spraying of liquid fertiliser on crop plants, measurement and logging of crop vigour, and other weed and crop management practices.

In order to facilitate a more detailed understanding of the nature of the invention a preferred embodiment of a spray boom and method for discriminating different types of ground vegetation will now be described in detail.

The method of the present invention involves the following steps:
1) segmentation of the image in living vegetation and non-vegetation regions;
2) detection of edges with orientation of the gradient at the individual pixels;
3) Extraction of statistical features which describe the relative orientation and spatial properties of the detected edges; and
4) Interpretation of the statistical features resulting in a measure of the monocot/dicot ratio.

Below is each of the steps described more detailed.

1. Segmentation

The segmentation serves to transform the raw image data into a measure which describes the likeliness that a given pixel is living vegetation. Within the domain there is primarily two ways which is typically used to accomplish this, one is normally referred to as Excessive green, the other as the normalized difference vegetation index.

Excessive green is defined as 2G – R – B where G defines the green part of the plant reflection, R the red part and B the blue part. It relies on the fact that the plant has a high absorption of blue and red light, but a low absorption of green. Normalized difference vegetation index (NDVI) is normally defined as (NIR-Red)/(NIR+Red).

The method used is capable of mapping the raw images into a description where pixels with living plant material are separated from the rest.

The image is segmented so plant material and soil is clearly separated. Excessive green relies on the green peak seen at 550nm, where the normalised vegetation index relies on the high near infrared reflection (the use of the red channel is primarily a way of reducing false positives).

2. Edge detection

After the image segmentation, the edges in the image are located. This can be performed using a filter bank consisting of Gabor kernels, with constant size and scale but different orientations, using a structure tensor or various other methods. For the Gabor method the edge image is constructed using the maximum response from the filter bank. This edge image is thresholded and thinned until a single pixel wide edge remains. For each pixel still in the edge image, the orientation of the local edge is determined from the gabor responses. By looking at which Gabor orientation yielded the maximum value for that edge point, the orientation of the Gabor kernel yielding the maximum response then directly corresponds to the orientation of the edge when combined with the sign of the imaginary part of the response at the pixel.

For the edge detection the contour of the segmented objects is extracted. The contour description should contain both the spatial coordinates as well as the orientation of the edge, and on which side of the edge the segmented object is positioned.

The edge is extracted in order to be able to define some features based on the shape of the plant. In order to extract this information a filter bank consisting of Gabor filters is applied. Each of these filters is designed in such a way as to have maximum magnitude response, when the kernel is placed centre on an edge, with the orientation of the kernel matching that of the edge.

In order to calculate the kernel of the Gabor filter, division into three parts is required; the propagating wave, the damping and the rotation of the kernel. The propagating wave simply relies on the definition of complex numbers which says that we can describe a complex wave as an exponential as:

$$e^{j\Theta} = \cos(\Theta) + j \cdot \sin(\Theta)$$

Applying this to the propagating wave of the Gabor it can described as:

$$e^{2\pi \cdot f \cdot x' j} = \cos(2\pi \cdot f \cdot x') + j \cdot \sin(2\pi \cdot f \cdot x')$$

Where *f* denotes the frequency, and x' denotes the position in the kernel given along the wave's direction of propagation.

The dampning can be described as an exponential decay towards the edge of the kernel as

$$e^{-(\alpha^2 \cdot x'^2 + \beta^2 \cdot y'^2)}$$

Where α describes the sharpness of the Gaussian bell along the wave and β describes the sharpness of the Gaussian bell across the wave. x' still denotes the position in the kernel along the wave propagation and *y´* denotes the position across the wave.

This allows the Gabor kernel to be expressed as:

$$G(x, y) = e^{-(\alpha^2 \cdot x'^2 + \beta^2 \cdot y'^2)} \cdot e^{2\pi \cdot f \cdot x' \cdot j}$$

x' and *y'* can be defined by a rotation given by the angle Θ as:

$$x' = x \cdot \cos(\Theta) + y \cdot \sin(\Theta)$$

$$y' = y \cdot \cos(\Theta) - x \cdot \sin(\Theta)$$

Where x, *y* defines the position in the kernel along the horizontal and vertical direction in the image.

For the Gabor filters there is a set of parameters which must be selected

1. Frequency
2. Sharpness / damping of Gaussian along and across the direction of propagation
3. Amount of different angles (how large should the filter bank be)
4. Size of filter mask

Each of these parameters is a compromise.

For selecting the frequency, the lower bound is defined by how small blobs should be detected; if the frequency is too low, it will not be able to detect the smaller weed blobs. If the frequency is too high we will have an increased sensitivity to noise. As the images the Gabor filter is working on is near binary, the edge can considered a Heavyside step function, therefore energy will be present at all frequencies. Since the blobs of the weed is sometimes fairly small (down to 4 pixels across a leaf) in the test dataset, a high frequency of $f = 0.4$ has been chosen (normalized frequency (cycles per pixel)).

Sharpness of the filter along the wave propagation should ensure that the sampling of the edge is localized and as we do not wish to be extra sensitive to texture only a single period should be contained within the Gaussian bell, the sharpness has been set to $\alpha = 0.8$, which results in that more than 99% of the contribution comes from the pixels which lies in a distance of less than or equal to 2 pixels away from the pixel being measured. Across the direction of propagation the sharpness defines how many of the neighbouring pixels aid in the definition of the orientation of the edge. If the bell is to narrow then the angle will be noisy, if it is too large it will be insensitive to sharp curves, we have chosen a sharpness of $\beta = 0.8$.

The amount of different angles is another compromise primarily between computational efficiency and the angular resolution, as computational efficiency is not a parameter for this project no further time has been spend on optimizing this parameter, and tests has been performed using 8 Gabor filters which equals a resolution of 22.5°.

A core feature of the present invention is the detection of dicots by estimating the curvature of the leaves by sampling locally distributed points placed on the edges of the leaves, and measuring the orientation of the edge at the points in a global coordinate frame;

By measuring the orientation of the edge at a local point in a global coordinate frame, a description of each edge point can be obtained, if each point is combined along the edge with the other points on the edge as shown in Figure 5. The relation of each combination of two edge points can be described. Using this description on all points which is a distance less than a maximum distance (e.g. 125 pixels), a set of fingerprints can be created for an image based on a histogram of the description. From these fingerprints the density of a set of strategically chosen areas is measured. From these measurements an evaluation can be performed to estimate the amount of leaf coverage. For this work the estimation was performed by performing a non-linear regression on a known reference using a genetic algorithm.

3. Feature extraction

To describe the shapes in the image, the relative location and orientation of pairs of edge pixels are examined. The relative measures are used in order to obtain spatial and rotational independence. The relative location of two edge pixels is described using the parameters: x, y and \theta. By looking at all pairs of edge pixels with an internal distance lower than a given threshold (e.g. 125 pixels), the distribution of the three parameters x, y and Θ can be investigated using 2D histograms. These histograms are the “fingerprints” of the examined structure represented in a rotation and position invariant way.

4. Interpretation

The statistical features can be visualized as a kind of “fingerprint” image. Three such fingerprints are shown in figure 6, one for pure monocots, pure dicots and finally a mixture of the two plant types

Mixture (nightshade and maize)

Based on the illustrated fingerprints and variation of these it is possible to quantify the amount and ratio between monocotyledons (cereal crops and grass weed) and dicotyledons (weeds) in a computational efficient manner. For interpreting the fingerprints a set of 9 features has been created, each of these features is a subset of the points selected to

approximate a given property of the plant. A feature is defined as a measure of the points density within a given area of the fingerprint. Even though some of the properties is not always approximated closely, in some cases the features has been kept as they have shown a strong correlation to the weed coverage. The 9 features are

- Straightness - describes the straightness of the plant
- Mean distance
- Width consistency
- Colinearity
- Colinearity 2. attempt
- Energy at 90 degrees
- Energy at 90 degrees measured at a distance of 50 pixels
- Energy at 90 degrees measured at a distance of 90 pixels
- Rotational variance

The initial results based simulations using 1000 artificial images with varying densities of maize (monocot) and weeds (dicots) is illustrated below. The results has been obtained using the data estimation tool Eureqa, made by Cornell University, which uses a Genetic Algorithm to find the equation which best describes a point cloud. When optimizing for the lowest mean error this results in a mean error of 0.54% and an maximum error of 41%. When optimizing for lowest maximum error, the mean error is 7.8% with a maximum error of 24.8%.

Referring to Figure 2 there is shown 1000 test images with changing weed densities were analyzed with Modivoci. The figure show the relation between the actual weed density and the estimated weed density.

All samples were ordered according to the actual weed density (plotted as the thick black line). For all samples were the estimated weed density shown as black circles. The figure proves that the estimated weed pressure provided by Modicovi is strongly correlated to the actual weed pressure.

Referring to Figure 3 the correlation between the actual weed pressure and the predicted weed pressure is shown. The samples used for training the estimator are marked with circles and the test samples are marked with solid dots.

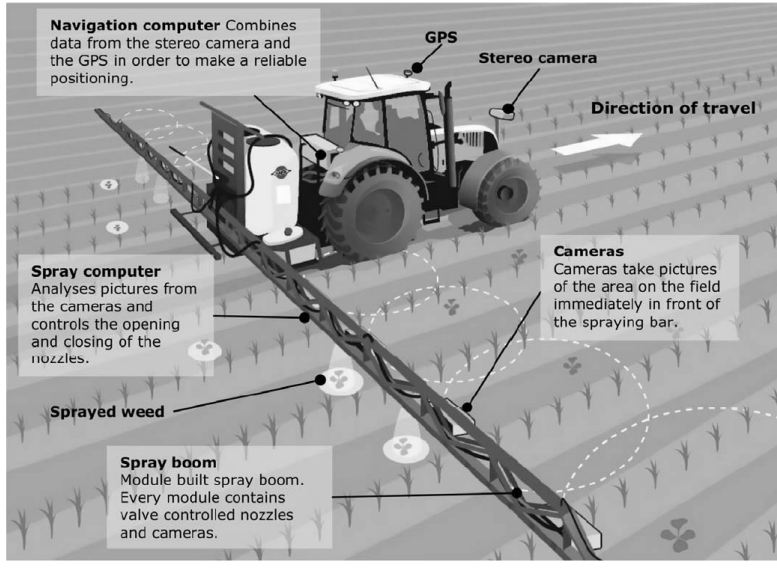
Navigation computer Combines data from the stereo camera and the GPS in order to make a reliable positioning.
GPS
Stereo camera
Direction of travel
Spray computer Analyses pictures from the cameras and controls the opening and closing of the nozzles.
Cameras Cameras take pictures of the area on the field immediately in front of the spraying bar.
Sprayed weed
Spray boom Module built spray boom. Every module contains valve controlled nozzles and cameras.

Figure 1

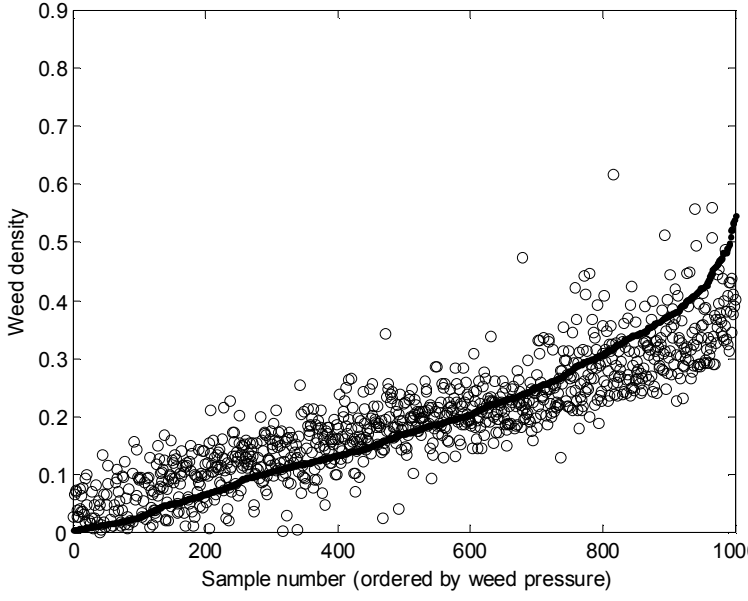
Weed density
Sample number (ordered by weed pressure)
0
0.1
0.2
0.3
0.4
0.5
0.6
0.7
0.8
0.9
0
200
400
600
800
1000

Figure 2

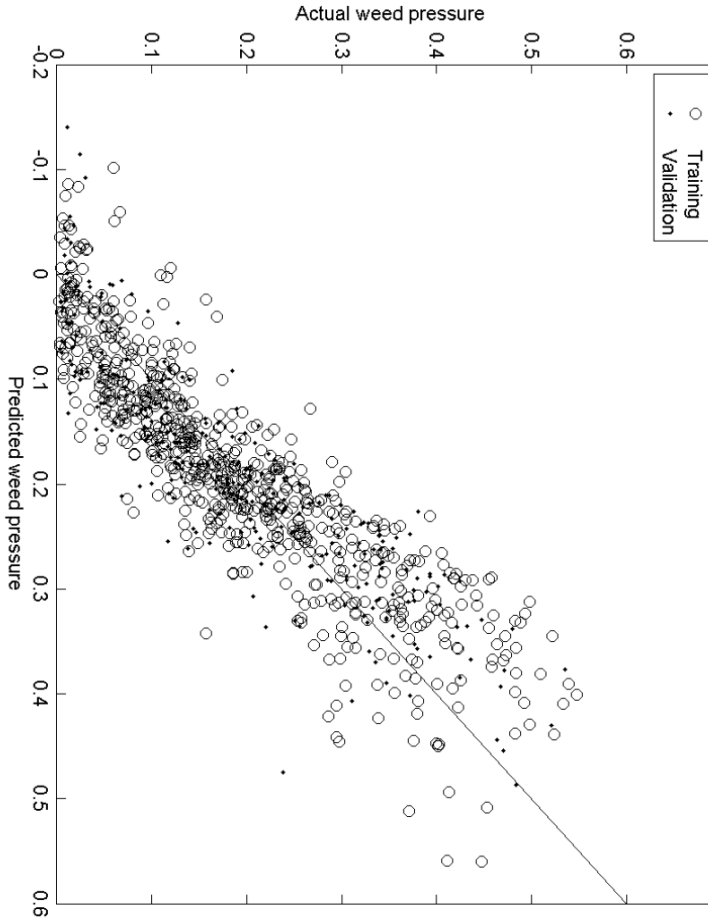
Actual weed pressure
Predicted weed pressure
Training
Validation
0.6
0.5
0.4
0.3
0.2
0.1
0
-0.1
-0.2

Figure 3

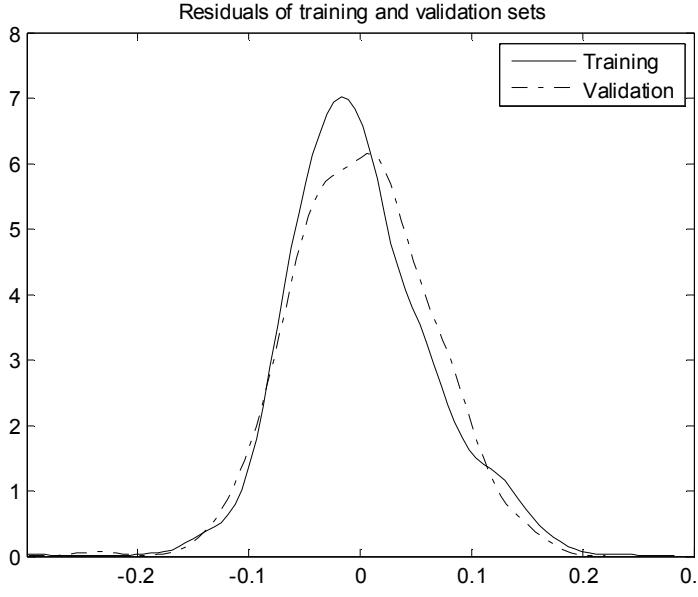
Residuals of training and validation sets
Training
Validation
8
7
6
5
4
3
2
1
0
-0.2
-0.1
0
0.1
0.2
0.3

Figure 4

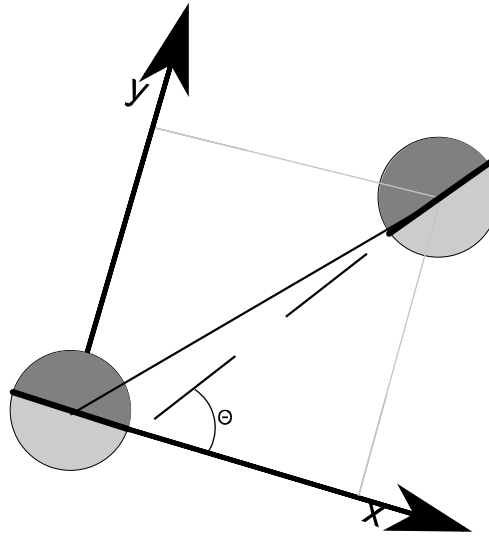

Figure 5

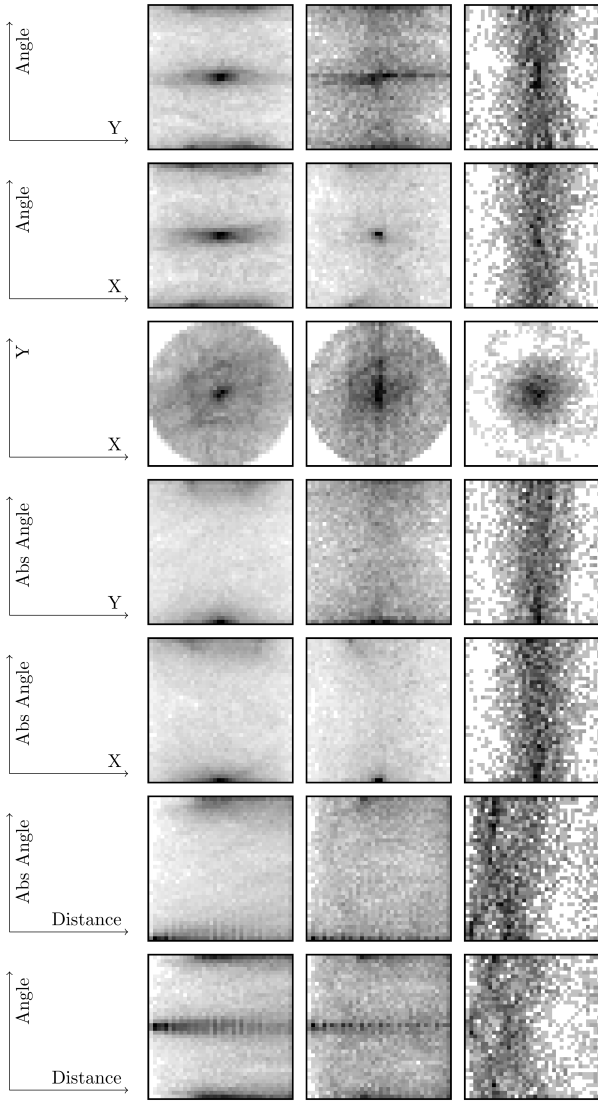
Angle
Y
Angle
X
Y
X
Abs Angle
Y
Abs Angle
X
Abs Angle
Distance
Angle
Distance

Figure 6

CLAIMS

1. A spray boom for selectively spraying a herbicidal composition onto dicots in a living vegetation, the spray boom comprising:

- means for digitally recording an image of a selected area to be treated by a nozzle on the spray boom, whereby a plant material is identified based on a segmentation procedure that transforms the raw image data of the image into a measure which describes the likeliness that a given pixel or point of the image is living vegetation, such as leaves;
- means for detecting dicots by estimating the curvature of the leaves by sampling locally distributed points placed on the edges of the leaves, said means for estimating the curvature measuring the orientation of the edge at the points in a global coordinate frame;
- a plurality of spray nozzles evenly distributed along the spray boom;
- means for activating one or more of the spray nozzles in response to detected dicots so as to selectively apply the herbicidal composition onto the sensed area containing the dicots.

2. A spray boom according to claim 1, wherein the selected area to be treated is less 250 mm x 200 mm.

3. A spray boom according to claim 1 or 2, wherein the measure which describes the likeliness that a given pixel is living vegetation is based on thresholding Excessive Green (2xGreen – Red – Blue) or NDVI ((NIR-Red)/(NIR+Red).

4. A method for selectively spraying a herbicidal composition onto dicots in a living vegetation, said method comprising the following steps:

- segmentation of an image into points of a selected area of a field in living vegetation and non-vegetation regions;
- detection of dicots by determining the curvature of the leaves through sampling locally distributed points placed on the edges of the leaves and measuring the orientation of the edge at the points in a global coordinate frame; and
- spraying the herbicidal composition to the selected area , wherein dicots have been detected.

ABSTRACT

There is provided a method and spray boom for discriminating cereal crop (monocot) and weeds (dicots). The spray boom includes means for digitally recording an image of a selected area to be treated by a nozzle on the spray boom, whereby a plant material is identified based on a segmentation procedure; and means for detecting the edges and estimating the angles of the edges of the leaves so as to discriminate between dicots and monocots; and means for activating one or more of the spray nozzles in response to detected dicots so as to selectively apply the herbicidal composition onto the sensed area containing the dicots.

Paper III

Estimating plant stem emerging point of beets in early growth stages

Estimating plant stem emerging point of beets in early growth stages. / Midtiby, Henrik Skov; Mosgaard Giselsson, Thomas; Jørgensen, Rasmus Nyholm. Biosystems Engineering, Vol. 111, p. 83-90, 2011.

Accepted by Biosystems Engineering.

Available online at www.sciencedirect.com

SciVerse ScienceDirect

journal homepage: www.elsevier.com/locate/issn/15375110

Research Paper

Estimating the plant stem emerging points (PSEPs) of sugar beets at early growth stages

Henrik S. Midtiby, Thomas M. Giselsson, Rasmus N. Jørgensen*

Institute of Chemical Engineering, Biotechnology and Environmental Technology, University of Southern Denmark, Niels Bohrs Allé 1, 5230 Odense M, Denmark

ARTICLE INFO

Article history:
Received 11 February 2011
Received in revised form
12 October 2011
Accepted 31 October 2011
Published online 21 November 2011

Successful intra-row mechanical weed control of sugar beet (*beta vulgaris*) in early growth stages requires precise knowledge about location of crop plants. A computer vision system for locating plant stem emerging point (PSEP) of sugar beet in early growth stages was developed and tested. The system is based on detection of individual leaves; each leaf location is then described by centre of mass and petiole location. After leaf detection were the true PSEP locations annotated manually and a multivariate normal distribution model of the PSEP relative to the located leaf was built. From testing the system, PSEP estimates based on a single leaf have an average error of ~3 mm. When several leaves are detected the average error decreases to less than 2 mm.

© 2011 IAgrE. Published by Elsevier Ltd. All rights reserved.

1. Introduction

Mechanical inter-row weeding between crop rows has been used for a long time. However, mechanical intra-row weeding within rows between the single crop plants is relatively new. Physical intra-row methods can, in general, rely on three different strategies (Griepentrog & Dedousis, 2010: chap. 11): (1) soil coverage of weeds or (2) weed root/stem cutting or (3) uprooting of weeds (whole plant or partly). The first option is only relevant in some crop types such as cereals and potatoes. Sugar beet (*beta vulgaris*) at dicotyledon stage does not belong to these groups (Kouwenhoven, 1997; Melander, 2000) and only strategy (2) and (3) may be used.

Several intra-row mechanical weed management methods need to know where the crop plants are located, especially with concern to the plant stem emerging point (PSEP) which is defined as the point where the plant stem emerges from the soil surface. Computer vision was used by Tillett, Hague, Grundy, and Dedousis (2008) to locate transplanted cauliflower plants, before a cultivation disc was used so that the crop plants were not harmed. RTK-GPS has been used to mark the position of crop seeds during sowing (Griepentrog, Nørremark, Nielsen, & Blackmore, 2005), but the PSEP is not identical to the planted seed position, as the orientation of the seed is not taken into account. Nørremark, Griepentrog, Nielsen, and Søgaard (2008) used RTK-GPS coordinates to control a cycloid hoe doing intra-row weed control based on seed positions. Uncertainty in seed orientation, PSEP, and GPS accuracy limited the achievable precision to approx 30 mm. Sun et al. (2010) used RTK-GPS for mapping transplanted tomatoes; 95% of the plants were within 51 mm from the true plant position. Based on vision input crop plant positions may be determined with a higher accuracy and precision as Åstrand and Baerveldt (2002) indicated by guiding an autonomous weed robot with 20 mm accuracy along crop rows. Earlier work on extraction of individual leaves from images included that of Franz, Gebhardt, and Unklesbay (1991) which analysed boundary curvature by comparing with a known leaf shape and Neto, Meyer, and Jones (2006) which detected individual leaves in complex scenes based on

* *Corresponding author*. Tel.: +45 21356105.
E-mail address: hemi@kbm.sdu.dk (H.S. Midtiby).
1537-5110/$ – see front matter © 2011 IAgrE. Published by Elsevier Ltd. All rights reserved.
doi:10.1016/j.biosystemseng.2011.10.011

Symbols and description

$\vec{S}$	Petiole location, mm
$\vec{C}$	Leaf centre of mass, mm
$\vec{z}_k$	List of boundary coordinates, mm
k	Index variable
Δ	Smoothing length
l	Temporary distance threshold, mm
$\vec{x}_{lc}$	Average PSEP location in plant frame, mm
Σ_{1c}	Covariance matrix of PSEP location in plant frame, mm^2
$\chi^2_{2,\alpha}$	Chi square distribution with two degrees of freedom at the level 1 - α
x,y	Coordinate in plant frame, mm
$P_A(\vec{x}), P_B(\vec{x}), P_C(\vec{x})$	Probability distribution of PSEP location in global frame, mm^{-2}
$\vec{x}^A_c, \vec{x}^B_c, \vec{x}^C_c$	Average PSEP location in global frame, mm
$\Sigma_A, \Sigma_B, \Sigma_C$	Covariance of PSEP location in global frame, mm^2
$D_1, \ldots, D_6$	Sets of PSEP estimates produced by different methods

Abbreviations

MR	Missed root
BBCH	Growth stage classification scheme by Biologische Bundesanstalt, Bundessortenamt and chemical industry
FP	False positive
PSEP	Plant stem emerging point
RTK-GPS	Real time kinematics GPS
GPS	Global positioning system
NDVI	Normalised difference vegetation index

Gustafson–Kessel clustering. This paper describes and evaluates a vision based method which detects single crop leaves and predicts where the corresponding PSEP is located.

2. Materials and methods

The current work consists of three parts: (1) development of a leaf detector, (2) building of a relative PSEP model, and (3) using the relative PSEP model to predict true PSEP based on detected leaves. An example image of sugar beet plants in early growth stages is shown in Fig. 1. The leaves can be described as convex objects with a thin stem (petiole). Leaves are detected by locating convex regions of the plant contour. The relative PSEP model is generated by comparing manually marked PSEP locations (i.e. ground truth values) with the detected leaves. Based on the relative PSEP location model and detected leaves, estimates of the true PSEP locations are obtained automatically. Finally, the methods for evaluating performance are described.

2.1. *Image acquisition and segmentation*

Images from sugar beet fields were acquired using a bi-spectral line scanning camera mounted on the Robovator (Poulsen, 2010) intra-row mechanical weeding robot. The setup for image capturing is shown in Fig. 2. The imaged sugar beet plants were part of field emergence trials conducted by Maribo Seed, Højbygårdvej 31, 4960 Holeby, Denmark in 2009. Precise plant placement is not required for field emergence trials which can be seen directly in the acquired images where sugar beet plants are distributed randomly over the captured region. The plants were in growth stages BBCH10-14. The captured area was illuminated with two 55 W halogen lamps. Each line in the acquired image consists of 256 pixels and a typical data file consisted of approximately 13,000 scan lines. A single pixel measured approximately 1.1 mm × 1.1 mm. A sample image can be seen in Fig. 1. For each pixel both a red and a near infrared value were available. Combining red and near infrared values makes it possible to segment images into plant material and soil which was done by calculating the normalised difference vegetation index (NDVI) value for each pixel (Backes & Jacobi, 2006). After this operation a single channel image was obtained with plant material having a high NDVI value compared to soil. This image is segmented using a threshold of 0.2 to form a binary image, the threshold was found by trial and error. These binary images are the basis for the data material used in this paper. Before further analysis the connected components are located. It was assumed that a leaf will only contribute to one connected blob. To remove noise, only blobs with areas larger than 160 pixels were kept.

2.2. *Leaf extraction*

For detecting leaves the general leaf structure was exploited. Examples of leaf shapes are shown in Fig. 1. The structure consisted of a large mainly convex region attached to the rest of the plant via a thin stem (petiole) (Meier, 2001). The leaf extraction method works in two steps. First convex regions are located and marked as leaf tip candidates; this is described in

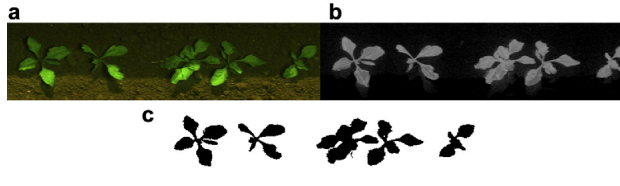

Fig. 1 – Plant segmentation was done in two steps. First were NDVI values calculated for each pixel, then was the image thresholded. The shown images are (a) pseudo RGB image of raw data (red is shown as red and NIR is shown as green while the blue channel is set to zero) (b) NDVI image before thresholding and (c) after thresholding.

Section 2.3. From the located leaf tip candidate a search for the corresponding petiole is then initiated, the search process is described in Section 2.4. If a petiole was located a leaf was found. When a leaf was detected the leaf location and orientation was described by petiole location $\vec{S}$ and the leaf centre of mass $\vec{C}$.

2.3. *Leaf tip candidate location*

Leaf tip candidates were found at local curvature minima in curvature of the plant boundary. At this stage the plant boundary was specified as the list of coordinates $\vec{z}_k$ where $k \in [1,\ldots,n]$ and the boundary was followed in a clockwise direction. The curvature was then defined as the angle between the line connecting point $k-\Delta$ and k and the line connecting point k and $k+\Delta$. The sign of the direction change indicated whether the current location of the boundary was concave or convex. The parameter $\Delta = 12$ was used together with a running average of the five nearest points. Plant boundary and curvature along the boundary was visualised in Fig. 3. Local maxima corresponds to concave regions, which were often located at leaf intersections or near the sugar beet growth point, which was assumed to be vertically above PSEP where several leaves are connected to a common area. Local minima corresponded to convex regions such as leaf tips.

To locate a candidate single leaf tip for each leaf, the following steps were used: (1) division of the boundary into concave and convex regions, (2) location of the minima in each convex region and (3) thresholding of the located minima. The purpose of the first step was to split the boundary into segments that at most contained a single leaf tip. Splitting points were used as locations where the curvature changes from positive to negative or from negative to positive values. The second step found the most likely leaf tip location, which were the points along the boundary where the boundary was convex and the change of direction was maximised. Step three removed possible leaf tip locations according to change of direction, if the change of direction was too small (i.e. less than 1 radians) the candidate was eliminated.

Fig. 2 – The camera unit consisted of camera combined with halogen lamp. During image acquisition were eight such units mounted in front of a tractor.

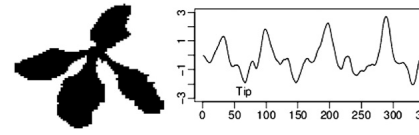

Fig. 3 – Example of plant boundary and the calculated curvature along the boundary. The boundary is followed clockwise. Leaf tips are local minima and locations near the PSEP corresponds to peaks.

2.4. *Location of corresponding petiole*

From each of the candidate leaf tips a search for the corresponding petiole was then initiated. Two walkers were placed at the leaf tip with the goal of following the boundary in each direction, one clockwise and one counter-clockwise. The movement of the walkers was controlled such that they reached the petiole nearly simultaneously. Each walker was then moved forward until the next step along the boundary brought the Euclidean distance between the walker and the leaf tip point above the specified threshold distance l. The distance between the walkers was then measured. This process (walker movement and distance measurement) was repeated with increasing values of l. In Fig. 4 the search strategy is visualised. For each value of the distance threshold the corresponding circle was drawn together with the two walker locations.

To locate the petiole, the distance between the walkers was investigated as follows: (1) search for a narrow leaf region which initiated the region in which the petiole could be located followed by (2) a search for a broadening of the leaf width which ends the region in which the petiole could be found. This strategy was implemented as a state machine. The state machine started in the leaf tip state and remained

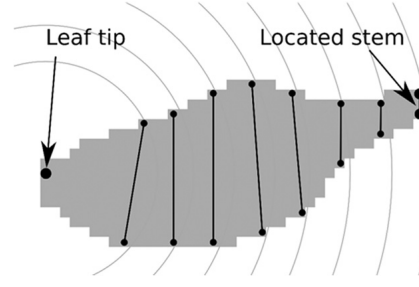

Fig. 4 – Visualisation of the search strategy. The boundary was followed from the leaf tip until the Euclidean distance between the current location and the leaf tip exceeded a specified threshold. This was done in both directions and distance between the located points was measured. The procedure was repeated with increasing distance thresholds illustrated by concentric circles. When the distance between located points was minimised the leaf cut-off location was found.

there until the distance between the two walkers got below half of the maximum distance between the walkers. At this point the state was changed to the leaf–stem state. In the leaf–stem state the system kept a track of the minimum distance between the walkers and corresponding walker locations. When the distance between the walkers exceeded three times the minimum distance observed in the leaf–stem state the search was terminated. The leaf boundary cut-off positions were given by the location of the walkers where the distance between the walkers was minimised within the leaf–state. The petiole location was set to the midpoint of the two boundary cut-off positions. To avoid infinite loops the petiole search was terminated if one of the walkers reached a leaf tip candidate or the two walkers passed each other.

2.5. *Manual marking of root/leaf relative locations*

After the automatic extraction of plant leaves, as described in Section 2.2, real PSEP locations were marked manually. A program showed each plant and the user then marked the pixel nearest the true PSEP. Fig. 5 illustrates a sample image with PSEPs marked with red spots and detected leaves marked by orange. To describe the marked PSEP location relative to the extracted leaf, the leaf coordinate system is placed with origin located at the petiole $\vec{S}$ and direction of the x axis parallel to the vector $\vec{C}-\vec{S}$. An example is shown in Fig. 6.

The manual annotation of the location of the true PSEP locations was prone to errors. PSEP locations were marked with a single pixel, so the average quantisation error will be ~0.5 mm along each dimension. The true PSEP locations marked by an operator will also have an uncertainty. To estimate size of the typical error in this process the same image was annotated by two persons. Differences in PSEP locations were calculated and mean distance between annotations was determined.

2.6. *PSEP location model*

A multivariate normal distribution was used to model the PSEP location within the leaf coordinate system. The model was defined as:

$$p(\vec{x}) = \frac{1}{2\pi|\Sigma_{lc}|}\exp\left[\frac{-1}{2}(\vec{x}-\vec{x}_{lc})^T\sum_{lc}^{-1}(\vec{x}-\vec{x}_{lc})\right] \quad (1)$$

where $\vec{x}_{lc}$ is the centre of the true PSEP estimate and $\sum_{lc}$ is the covariance matrix. Both $\vec{x}_{lc}$ and $\sum_{lc}$ are expressed in the leaf coordinate system. Ellipses were used to visualise the multivariate normal distribution, contours of certain values are drawn such that a given fraction of the probability is inside the ellipses. To calculate the ellipses the formula below is used:

$$(\vec{x}-\vec{x}_{lc})^T\sum_{lc}^{-1}(\vec{x}-\vec{x}_{lc}) = \chi^2_{2,\alpha} \quad (2)$$

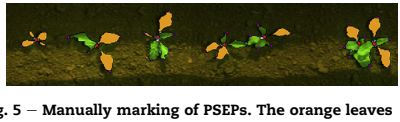

Fig. 5 – Manually marking of PSEPs. The orange leaves were detected by the leaf detector. PSEPs are marked with red spots.

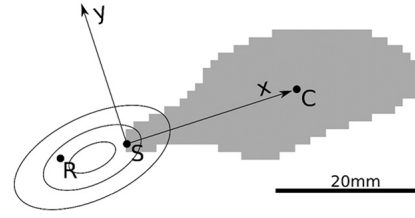

Fig. 6 – PSEP location as specified in the leaf coordinate system. Where the centre of mass is C, stem attach point S and PSEP location R. The PSEP location model is indicated by the three concentric ellipses. According to the PSEP location model, 68% of the true PSEP locations will be placed within the central ellipse, the two other ellipses will contain 95% and 99.7% respectively.

where $\chi^2_{2,\alpha}$ is the χ^2 distribution with 2 degrees of freedom and P value $1-\alpha$. Typical fractions used for visualisation are 68%, 95% and 99.7%. As the PSEP is defined relative to the leaf (Fig. 6) the x and y coordinate values were translated to a displacement along the major leaf axis and displacement perpendicular to the same axis respectively. The PSEP was expected to lie in extension of the primary leaf axis (low y values) shifted to negative x values. For later analysis position and uncertainty parameters were converted to the global coordinate system using a coordinate transformation based on rotation and translation.

2.7. *Combination of relative PSEP location models*

In many cases it is possible to detect more than a single leaf, an example is shown in Fig. 7. In the figure 99.7% ellipses of the two estimates of the true PSEP share a common region and it could be expected that the true PSEP was located within this region. To combine two PSEP models ($p_A(\vec{x})$ and $p_B(\vec{x})$) the probability densities are multiplied and normalised.

$$p_c(\vec{x}) \propto p_A(\vec{x})\cdot p_A(\vec{x}) \quad (3)$$

If the PSEP models are defined by the parameters $\sum_A, \sum_B$, $\vec{x}_c^{\,A}$ and $\vec{x}_c^{\,B}$ the parameters of the combined model expressed as (Gales & Airey, 2006)

$$\sum_C^{-1} = \sum_A^{-1} + \sum_B^{-1} \quad (4)$$

$$\vec{x}_c^{\,C} = \sum_C\left(\sum_A^{-1}\vec{x}_c^{\,A} + \sum_B^{-1}\vec{x}_c^{\,B}\right) \quad (5)$$

This combination of PSEP models was based on the same principle as least squares estimation used in the Kalman filter.

2.8. *Generation of position predictions*

To test the developed method for PSEP estimation, the method was applied to a test image. True plant locations were determined manually and compared to six sets $D_{1,\ldots,6}$ of predicted PSEP locations. These sets were used to measure accuracy of

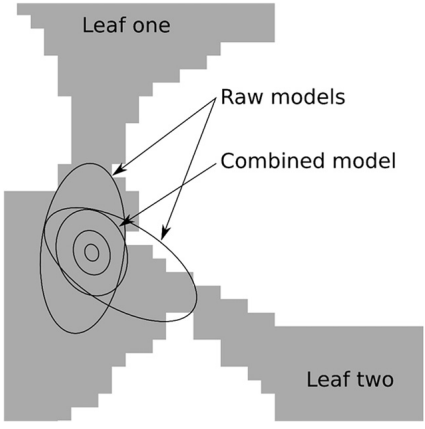

Fig. 7 – Combination of two PSEP location models. The ellipses are similar to those shown in Fig. 6. For the raw models the ellipses for 99.7% are shown and for the combined model 68%, 95% and 99.7%, respectively.

the located PSEPs under different conditions, eg. different number of detected leaves per plant.

From all the detected leaves a PSEP were generated (using only information from this leaf). This was a set D_1. D_2 containing PSEPs calculated from two detected leaves. All possible combinations were tested and leaf pairs were combined if distance between centres of their PSEP models was less than 20 mm. D_3 and D_4 were similar to D_2 except that 3 and 4 leaves are used for calculating the PSEP. For a plant where n leaves were detected, the set D_k would contain $\binom{k}{n}$ elements related to that plant. Not all plants had all four leaves detected, therefore they did not contain PSEPs associated to these plants. Thus the number of leaves used to calculate PSEPs increased, the precision of the located PSEPs increased, but a larger fraction was missed. D_5 was a compromise between large coverage and low placement error. The set was built on D_1 by merging PSEP models with a distance between predicted plant centres of 20 mm or less. This merging scheme generated combined PSEP models based on position information from up to 4 leaves. In addition was a set, D_6, generated by manual annotation by a different person than the one who marked the reference PSEPs. D_6 covered only one third of the test image and was used to estimate the uncertainty of the manually marked PSEPs.

2.9. *Performance evaluation*

Performance of the PSEP location models was judged according to the following values:

False positives (FPs): If a leaf was falsely found by the leaf separator method it constituted a FP. These cases were characterised by having a long distance from the predicted PSEP to the nearest true PSEP. FPs were detected by setting a threshold on the allowed distance from predicted leaf location to the nearest true PSEP.

Missed PSEP locations: If none of a plant's leaves were detected a PSEP was missed. It was characterised by having a long distance from the true PSEP to the nearest predicted PSEP. Missed PSEPs were detected by setting a threshold on the allowed distance.

Predicted position error: The errors in the predicted PSEP location were averaged for all predicted PSEP locations with an error less than a threshold of 20 mm.

3. Results

3.1. *Leaf detector performance*

For evaluating performance of the leaf detector, the 805 leaves present in the test images were counted manually. The leaf detector located 46.6% (395) leaves, of those 2.4% (19) were FPs.

3.2. *Relative PSEP model*

The leaf detector was applied to three datasets. True PSEPs were marked by hand in all three datasets. Additionally leaves were detected by the leaf detector method and their location specific information recorded. Analysing leaves and PSEPs led to the generation of 223 data points. In the local leaf coordinate system the multivariate normal distribution model was described by the parameter values:

$$\vec{x}_{lc} = \begin{pmatrix} 5.40 \\ 0.24 \end{pmatrix} \text{mm} \qquad \sum_{lc} = \begin{pmatrix} 12.65 & 1.28 \\ 1.28 & 2.35 \end{pmatrix} \text{mm}^2 \tag{6}$$

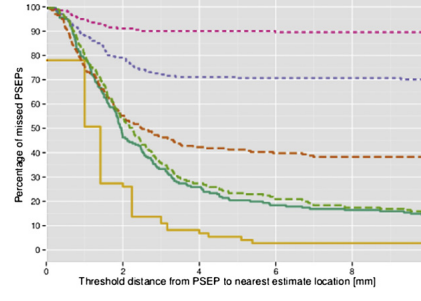

Fig. 8 – Fraction of missed PSEPs as a function of the threshold distance. When the number of leaves used to estimate true PSEPs was increased, the fraction of missed PSEPs also increased. The following colour coding is used: D1: dashed green line, D2: dashed dark orange line, D3: dotted blue line, D4: dotted pink line, D5: green line and D6: orange line.

Table 1 – Performance statistics of the PSEP estimates. Count; number of position estimates. FP; false positives, percentage of predicted plant positions with a distance to the nearest true plant location larger than 20 mm. MR; missed roots, percentage of true PSEPs within 20 mm of a predicted PSEP location. Avg; average estimate error in mm. 95%; the 95% quantile of estimate errors in mm.

Set	Number of leaves	Count	FP	MR	Avg	95%
D_1	1	395	4.8%(19)	10.0%	3.29 ± 0.14	15.76
D_2	2	313	1.6%(5)	37.3%	1.88 ± 0.07	4.62
D_3	3	132	0.8%(1)	70.1%	1.42 ± 0.09	3.02
D_4	4	29	0.0%(0)	89.1%	1.22 ± 0.20	2.39
D_5	1–4	188	8.0%(15)	10.4%	2.66 ± 0.21	49.51
D_6	na	71	0.0%(0)	2.7%	1.37 ± 0.26	3.58

3.3. *Fraction of PSEP locations found*

The fraction of missed PSEPs was visualised as a function of the chosen threshold in Fig. 8. All six PSEP prediction methods showed the same trend. At first the fraction of missed PSEPs decreased linearly until the curve flattened out. The point where the curve flattened out indicated the maximum error of the position estimate and the fraction of PSEPs that were not found. Note that humans were good at locating a large fraction of the PSEPs. The fraction of roots not found within 20 mm is shown in the missed root (MR) column in Table 1. If a single leaf (D_1) was used to predict PSEPs, approximately 10% of the true PSEPs were missed, this number increased strongly when the number of leaves used in the prediction was increased. Approximately 37% of the true PSEPs were missed with estimates based on two leaves and this number increased to ~89% when four leaves were used to generate estimates. This increase in the fraction of missed PSEPs was only to be expected, as the plants with one or two detected leaves were not present in D_3 and D_4.

3.4. *Fraction of FPs*

To gain insight in the accuracy of PSEP location estimates the fraction of FPs was visualised as a function of threshold distance in Fig. 9. The figure was divided into four regions, each representing a dataset. Dataset *One* is the PSEP near which the leaf detector found a single leaf; *Three* is when the leaf detector located three leaves. From the green curve it is seen that ~20% of the D_1 position estimates had a distance (error) > 4 mm to the nearest true PSEP, for comparison the corresponding distance for D_2 was 3 mm. The figure shows that when the number of leaves used to generate a PSEP location estimate was increased the error in the estimate was reduced significantly. The figure was divided into four underlying datasets such that each dataset could be weighted appropriately. If all the data was shown in one plot it would have been difficult to interpret because each set of location estimates was based on a unique dataset. The number of FPs and MRs for each of the estimate sets is given in Table 1. The listed values were found using a threshold distance of 20 mm. In addition the estimate error (distance from estimate to nearest PSEP) was described using the average value and the 95% quantile (i.e. 95% of the predicted PSEP had an error of less than that value).

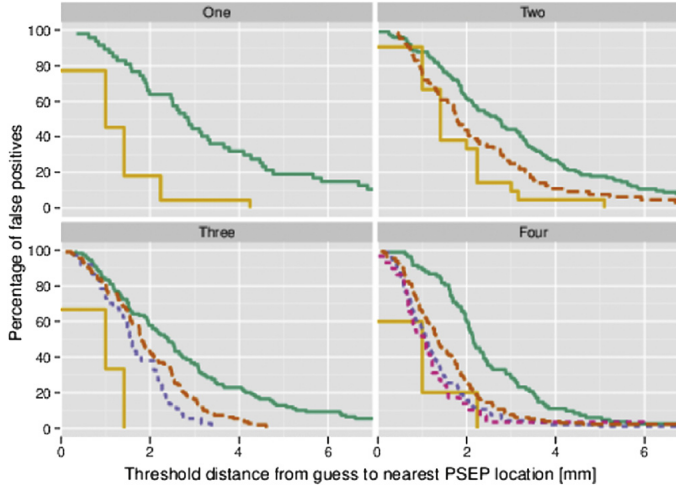

Fig. 9 – Fraction of false positives as a function of the threshold distance. Error of PSEP location estimates was seen to decrease when the number of leaves used to make the estimate increased. Colour codings as in Fig. 8.

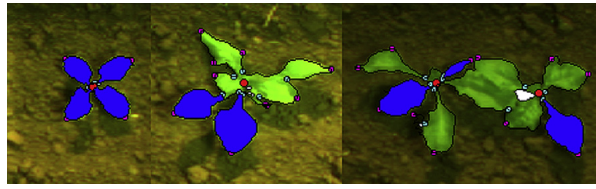

Fig. 10 – Easy and difficult cases for the leaf detector. Leaf tip candidates are marked by purple squares. Cyan indicates concave locations. Detected leaves are marked in blue.

4. Discussion

The leaf detector was not able to locate all leaves in the test images. This was due to overlapping leaves, leaves with irregular shapes and, to a certain extent, limitations in the implemented algorithm. Some typical cases are shown in Fig. 10. The petiole search was fragile and failed if more than a single leaf tip candidate was found in one leaf. In the used leaf definition (convex area with a thin petiole) overlapping leaves could have influenced both criteria: the combined leaf area was not guaranteed to be convex and the petiole region could have been hidden or widened. Rarely will the relative location of leaf tip estimate and petiole cause the petiole search strategy to fail; this is the case when the distance between petiole and leaf tip estimate is less than the distance between leaf tip estimate and the true leaf tip. To reduce the fraction of missed PSEPs the leaf detector must be improved. If a PSEP is not located none of the associated leaves have been detected.

Before evaluation of the implemented algorithms the uncertainty of the true PSEP position should be investigated. This can be achieved by comparing true PSEPs with PSEPs determined by a person different from the one who determined the true PSEPs initially. The difference between such two manual annotations can be used as an estimate of the position uncertainty of the true PSEPs. On average the difference was 1.37 mm and in 95% of the cases the difference between the two human annotations was < 3.58 mm. Two sources contributed to this difference (1) quantification errors and (2) the uncertainty / unreliability of the human annotation. The quantification error originated from the annotation program, which used integer coordinates to describe PSEPs. A rough estimate of this error is ~ 0.5 mm along the two coordinate axes. The human annotation unreliability originated from differences in test image interpretation.

When the leaf detector found two leaves of a single plant the corresponding true PSEP will, with a probability of 95%, be within a distance of 5 mm or less from the estimate. This and similar values are shown in Table 1. Sun et al. (2010) were able to measure the position of transplanted crops with an RTK-GPS unit within 51 mm for 95% of the plants. The accuracy of the vision system was therefore one order of magnitude better than RTK-GPS seeding of plants. When three or more leaves were used to predict PSEPs the accuracy was comparable to the human annotation. One interpretation of this is that the developed method can predict PSEPs with a higher accuracy than the reference predictions based on manual annotation given that two or more leaves are detected for each PSEP.

5. Conclusion

A system for automated PSEP estimation of sugar beet plants (in growth stages BBCH10-14) based on leaf detection has been developed and tested. In a set of test images the system detected 46.7% of the present leaves. A multivariate Gaussian PSEP model was built based on the detected leaves and manual annotation of true PSEPs. Given centre of mass and attach point of a single leaf the model stated that the average true PSEP was at a distance of 6.2 mm from the petiole attachment point and placed on the line connecting the leaf attach point and the leaf centre of mass. Ninety-five % of the volume below the multivariate Gaussian was contained within an ellipse with semi-major and semi-minor axes of 12 mm and 6 mm respectively.

In the set of test images the detected leaves were used to predict the true PSEPs. With PSEP predictions based on single leaves 90% of the true PSEPs were located within 20 mm of at least one predicted PSEP location. In this case the average distance from the predicted location to the true PSEP was 3.3 mm. When several leaves of the same plant are detected, the PSEP models can be combined using least-squares estimation and thus produce an even better estimate of the true root location. For example, by combining two leaves the average error was reduced to 1.9 mm. Precise quantification of the error in three and four leaf based PSEP estimates is hindered as these methods performed on par with the human annotation used as reference.

REFERENCES

Åstrand, B., & Baerveldt, A.-J. (Jul. 2002). An agricultural mobile robot with vision-based perception for mechanical weed control. *Autonomous Robots*, 13(1), 21–35. http://dx.doi.org/10.1023/A:1015674004201.

Backes, M., & Jacobi, J. (2006). Classification of weed patches in Quickbird images: verification by ground truth data. *EARSeL European Association of Remote Sensing Laboratories*, 5(2), 172–179. http://www.eproceedings.org/static/vol05_2/05_2_backes1%.html.

Franz, E., Gebhardt, M.Unklesbay, K. (1991). Shape description of completely visible and partially occluded leaves for identifying plants in digital images. 34. p. 673–681.

Gales, M., & Airey, S. (Jan. 2006). Product of Gaussians for speech recognition. *Computer Speech & Language*, 20(1), 22–40. http://

www.sciencedirect.com/science/article/B6WCW-4FBH%W7F-1/2/b1001c29af3057ecce30bfe8e9592955.

Griepentrog, H. W., & Dedousis, A. P. (2010). *Mechanical weed control, Vol. 20*. Heidelberg: Springer Berlin, 171–179.

Griepentrog, H. W., Nørremark, M., Nielsen, H., & Blackmore, B. S. (2005). Seed mapping of sugar beet. *Precision Agriculture, 6*, 157–165. doi:10.1007/s11119-005-1032-5. http://dx.doi.org/10.1007/s11119-005-1032-5.

Kouwenhoven, J. K. (1997). Intra-row mechanical weed control–possibilities and problems. *Soil and Tillage Research, 41*(1–2), 87–104. http://www.sciencedirect.com/science/article/B6TC6-3RGT%BJD-7/2/3ce3ed554667f0adfed53ebb227deeb6.

Meier, U. (2001). Growth stages of mono-and dicotyledonous plants. http://www.bba.de/veroeff/bbch/bbcheng.pdf.

Melander, B. (2000). Mechanical weed control in transplanted sugar beet. In: 4th EWRS Workshop on Physical Weed Control. http://orgprints.org/1542/1/Abstract_Elspeet1.pdf.

Neto, J. C., Meyer, G. E., & Jones, D. D. (Apr. 2006). Individual leaf extractions from young canopy images using Gustafson-Kessel clustering and a genetic algorithm. *Computers and Electronics in Agriculture, 51*(1–2), 66–85. http://www.sciencedirect.com/science/article/B6T5M-4J2M%44F-1/2/b947a39d2c204692a56e44750203ac42.

Nørremark, M., Griepentrog, H., Nielsen, J., & Søgaard, H. (2008). The development and assessment of the accuracy of an autonomous gps-based system for intra-row mechanical weed control in row crops. *Biosystems Engineering, 101*(4), 396–410. http://www.sciencedirect.com/science/article/B6WXV-4TX6%W5S-1/2/8aede62984cd66ed1ef62aa58e1518f3.

Poulsen, F. (2010). Measuring emerging plants using machine vision. http://www.visionweeding.com/Products/Plant-Counting/Plant-Counting.htm.

Sun, H., Slaughter, D. C., Ruiz, M. P., Gliever, C., Upadhyaya, S. K., & Smith, R. F. (Apr. 2010). Rtk gps mapping of transplanted row crops. *Computers and Electronics In Agriculture, 71*(1), 32–37.

Tillett, N., Hague, T., Grundy, A., & Dedousis, A. (2008). Mechanical within-row weed control for transplanted crops using computer vision. *Biosystems Engineering, 99*(2), 171–178. http://www.sciencedirect.com/science/article/B6WXV-4R5H%1V8-2/2/4487816230cc4673f885d6bd784c79a2.

Paper IV

Performance evaluation of a crop / weed discriminating microsprayer

Performance evaluation of a crop / weed discriminating microsprayer. / Midtiby, Henrik Skov; K. Mathiassen, Solvejg; Andersson, Kim Johan; Jørgensen, Rasmus Nyholm. Computers and Electronics in Agriculture, Vol. 77, Nr. 1, 2011, p. 35-40.

Accepted by Computer and Electronics in Agriculture.

Computers and Electronics in Agriculture 77 (2011) 35–40

Contents lists available at ScienceDirect

Computers and Electronics in Agriculture

journal homepage: www.elsevier.com/locate/compag

Performance evaluation of a crop/weed discriminating microsprayer

Henrik Skov Midtiby [a,*], Solvejg K. Mathiassen [b], Kim Johan Andersson [a], Rasmus Nyholm Jørgensen [a]

[a] University of Southern Denmark, Niels Bohrs Allé 1, 5230 Odense M, Denmark
[b] Department of Integrated Pest Management, Research Centre Flakkebjerg, Forsøgsvej 1, 4200 Slagelse, Denmark

ARTICLE INFO

Article history:
Received 23 March 2010
Received in revised form 8 March 2011
Accepted 20 March 2011

Keywords:
Machine vision
Weed crop discrimination
Microsprayer
Herbicide reduction
Site-specific
Close-to-crop

ABSTRACT

An intelligent real-time microspraying weed control system was developed. The system distinguishes between weed and crop plants and a herbicide (glyphosate) is selectively applied to the detected weed plants. The vision system captures 40 RGB images per second, each covering 140 mm by 105 mm with an image resolution of 800 × 600 pixels. From the captured images the forward velocity is estimated and the spraycommands for the microsprayer are calculated. Crop and weed plants are identified in the image, and weed plants are sprayed. Performance of the microsprayer system was evaluated under laboratory conditions simulating field conditions. A combination of maize (*Zea mays* L.), oilseed rape (*Brassica napus* L.) and scentless mayweed (*Matricaria inodora* L.) plants, in growth stage BBCH10, was placed in pots, which were then treated by the microspray system. Maize simulated crop plants, while the other species simulated weeds. The experiment were conducted at a velocity of 0.5 m/s. Two weeks after spraying, the fraction of injured plants was determined visually. None of the crop plants were harmed while 94% of the oilseed rape and 37% of the scentless mayweed plants were significantly limited in their growth. Given the size and shape of the scentless mayweed plants and the microsprayer geometry it was calculated that the microsprayer could only hit 64% of the scentless mayweed plants. The system was able to effectively control weeds larger than 11 mm × 11 mm.

© 2011 Elsevier B.V. All rights reserved.

1. Introduction

Effective weed control is a vital part of agriculture. Conventionally, weeds are controlled by an overall application of herbicides to the field. It has become apparent that herbicides place a heavy burden on the environment. Herbicide usage is already controlled by European laws, but in the future these restrictions are expected to increase significantly. Increased restrictions will reduce the number of herbicides and thus there exists a demand for new weed control methods. With the microsprayer approach developed in this article, herbicides are mainly deposited on weed plants.

In patchspraying, the entire field is divided into smaller patches and then the herbicide is adjusted according to the presence of weeds (Christensen et al., 2009). When the patch size is reduced, the potential reduction in herbicide use is increased (Lund et al., 2008). When the patch size reaches the size of a single plant, the process is denoted microspraying. The microspraying technique has two significant advantages: (1) high reduction of the amount of herbicide deposited on the soil, which minimizes the issue of herbicide leaching and (2) almost no deposition of herbicide on crop plants, which eliminates the potential presence of herbicide residues in the harvested crop plants and potential damages to the crop. In addition microspraying can use both selective and non-selective herbicides. Non-selective herbicides, like glyphosate used in this experiment, harm any plant while selective herbicides are tolerated by specific crop plants but can cause yield loss.

Lee et al. (1999) used a microsprayer to control weeds in tomato. The spraying system moved forward with a continuous velocity of 0.22 m/s. A camera grabbed images of the ground in front of the spraying device. A grid consisting of 8 × 18 cells were imposed on the image, and the cells containing weed plants were marked for spraying. The system was able to spray 47.6% of the weeds while 24.2% of the tomato plants was also sprayed. A similar spraying device was used by Lamm et al. (2002), to spray weeds with elongated leaves in a cotton field. The system sprayed 89% of the weeds and 22% of the cotton plants.

Søgaard and Lund (2005) investigated the accuracy and precision of a robotic system carrying a microsprayer hitting weed markers (circles with a diameter of 12 mm). The robotic system switched between two modes: image analysis and forward motion while spraying the detected circles. During the image analysis step where a single image was acquired, targets were identified and marked in a spray plan. The spray plan was represented as an 8 × 16 grid and each cell could either be marked for spraying or not. After the spray plan was generated, the robotic system moved 180 mm forward with a velocity of 0.2 m/s. During this motion the microsprayer was activated according to the spray plan. When the

* Corresponding author. Tel.: +45 21 35 61 05; fax: +45 65 50 73 54.
E-mail addresses: hemi@kbm.sdu.dk (H.S. Midtiby), Solvejg.Mathiassen@agrsci.dk (S.K. Mathiassen), kja@kbm.sdu.dk (K.J. Andersson), rasj@kbm.sdu.dk (R.N. Jørgensen).

0168-1699/$ - see front matter © 2011 Elsevier B.V. All rights reserved.
doi:10.1016/j.compag.2011.03.006

movement ended a new image was acquired and the entire process repeated. The system was able to hit the weed markers with an average position error of 2.8 mm.

Nieuwenhuizen et al. (2010) evaluated a microspraying system consisting of five nozzles used for controlling volunteer potatoes in sugar beet. Average color information was calculated for 11×11 pixel bins and used to distinguish between crop and weed plants using an adaptive Bayesian classifier. With a forward speed of 0.8 m/s the system controlled growth of 77% of the volunteer potatoes and killed up to 1% of the crop plants.

In present paper a spray targeting system that does not rely on a fixed cell grid is evaluated. By avoiding the fixed grid, the ability to hit small targets is expected to increase. When controlling a microsprayer it is important to trigger the sprayer when it is directly above the target. Using a fixed grid, the set of possible activation-times is reduced. None of the above mentioned microspray systems can move at a speed above 0.3 m/s and maintain a weed control efficiency higher than 90%. The relative low speed of the spray systems severely limits the number of plants that can be processed in a given period and a low weed control efficiency renders the systems economically unattractive. Compared to other microspray systems, our system has a higher speed relative to the treated plants and can therefore control weeds more efficiently.

Present article covers: (1) a detailed description of the vision control system and microsprayer setup, (2) calculations of the achievable hit rate given the geometry of the microsprayer and size and shape of the treated plants and (3) a performance evaluation of the entire system conducted under laboratory conditions.

2. Materials and methods

The system is a combination of three separate subsystems, (1) vision system, (2) spray planner using the acquired images and (3) physical microsprayer. The vision system captures images (Fig. 1a) which are processed by two different subsystems: a plant recognizer and a velocity estimator. The velocity estimator compares two consecutive images and determines the displacement of their common content. The plantrecognizer analyses each image and locates green objects in the image. These objects are then classified as crop or weed plants, in this process a crop and weed map is generated (Fig. 1b). The map is an interpreted version of the input image covering the same area. Based on this map and the estimated forward velocity spraycommands are generated and sent to the microsprayer controller.

2.1. Vision system

Homogeneous illumination of the field of view is provided by 18 3W white LEDs (ProLight PG1X-3LXS-SD) that are directed on the white inner surface of a half cylinder placed over the spray location. When placed in direct sunlight, the half cylinder ensures that the area to be captured is kept free of hard shadows and the homogeneous illumination eliminates specular highlights. These properties have been verified in small scale experiments with the half cylinder placed approximately 100 mm above the soil surface and exposed to direct sunlight.

Images were acquired by a CMOS camera (PixeLINK PL-B742F-R) pointing downwards. The field of view was 140 mm $\times$ 105 mm and was acquired as an 800×600 pixel image. The spray system consisted of six nozzles each with a fixed location and all pointing directly downwards. The six areas that could be targeted by the spraynozzles were all within the captured area, as well as the soil and plants that would pass below the microsprayer during the next 100 mm of movement. To determine the spraycells, the spraynozzles were activated while the sprayer was at rest and an image was acquired. The spraycells were then set to the sprayed locations in the acquired image. Images were acquired with a short exposure time of 9 m/s to reduce motion blur and 40 images were captured per second. The acquired images were transferred to the image processing computer via a Firewire connection. Image processing were performed on a Lenovo ThinkPad W700 laptop equipped with an Intel Core 2 Duo T9600 2.8 GHz processor and 4 GB ram running Windows XP. The software was developed using the C++ programming language and consisted of three separate threads which handled image acquisition, image analysis and sprayplanning, respectively. The software library OpenCV (Bradski and Kaehler, 2008) was used for the implementation of the image processing methods.

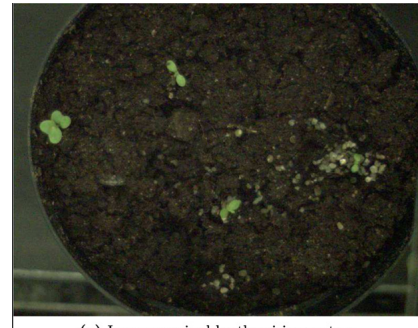

(a) Image acquired by the vision system.

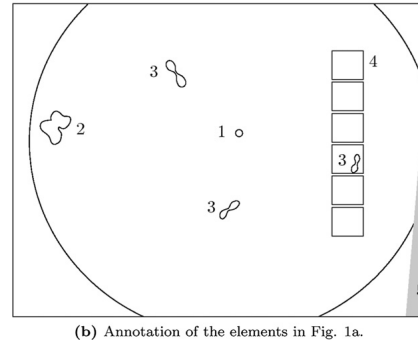

(b) Annotation of the elements in Fig. 1a.

Fig. 1. An example of the images acquired by the vision system. The numbers in (b) describes the elements at the shown locations. (1) Maize, (2) oilseed rape, (3) scentless mayweed, (4) target areas of the six spraynozzles and (5) part of the microsprayer. One of the scentless mayweed plants is located in the target area of spraynozzle 4. Part (4) and (5) are fixed in the image while (1)–(3) moves from left to right.

2.2. Ground velocity estimation

Velocity of the spray system relative to the soil surface was estimated from the acquired sequence of images, based on the assumption that perspective distortions can be ignored. After image N has been captured, it was compared to image $N-1$ and the relative motion between the two images was estimated. Using

the relative motion and the difference between the time of image acquisition for the two images the velocity was calculated.

Initially both images were scaled down to a resolution of 200×150 (from 800×600). An area measuring 100×125 pixels was extracted from the central part of image $N-1$, this part of the image was used as a template. The cross correlation between the template and image N was determined, as a function of the relative position of the template with respect to image N. The location where the template has the highest correlation with image N was determined. Then the offset between the template location in image $N-1$ and the best matching location in image N was determined. This offset was used as an estimate of the velocity of the field of view, e.g. how fast one object moved across the field of view measured in pixels per unit of time. The template matching can be calculated efficiently using Fast Fourier Transforms. Template matching used on average 5.1 m/s per frame. If no objects are present in the images, the best matching location is not well defined which then will result in a random location being selected as the best matching location.

2.3. Plant detection

To locate plants in the acquired image, the excess green color index (ExG) introduced by Woebbecke et al. (1995) was used:

$$\mathrm{ExG} = 2G - R - B \tag{1}$$

where R, G and B are the red, green and blue pixel values of the current pixel. The pixel values are stored as integer values in the range $[0;255]$. The generated excess green image is then smoothed and binarized using a threshold value of 55. The threshold value was chosen based on the images acquired by the vision system.

Connected regions in the segmented image are located, and for each of the regions the size and some shape descriptors are determined. The shape descriptors used are the seven scale, translation and rotation invariant moments introduced by Hu and February (1962). Regions that intersect the border are considered incomplete and therefore discarded.

2.4. Classifier

For classification between crop and weed plants a nearest neighbor Bishop (2007) classifier was used. As the calculated features have different magnitudes (size ~1000 and Hu1 ~0.1) the features are rescaled before classification. The rescaling consists of multiplying the features with the weights given in Table 1. The weights were chosen based on the typical magnitude of the features. Features with high noise levels were given a decreased weight to decrease the influence of the noise. Performance of the classifier was not investigated directly, but small experiments on the experimental setup showed a relative high classification accuracy.

After classification the presence of crop and weed plants are stored in a crop/weed map. The crop/weed map is an image with similar dimensions as the original image where pixels belonging to a weed plant have the value 1 and crop plant pixels have the value 255. Areas with no plants present are identified by the value 0.

Table 1
Feature weights used in the classifier.

Feature	Weight
Size	0.001
Hu1	6.667
Hu2	8.403
Hu3	71.428
Hu4-7	100.000

2.5. Sprayplanning

Sprayplanning was performed once for each of the individual spraynozzles. For each nozzle, the area that the nozzle was expected to pass, was examined in the crop/weed map. Presence of crops and weeds were determined as a function of the distance to the current nozzle. Regions where only weeds were present were marked for spraying. When a weed was found in the course of the nozzle, a command is sent to the microsprayer controller that the nozzle should be opened at the time t_{spray}, which was calculated based on the acquisition time of the processed image t_{img}, the distance to the weed d_{weed}, the current forward velocity v and the delay t_{delay} caused by the entire system. The relationship is:

$$t_{\mathrm{spray}} = t_{\mathrm{img}} - t_{\mathrm{delay}} + \frac{d_{\mathrm{weed}}}{v} \tag{2}$$

The delay parameter was adjusted during the calibration phase before the experiment.

2.6. Spray system

The spray system was based on a Willett 3150 Si/800 inkjet printer head. Off the shelf the printer head has seven nozzles which can be controlled individually; six of these were used, as one was malfunctioning. The six nozzles are spaced evenly over a distance of 53 mm, which corresponds to a distance of 10.5 mm between two adjacent nozzles. In the experimental setup there was a distance of ~100 mm between soil surface and nozzle.

The computer sends spraycommands to a microcontroller via a USB connection. After receiving the commands, the microcontroller immediately opens the requested nozzles for 1 ms and 0.2 μL spray liquid is ejected. The spray liquid consists of water mixed with RoundUp Bio (360 g/L glyphosate as an isopropylamine salt, Monsanto Europe) with a concentration of 5 g/L. This ensures that in one spray application there will be enough glyphosate to effectively control the growth of the weed seedling. According to Søgaard et al. (2006), 0.8 μg of glyphosate is enough to effectively control the growth of *Solanum nigrum* L. seedlings. Unpublished results show that oilseed rape seedlings are effectively controlled by a similar amount of glyphosate.

2.7. The experimental setup

Crop and weed plants were seeded in pots with a diameter of 130 mm and a volume of 1 L. The plants were raised in glasshouse. The pots had to be moved below the spray system with a small error in the transversal direction as the plants are placed in a 50 mm wide band inside the pots and the spray system can only treat a 60 mm band. To run the experiments, the microsprayer including illumination, vision and control systems was mounted above a conveyor belt, such that the distance between spraynozzles and soil surface in the pots was approximately 100 mm. The purpose of the conveyor belt was to move potted plants below the operating microsprayer system in a steady motion.

2.8. Experimental method

Three species were used: maize, oilseed rape and scentless mayweed. At the time of the experiment, the cotyledons had just emerged, which equals growth stage 10 on the BBCH scale (Meier, 2001). Weed control should be performed before growth stage BBCH12 according to Danish recommendations (Petersen and Jensen, 2010). One crop (maize) plant was placed near the pot centre, while 1–2 oilseed rape and 2–3 scentless mayweed plants were placed randomly in a 50 mm wide band centred on the maize

plant. The plants were placed such that no leaves overlapped other plants.

Four pots were randomly selected as control pots. These pots received no treatment by the microsprayer system and the plants inside the pots were used to train the classifier. The classifier database was filled with the control plants, where maize was marked as crop and oilseed rape and scentless mayweed were marked as weeds. In total four maize, eight rape and 10 mayweed plants were present in the four control pots. The 33 remaining pots were placed on a conveyor belt, which carried the pots below the microsprayer at a velocity of 0.5 m/s, while the spray system was activated. In total 33 maize, 54 oilseed rape and 76 scentless mayweed plants were treated by the microsprayer.

Two weeks after the microspraying, the status of each individual plant was visually evaluated using two categories: plants following the expected growth rate and plants severely behind the expected growth rate. The expected growth rate was estimated using the observed growth in the four control pots. Dry weight measurements of the oilseed rape plants were made directly after the visual evaluation.

2.9. Interpretation of experimental results

The experiment consisted of exposing a number of plants n to the microsprayer treatment. Two weeks after the treatment, the number of normal growing plants k was determined. The normal growth fraction f of the plants exposed to treatment can be estimated from $f = k/n$. In addition to the normal growth fraction, the uncertainty of this fraction was estimated. The credible interval is used to describe the uncertainty of the determined normal growth fraction. Using the Binomial distribution, the experimental support for a given normal growth fraction hypothesis can be expressed as being proportional to

$$p(f|n,k) \propto f^k \cdot (1-f)^{n-k} \tag{3}$$

Note that this value is maximized for $f = k/n$. We assume that $p(f|n,k)$ is normalized, such that

$$\int_0^1 p(f|n,k)\,df = 1 \tag{4}$$

The probability q, that the real plant growth fraction is inside the interval $[f_l; f_h]$ is then

$$q = \int_{f_l}^{f_h} p(f|n,k)\,df \tag{5}$$

The shortest interval $[f_l; f_h]$ that covers a given fraction q was used as a credible interval at the q level, this approach was described by Ross and Nov. (2003).

2.10. Probability of hitting small plants

When a small plant passes below the microsprayer between two of the nozzles, it is not always possible for the spray system to hit the plant. This can be explained by the geometry of the spray system, where the distance between two adjacent nozzles is larger than the width of the sprayed area of one nozzle. The area between two nozzles that cannot be sprayed is denoted the deadzone (Fig. 2). If a plant is in the deadzone throughout the entire passage, the spray system has no chance of hitting it. The following values are used to describe the setup: w is the distance between two adjacent nozzles, w_s is the width of the area that are sprayed by a single nozzle, θ is the plant orientation and $w_{\text{eff}}(\theta)$ is the effective width of the plant (Fig. 2). The effective width of a plant is its width measured in the direction perpendicular to the moving direction. If the effective width is larger than the deadzone width

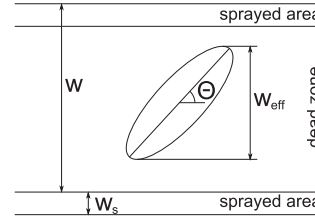

Fig. 2. Illustration of the effective plant width w_{eff} and the parameters w and w_s for the microsprayer setup.

($w_{\text{eff}} > w - w_s$), some part of the plant will always overlap an area that can be sprayed and thus it is possible to hit the plant. In the other case where $w_{\text{eff}} < w - w_s$ the probability of hitting the plant with random location is given by the fraction $\frac{w_{\text{eff}}+w_s}{w}$. To calculate the probability of hitting a plant with random orientation and location the following expression is used.

$$p_{\text{hit}} = \frac{w_s}{w} + \frac{1}{\pi}\int_0^{\pi} \frac{\min(w - w_s, w_{\text{eff}}(\theta))}{w}\,d\theta \tag{6}$$

To simplify the calculations, the plant shape is described by an ellipse, with the major axis a and the minor axis b. The ellipse shape parameters were chosen such that the ellipse covered the entire plant. Eq. (6) can then be evaluated numerically using the values relevant for the used microsprayer setup ($w = 10$ mm,$w_s = 2$ mm), and the parameters describing the plant shape. Note that the calculated values are based on two assumptions: (1) that all the plants have the same shape and size and (2) that all the plants are located and oriented randomly. The estimated hit probability is a statistical upper bound of the performance of the optimal vision and spray control system.

The difference between the observed normal growth fraction and estimated probability of not being able to hit the plant species, $f - p_{\text{miss}}$, is a measure of the performance of the spray system. A low value indicates that the system can effectively target the given plant species at this growth stage, and a high value shows that the system did not hit all plants that it should be able to. Using this measure it is possible to compare the targeting performance of the spray system when targeting different objects, varying in size and shape.

3. Results and discussion

Table 2, lists the plant shape parameters used for the estimation as well as the obtained hit probabilities. The hit probabilities reveals that the geometry of the microspray system is suitable for targeting plants larger than 11 mm × 11 mm but is unsatisfactory for smaller plants.

There was a clear difference between control and treated group. All plants in the control pot, Fig. 3a, were now in a more developed growth stage than at the time of spraying. For the treated pot in Fig. 3b, the maize plant and a single scentless mayweed plant had evolved into a more developed growth stage. For the maize and oilseed rape plants, there were no doubt of which category to place the plants into, as they either grew as expected or their growth were stopped at the BBCH 10 stage. The scentless mayweed plants were more difficult to classify, as only a part of the plants grew as expected (48 plants) or stopped their growth at the BBCH 10 stage (18 plants). The remaining fraction (10 of 76) were somewhere between these two stages. Table 2 lists the number of treated plants and the number of the ones that followed the expected

Table 2
Short summary of the experimental results. (a and b): major and minor axes of the ellipse shaped plant model (p_{miss}): probability of the system not being able to hit the plant model (k): number of plants that grow unaffected after the microspray treatment. (n): number of plants treated by the microsprayer system. (f): normal growth fraction. (95% CI): the shortest credible interval for the rate of normal growth. ($f - p_{miss}$): miss rate that cannot be explained by plant size.

Plant	Spray probability			Experimental results				$f - p_{miss}$
	a [mm]	b [mm]	p_{miss}	k	n	f	95% CI	
Maize(crop)	3.5	3.5	0.55	33	33	1.00	[0.92; 1.00]	0.45
Scentless mayweed	8.0	2.5	0.34	48	76	0.63	[0.52; 0.73]	0.29
Oilseed rape(weed)	13.7	11.0	0.00	3	54	0.06	[0.01; 0.14]	0.06

(a) Control pot **(b)** Sprayed pot

Fig. 3. Comparison of a control pot and a sprayed pot. In the sprayed pot, the oilseed rape plant is severely damaged by the herbicide while the maize plant appears unaffected. Of the two scentless mayweed plants that are present in the sprayed pot one is severely injured while the other grows unaffected.

growth pattern. Three of the treated oilseed rape plants had a dry weight comparable to the control plants. The weight distribution of the control and the treated plant populations are visualized in Fig. 4.

The oilseed rape plants, which had the largest leaf area per plant, were effectively controlled by the microsprayer. Only 6% of the treated plants followed the expected growth pattern for untreated plants, while 94% was effectively controlled. In comparison only 37% of the scentless mayweed plants were sprayed, which is much less than the expected hit probability of 66%. This difference indicates that the system is not able to locate and target small objects effectively. The reason could be timing problems of the microsprayer control system, imprecise calibration of the delay parameter t_{delay} or faulty classification of the plants as crop plants. The $f - p_{\text{miss}}$ measure is not relevant for the maize plants, as they were not targeted for spraying. All of the 33 treated maize plants followed the expected growth pattern, this indicates the system was able to correctly classify the plants as crops.

A main disadvantage with the experiment is that the input to the vision system was discarded during the experiment. Therefore it is not possible to investigate how the system failed in the cases where plants were not hit. By storing all the acquired images before they are processed, it should be possible to redo the image analysis and the following sprayplanning.

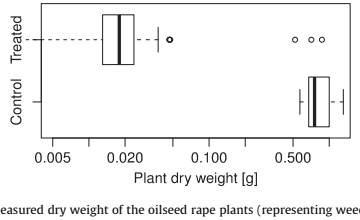

Fig. 4. Measured dry weight of the oilseed rape plants (representing weeds) in the control ($n = 8$) and treated ($n = 53$) groups two weeks after microspraying. Three outliers can be identified in the treated group, these are the plants that the microsprayer missed during the treatment.

The system by Søgaard and Lund (2005) relies on controlling the motion of the vision and spray system, this makes the system infeasible to mount on an existing platform. Our system is self contained and needs only to be moved in a steady motion above the area that should be treated. The volunteer potato controlling system described in Nieuwenhuizen et al. (2010) and our system have many common properties. The main difference is the geometry of the microsprayer setup, the nozzle spacing is narrower in our setup, this increases the resolution of the spray system which can then target weed plants closer to crop plants.

A direct limitation of the described system is the narrow region (60 mm) in which weeds can be controlled. By replacing the microsprayer unit with a larger one, the region can be extended to cover the full range of the vision system $\sim$ 100 mm. If the region should be larger the vision system has to be redesigned.

The future of the microsprayer technique depends on several things. The system presented can reliably detect and control weed plants with a size larger than 11 mm $\times$ 11 mm when in a steady forward motion with a velocity of 0.5 m/s. The forward velocity of 0.5 m/s is probably not enough to make the system economically feasible. The challenge will be to move the system from controlled indoor facilities to more challenging circumstances in the field. Use of controlled illumination and shielding from direct sunlight is expected to make the system more resistent to changes in the natural illumination. The main change will be to go from the steady motion to a more shaky motion. Under a steady forward motion is it possible to predict the weed trajectory relatively to the vision system with high accuracy, when the motion is disturbed the quality of such a path prediction will decline rapidly, deteriorating spray accuracy.

4. Conclusion

A machine vision system was developed for controlling a microsprayer system. The goal was to develop a system that can

detect, classify and effectively control weed plants while the system was moving with a velocity of 0.5 m/s. The system was tested in a relatively simple situation with two weed species (scentless mayweed and oilseed rape) in maize. With a velocity of 0.5 m/s between the soil surface and the microsprayer system, the system was able to effectively control weeds larger than 11 mm × 11 mm. But only 37% of the smaller scentless mayweed plants were effectively controlled. The low success rate cannot be explained by the small plant size alone, but may be explained by a sub optimal sprayplanning system, problems related to depositing enough herbicide on the small leaves or a combination of both.

Acknowledgements

Henning Tangen Søgaard provided a lot of constructive critique during the writing of this paper. During development of the system we had constructive discussions with Ivar Lund (University of Southern Denmark, Department of Industrial and Civil Engineering) and Michael Nørremark (Aarhus University, Department of Biosystems Engineering). Michael also provided access to the used microsprayer device.

References

Bishop, C.M., 2007. Pattern Recognition and Machine Learning (Information Science and Statistics), first ed. Springer.

Bradski, G., Kaehler, A., 2008. Learning OpenCV. O'Reilly Media.

Christensen, S., Søgaard, H.T., Kudsk, P., Nørremark, M., Lund, I., Nadimi, E.S., Jørgensen, R., 2009. Site-specific weed control technologies. Weed Research 49 (3), 233–241.

Hu, M.-K., 1962. Visual pattern recognition by moment invariants. IRE Transactions on Information Theory 8 (2), 179–187.

Lamm, R.D., Slaughter, D.C., Giles, D.K., 2002. Precision weed control system for cotton. Transactions American Society of Agricultural Engineers (ASAE) 45, 231–248 (shutter speed: 1/250 s).

Lee, W.S., Slaughter, D.C., Giles, D.K., 1999. Robotic weed control system for tomatoes. Precision Agriculture 1, 95–113.

Lund, I., Christensen, S., Jensen, L.A., Jensen, P.K., Olsen, H.J., Søgaard, H.T., Bligaard, J., Jensen, J.E., 2008. Cellesprøjtning af ukrudt i majs. Technical Report, Miljøstyrelsen.

Meier, U. (Ed.), 2001. Growth stages of mono-and dicotyledonous plants. BBCH Monograph, second ed. Federal Biological Research Centre for Agriculture and Forestry.

Nieuwenhuizen, A., Hofstee, J., van Henten, E., 2010. Performance evaluation of an automated detection and control system for volunteer potatoes in sugar beet fields. Biosystems Engineering 107 (1), 46–53.

Petersen, P.H., Jensen, J.E., 2010. Ukrudt i majs. Available from: <http://www.landbrugsinfo.dk/Planteavl/Plantevaern/Ukrudt/Kemisk-bekaempelse/Sider/pl_pn_10_102.aspx>.

Ross, T.D., 2003. Accurate confidence intervals for binomial proportion and poisson rate estimation. Computers in Biology and Medicine 33 (6), 509–531.

Søgaard, H., Lund, I., Graglia, E., 2006. Real-time application of herbicides in seed lines by computer vision and micro-spray system. Transactions American Society of Agricultural Engineers (ASAE), 061118.

Søgaard, H.T., Lund, I., 2005. Investigation of the accuracy of a machine vision based robotic micro-spray system. Precision Agriculture '05, 613–619.

Woebbecke, D.M., Meyer, G.E., Von Bargen, K., Mortensen, D.A., 1995. Color indices for weed identification under various soil, residue, and lighting conditions. Transactions American Society of Agricultural Engineers (ASAE) 38 (1), 259–269.

Paper V

Upper limit for context based crop recognition

Upper limit for context based crop recognition. / Midtiby, Henrik Skov; Åstrand, Björn; Jørgensen, Ole; Jørgensen, Rasmus Nyholm.

Submitted to Biosystems Engineering, january 2012.

Upper limit for context based crop classification

Henrik Skov Midtiby[a,*], Björn Åstrand[b], Ole Jørgensen[c], Rasmus Nyholm Jørgensen[a]

[a] *Institute of Chemical Engineering, Biotechnology and Environmental Technology, University of Southern Denmark, 5230 Odense M, Denmark*
[b] *Intelligent Systems Laboratory, Halmstad University, E-301 18 Halmstad, Sweden*
[c] *Department of Biosystems Engineering, Aarhus University, DK-8830 Tjele, Denmark*

Abstract

Mechanical in–row weed control of crops like sugarbeet require precise knowledge of where individual crop plants are located. If crop plants are placed in known pattern, information about plant locations can be used to discriminate between crop and weed plants. The success rate of such a classifier depends on the weed pressure, the position uncertainty of the crop plants and the crop upgrowth percentage. The first two measures can be combined to a *normalized weed pressure*, λ. Given the normalized weed pressure an upper bound on the positive predictive value is shown to be $\frac{1}{1+\lambda}$. If the weed pressure is $\rho = 400m^{-2}$ and the crop position uncertainty is $\sigma_x = 0.0148m$ along the row and $\sigma_y = 0.0108m$ perpendicular to the row, the normalized weed pressure is $\lambda \sim 0.40$; the upper bound on the positive predictive value is then 0.71. This means that when a position based classifier predicts that a certain plant is a crop plant 71% of the times it will be correct.

Keywords:

1. Introduction

Typical work flows in agriculture are often based on crop plants placed in row structures. Cereals like barley and wheat are placed in rows with no clear structure within the row, while Maize, Sugar beets and other high value crops are placed in rows with a clear defined intra-row spacing between

*Corresponding author.
Email address: hemi@kbm.sdu.dk (Henrik Skov Midtiby)

crop plants. Given the position of a single sugar beet plant, it is possible to predict locations of nearby crop plants, based on information about plant distances within the row.

Plant classification based on spectral properties and plant morphology (Weis and Sökefeld, 2010) is vulnerable to variations in plant appearance. There can be a large variation of plant appearance within field, between fields and during growth season. Also the weed pressure and population varies. However, the sawing pattern is more stable. Therefore it is interesting to use classifiers that utilize the position information to discriminate between crops and weeds.

Tillett et al. (2001) used crop position information to distinguish between crop and weed plants in a field of *brassica*. The crops were transplanted to a square pattern with side lengths $0.48m$ in three adjacent rows. They state that it is practical to track crop plants using extended Kalman filtering, but gives no numbers of the achieved classification rate. Onyango and Marchant (2003) detected grid placement of cauliflower and used this information to distinguish between crop and weed pixels. The highest obtained correct crop and weed pixel classification rates were 96% and 92%.

The two earlier examples looked at plants placed in a 2D pattern, while Åstrand and Baerveldt (2004) used crop position information in a single row to classify crop and weed plants in sugar beet fields. In a field with a weed pressure of 50 plants/m^2, they recognized 96% of the crop plants as crop plants by searching for a pattern consisting of four plants placed in a row structure with the inter plant distance set to the known crop plant distance. The method was based on searching for four plants on a line with a known plant spacing. In Åstrand (2005) position information was combined with individual plant features for recognizing crop plants. In field conditions with low weed pressure (50 weeds/m^2) they achieve a positive predictive value (PPV) of 74% for recognizing crops when only using plant position information. When the weed pressure is increased to 400 plants/m^2 the PPV decreases to 47%. In both cases were the crop upgrowth around 70%. This decrease is explained by increase of plant occlusion / overlapping resulting in that the row structure can be difficult to recognize when the number of weed plants is large. To determine plants centres when some of the leaves are occluded the method described in Midtiby et al. (2012) should be considered.

Position information might not be sufficient, but what can is the limit of this group of methods? In this paper we investigate the upper limits of what can be achieved by using information about plant positions. Theoretical

considerations show that an important factor for explaining the achievable PPV is the normalized weed pressure, that depends on weed density and position uncertainty of crop plants. Four different strategies for localising crop plants based on plant locations was implemented and tested in a simulated environment. Results from testing the three strategies supports the theoretical considerations. Finally are results presented by Åstrand (2005) found to agree well with the derived theoretical upper bound.

2. Materials and methods

In this section the mathematical foundation for calculating the achievable PPV is presented. A central part of these calculations is the normalized weed pressure, a dimensionless quantity, which limits the achievable PPV. Four different algorithms using context information are then described and tested in a simulated environment. The test environment allow investigation of the influence from parameters like weed density and crop position uncertainty.

2.1. Normalized weed pressure

The normalized weed pressure is the average number of weed plants closer to a seeding point than the nearest crop plant. The crop plant position probability is modelled as a Gaussian distribution with centre at (0, 0) and the uncertainties σ_x, σ_y in the x and y directions respectively ($c \in \{x, y\}$).

$$p_{\sigma_c}(c) = \frac{1}{\sigma_c\sqrt{2\pi}} \exp\left(\frac{-c^2}{2\sigma_c^2}\right) \tag{1}$$

The position is described in terms of the distance along the crop row (x–coordinate) and the distance perpendicular to the crop row (y–coordinate). The next step is to determine the number of weed plants closer to the origin than the crop–point (x, y) using the Mahanolobis distance metric. The number of weed plants is the weed density ρ multiplied with the area of the ellipse going through (x, y) with semi–major axis along the x–axis and semi–major and minor axes proportional to σ_x and σ_y. See figure 2. The expected number of weeds is given by

$$n_w(x, y) = \rho\pi\sigma_x\sigma_y\left(\frac{x^2}{\sigma_x^2} + \frac{y^2}{\sigma_y^2}\right) \tag{2}$$

Symbol	Unit	Description
x	m	Coordinate along x-axis (direction along the crop row), $x = 0$ is the expected crop location
y	m	Coordinate along y-axis (perpendicular to the crop row), $y = 0$ is the expected crop location
σ_x	m	Crop position uncertainty along the x–axis
σ_y	m	Crop position uncertainty along the y–axis
α	1	Scaling factor
ρ	m^{-2}	Weed density
λ, NWP	1	Normalized weed pressure
$p_{\sigma_c}(c)$	1	Position probability distribution of variable c
$n_w(x, y)$	1	Expected number of weeds closer to the seeding location than the point (x, y)
$\vec{x}_k$	m	Coordinates of the kth plant
$\vec{x}_{\text{offset}}$	m	Coordinates of the first crop plant in the row structure
$\vec{d}$	m	Vector from one crop position to the next expected crop position
k, i, m	1	Index variables
l	1	Number of occurrences in a Poisson distribution
c_i	1	Position score associated to the ith plant
s	1	Scaling factor
N	1	Number of neighbour positions to examine
ϕ	1	Probability of not seeing any plants within 3σ
γ	1	Crop upgrowth
f	1	Fitting parameter for classifier performance
PPV	1	Positive prediction value
ePPV	1	Expected positive prediction value
oPPV	1	Observed positive prediction value
n_{crop}	1	Number of crop plants in dataset
n_{weed}	1	Number of weed plants in dataset
n_{total}	1	Total number of plants in dataset
$f(l, \beta)$	1	Probability of seeing l events in a Poisson process with an average number of events of β
x_n	m	nth crop location
n	1	Crop plant number
$\sigma_{\text{seed-plant}}$	m	Deviance between seed placement and resulting plant position
TP		True positives
FP		False positives4
TN		True negatives
FN		False negatives
CI		Credible interval

Table 1: Symbols and associated units used in the paper.

The average number of weeds closer to the seeding point than the nearest crop plant can then be expressed with the following double integral.

$$\lambda = \int_{-\infty}^{\infty} \int_{-\infty}^{\infty} p_{\sigma_x}(x) \cdot p_{\sigma_y}(y) \cdot n_w(x, y)\, dx\, dy \tag{3}$$

The value of the double integral is $\lambda = 2\pi\sigma_x\sigma_y\rho$ (see derivation in appendix Appendix A.2), this value is denoted the *normalized weed pressure* (NWP).

2.2. Positive predictive value given normalized weed pressure

If a classifier based on the plant positions chooses the plant nearest to the estimated grid position as crop, it is interesting to look at the probability of misclassification, which happens when there is a weed plant closer to the grid location than the nearest crop plant. To calculate this probability we will assume that the weeds are uniformly distributed and model the number of weed plants within an area with a Poisson distribution

$$f(l; \beta) = \frac{\beta^l e^{-\beta}}{l!} \tag{4}$$

with l as the number of observed weed plants and β the average number of weeds seen in an area of this size, calculated as weed density ρ times the size of the area. The case where no weed plants are observed in the area corresponds to $l = 0$, in which the probability is given by $\exp(-\beta)$. With a crop plant a (x, y) is the probability of not seeing a weed plant closer to the grid point $\exp(-n_m(x, y))$. By averaging this over all possible values of x and y while weighting with the probability of seeing a crop plant at these locations, the following integral appears.

$$\mathrm{PPV} = \int_{-\infty}^{\infty} \int_{-\infty}^{\infty} p_{\sigma_x}(x) \cdot p_{\sigma_y}(y) \cdot \exp\left(-n_w(x, y)\right)\, dx\, dy \tag{5}$$

The value of the double integral is $\mathrm{PPV} = \frac{1}{1+2\pi\sigma_x\sigma_y\rho}$ (see derivation in appendix Appendix A.3). This value can also be expressed in terms of the normalized weed pressure, then it is $\mathrm{PPV} = \frac{1}{1+\lambda}$. This is an upper bound on the achievable positive predictive value that can be reached using position information alone for recognizing crop plants. If the true seeding position is unknown the performance will be lower.

Figure 1: Row structure in sugar beets and cabbage. Images provided by Frank Poulsen Engineering, www.visionweeding.com, 2011.

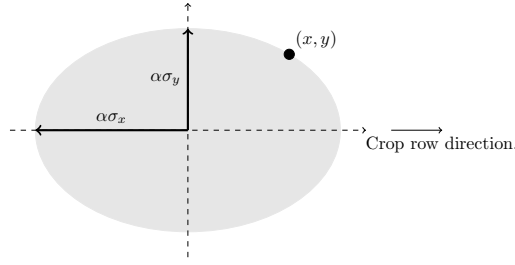

Figure 2: Given a crop plant at (x, y), the area that should be weed free for obtaining a correct classification is marked with a grey shading. All points in the shades area has a smaller Mahanolobis distance to the expected crop location than the observed crop at (x, y) The area of the shaded region is $\pi\sigma_x\sigma_y\left(x^2/\sigma_x^2 + y^2/\sigma_y^2\right)$. Origin is the expected crop plant position.

2.3. Crop localisation based on plant locations

The following subsection shows different methods for recognizing crop plants given plant positions as input. Four different methods are described, of which two are reference methods for establishing upper and lower bounds on classifier performance. All methods takes a list of all observed plant positions ($\vec{x}_k$, $k \in 1 \ldots, n_{\text{total}}$) as input together with the number of crop plants n_{crop} present in the dataset.

2.3.1. Random plant selector

From the set of plant positions $\vec{x}_k$ are n_{crop} plant positions drawn randomly with no replacements. This method uses no information about the row structure and can therefore be used as a lower bound on the achievable recognition rate.

2.3.2. Position scores

In this method a position score is calculated for all of the observed plant positions. Given a plant location, the position score depends on location of nearby plants. If the nearby plants follow the crop plant structure the calculated score is high. The score function probes the N adjacent expected crop locations and for each of them finds the plant closest to this position. If there are plants nearby the expected crop locations the score for that position is high, otherwise it is reduced.

$$c_i = \sum_{m=1}^{N} \left[\max_k \exp\left(\frac{-||\vec{x}_k - \vec{x}_i - m \cdot \vec{d}||^2}{2s^2\sigma_x\sigma_y} \right) \right] \tag{6}$$

The scaling factor s was set to 5, tests showed that values outside the interval $[2, 8]$ reduced the performance of the method, inside the interval the performance was unaltered. After calculating the position score for all observed plant locations the n_{crop} plant positions with the highest score were marked as crop plants.

2.3.3. Path scores

This method calculates plant position scores by looking at the position score of neighbouring plants. All plant position scores are divided in two parts, a base value of 1 and a contribution of a percentage of a neighbouring plants position score. The contribution percentage is determined by the

relative positions of the neighbouring plants, if the plant positions are likely neighbours the percentage is high and otherwise it is lowered. This percentage is modelled as an exponential function with the distance from expected to observed plant position squared divided with the crop position uncertainties. In this description it is assumed that the plant which position score should be calculated is positioned exactly at a grid location. Plants near the prior grid location are all investigated and it is determined which plant (and corresponding position score) can increase the current plants position score maximally. Such a measure can be computed efficiently, by calculating the position scores from left to right using dynamic programming. The position score of the i^{th} plant can then be expressed as

$$c_i = 1 + \max_k \left[c_k \cdot \exp\left(\frac{-||\vec{x}_k - \vec{x}_i - \vec{d}||^2}{2 \cdot (2\sigma_x) \cdot (2\sigma_y)} \right) \right] \tag{7}$$

2.3.4. Known seeding positions

In addition to the plant positions, this method also has access to information about all grid locations on which there is placed crop plants. For each of these grid locations the nearest plant is identified and marked as crop. This method is implemented for confirming the predicted upper bound on the achievable PPV given a normalized weed pressure λ.

2.4. Test suite

For evaluation of the implemented crop recognition methods, a simulation environment was implemented. Given a set of parameters (weed density and crop position uncertainty) the simulation environment would produce a set of crop plant positions and a set of weed plant positions. The generation of these position sets is described in 2.4.1. These two sets of positions was combined to one set which was then handed over to the method that should be tested. The performance of the method was then evaluated and a resulting PPV value was obtained. The evaluation procedure is described in 2.4.2.

2.4.1. Generation of plant positions

The n^{th} grid location had the position

$$\vec{x}_n = \vec{x}_{\text{offset}} + n \cdot \vec{d} \tag{8}$$

where $\vec{x}_{\text{offset}}$ is the position of the first plant and $\vec{d}$ is the distance from one crop plant to the adjacent crop plant. For each grid location a crop plant were placed on that point and adjusted with x and y displacements drawn from normal distributions with zero mean and σ_x and σ_y standard deviations.

Weed plant positions were drawn from a uniform distribution of the simulated area. The number of weed plants, n_{weed}, was adjusted to match the desired weed pressure. Crop and weed plant positions were then placed in a list and sorted by their x–coordinates.

2.4.2. Interpretation of results

The tested method then generated a list of the plants recognized as crops and combined with the knowledge of the true crop plant positions a confusion matrix was built. To avoid boundary effects on the result, the simulated field were split into three parts: beginning, middle and end. The parts beginning and end of the simulated field were defined as the space required for 20 adjacent crop plants. Only plants in the middle part contributed to the confusion matrix. The confusion matrix kept track of the number of true positives TP (crops classified as crops), false positives FP (weeds classified as crops), false negatives FN (crops classified as weeds) and true negatives TN (weeds classified as weeds). PPV was then calculated as

$$\text{PPV} = \frac{\text{TP}}{\text{TP} + \text{FP}} \tag{9}$$

2.5. Effect of upgrowth

The main difference between the obtained theoretical predictions and the observed classifier performance described in Åstrand (2005) was that the upgrowth in the experiments were less than assumed in the derivations (100%). The article states upgrowth γ together with number of crops found (TP) and number of weeds misclassified as crops (FP). If the used algorithm cannot find a plant near a predicted grid location (within 3σ) no plants are classified as crop for that location. The probability of not finding a plant within 3σ are given by

$$\phi = (1 - \gamma) \cdot \exp\left(-\lambda \cdot 3^2\right) \tag{10}$$

where $1 - \gamma$ is the probability of not having a crop plant at the grid location and $\exp\left(-\lambda \cdot 3^2\right)$ is the probability of not seeing any weeds within 3σ from the grid location.

If a crop plant is present at the investigated grid location, the expected PPV is given by $\frac{1}{1+\lambda}$. If no plants are within 3σ no action is taken and the observed PPV is not affected. The expected PPV value in a field with crop upgrowth γ is then

$$\text{ePPV} = \frac{1}{1+\lambda} \cdot \frac{\gamma}{1-\phi} \tag{11}$$

where $(1-\phi)$ is the proportion of grid locations were at least a single plant is within 3σ from the location.

3. Results and discussion

With the test framework described in 2.4, the implemented classification methods were evaluated. Fields containing 360 crop plants were used. PPV values were calculated for weed densities (ρ) in the interval $[0.03m^{-2}; 180m^{-2}]$ and crop positions uncertainties (σ_x, σ_y) in the interval $[0.015m; 0.200m]$. For each set of simulation variables the simulation was repeated 36 times.

By plotting the obtained PPV as a function of the normalized weed pressure, it is seen that the normalized weed pressure is a suitable combination of the weed pressure and the crop position uncertainty as the simulation results (black dots in figure 4) lie in a thin band. The visualized simulation data in figure 4 was from the known grid locations method. It is also seen that the simulation results closely resemble the predicted upper bound on PPV given a certain normalized weed pressure.

3.1. Influence of reduced upgrowth

The effect of reduced upgrowth is visualized in figure 4, based on the assumption that plants with a distance larger than 3σ from the nearest expected grid location are always classified as weed. At NWP above $\lambda \simeq 0.1$ is the effect of reduced upgrowth a direct reduction in the achievable PPV value. At lower NWP values the dependency on upgrowth is reduced, as the probability of finding a weed within 3σ is low.

3.2. Lower limits for crop positioning uncertainty

Crop plant position uncertainty depends on several factors like seed bouncing, displacement and difference between seed and seedling location (Nørremark

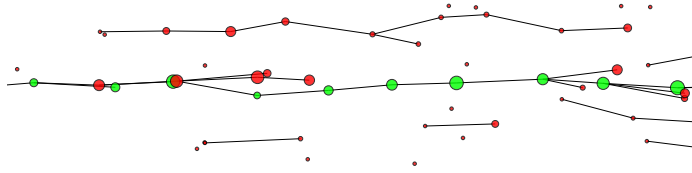

Figure 3: Example of tree built by the path score method. The circles mark plant positions (crops are green and weeds are red) and their radii are proportional to the assigned position score. Solid lines indicates the neighbouring plant position that is contributing to the current position score. The shown data is from a simulation with the parameters $\rho = 50m^{-2}$, $\sigma_x = 0.0240m$ and $\sigma_y = 0.0136m$. which gives the normalized weed pressure $\lambda = 0.1025$. These conditions resembles DS1 from Åstrand (2005).

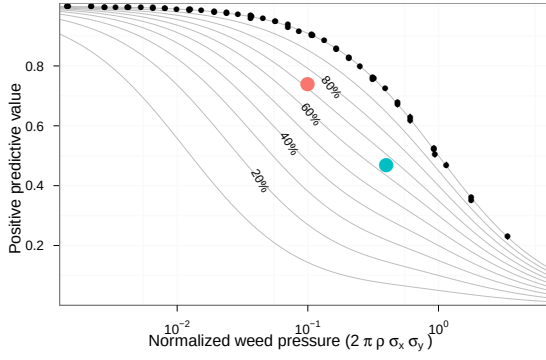

Figure 4: Visualisation of the predicted PPV as a function of the normalized weed pressure and the crop upgrowth, upgrowth percentages are indicated. The black dots are simulation results of the Known Grid Locations method for recognizing crop plants, it is seen to follow the prediction PPV. The two coloured dots are PPV from experiments described in Åstrand (2005).

et al., 2007). The position uncertainty will in general be larger in the direction of the crop row due to the seeding mechanism. Distances between seed and seedling location were quantified for light and heavy soil types by (Griepentrog et al., 2005). For light soils with fine seed beds the uncertainty was $\sigma_{\text{seed-plant}} = 12.4mm$ (Nørremark et al., 2007).

Consider the case with a high weed pressure of $\rho = 400m^{-2}$ and crop position uncertainties of $\sigma_x = \sigma_y = 30mm$. What is the effect of using a better sowing machine to reduce the crop position uncertainty by a factor of two in both x and y directions? The normalized weed pressures and expected PPV values in these two cases are

$$\lambda_1 = 2\pi \cdot 400m^{-2} \cdot 0.03m \cdot 0.03m = 2.26 \qquad \text{PPV} = \frac{1}{1+\lambda_1} = 0.31 \quad (12)$$

$$\lambda_2 = 2\pi \cdot 400m^{-2} \cdot 0.015m \cdot 0.015m = 0.57 \quad \text{PPV} = \frac{1}{1+\lambda_2} = 0.64 \quad (13)$$

This increase in PPV value indicates that for context based methods the precise placement of crop plants is vital for good performance.

3.3. Comparison with reported classification rates

Åstrand (2005) provides information on weed pressure and crop plant position uncertainties for two datasets, these numbers are provided in table 2. Given this information the upper bounds on PPV can be estimated using the relation derived in section 2.5. Table 3 contains information about classifier PPV in the cited paper and predicted upper bound on PPV given the circumstances. The observed PPV is calculated as

$$\text{oPPV} = \frac{\text{TP}}{\text{TP} + \text{FP}} \quad (14)$$

The 95% credible interval (CI) in table 3 was calculated using the *minimal length* method described in Ross (2003). In dataset DS1 the classifier performed slightly better than the predicted upper bound, but not significantly higher. In DS2 the classifier did not perform as well as the predicted upper bound, but the difference was not significant. For both datasets the theoretical predictions are close to the observed classifier performance, which support the theoretical predictions and indicate that the classifier implemented in Åstrand (2005) performed nearly optimal.

3.4. Performance of implemented methods

To compare performance of the different classifiers, PPV values for different circumstances are shown in figure 5. The position score classifier were used in four different configurations where the number of examined neighbour positions were 2, 5, 10 and 20 respectively. For each classifier configuration, the model

$$\mathrm{PPV} = \frac{1}{1 + f \cdot \lambda} \tag{15}$$

was fitted to the simulation results. The parameter f is a measure of the ability of the classifier to locate the true crop locations compared to the expected performance of a classifier using true crop grid locations. A value of 3 means that the classifier performs as a classifier using true crop grid locations in a field with a three times higher NWP.

The random classifier ($f = 19.18$) performs really bad, which is to be expected as it does not utilize knowledge about the row structure. The classifier based on position scores were tested in four different configurations where the number of examined neighbour sites (N) was varied. Using two neighbour sites the performance is much better than the random classifier, but the gap up to the ideal classifier is large. When the number of neighbours is increased from 2 to 5, 10 and 20 the performance of the classifier is gradually increased. The f values is seen to have the approximate dependency on N:

$$f = 1.94 + \frac{6.55}{N} \tag{16}$$

The path score classifier is seen to perform similar to the position score when examining 20 neighbour positions.

3.5. Is context information enough?

Is it possible to rely on context based classification only? Assume that a PPV of 95% is so precise that farmers will find that the decrease in yield due to falsely removed crop plants will be outweighted by the decreased cost of manual weed control. To reach PPV = 0.95 the NWP should be $\frac{1}{0.95} - 1 = 0.0526$ or lower. If the crop positioning uncertainty is $\sigma_x = \sigma_y = 1cm$ the weed pressure must not exceed $\sim 84m^{-2}$. Higher weed pressures is often observed and therefore is context based classification not enough to reach the required classification accuracy.

Dataset	$\rho[m^{-2}]$	$\sigma_x[m]$	$\sigma_y[m]$	λ	γ
DS1	50	0.0240	0.0136	0.1025	0.71
DS2	400	0.0148	0.0108	0.4017	0.73

Table 2: Weed pressure, crop upgrowth and crop position uncertainties for two example datasets and the derived normalized weed pressure. ρ: weed density, σ: crop position uncertainty, λ: normalized weed pressure, γ: upgrowth rate.

Dataset	# Loc.	# TP	# FP	oPPV	CI	$\frac{1}{1+\lambda} \cdot \frac{\gamma}{1-\phi}$
DS1	643	424	148	0.741	[0.70; 0.78]	0.728
DS2	273	120	135	0.471	[0.41; 0.53]	0.525

Table 3: Predictions based on Åstrand (2005). # loc: number of crop locations, # TP: number of correctly classified crop plants, oPPV: observed positive prediction rate, CI: credible interval of the true PPV given the observations.

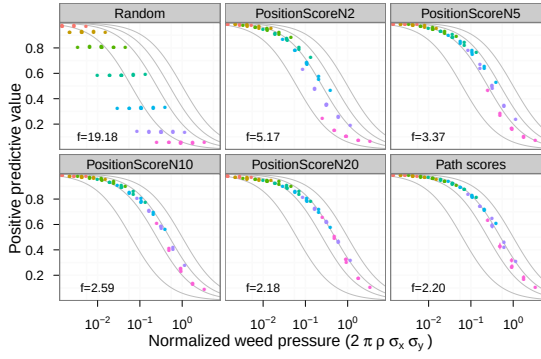

Figure 5: Comparison of performance of different context based crop recognition methods. The position score method is shown with results from four different number of neighbours. Simulation results based on the same weed pressure (but different crop position uncertainties) have identical colours. For each method the model $\frac{1}{1+f \cdot \lambda}$ is fitted and the f value is indicated in the figure.

3.6. Error types

The observed errors can be divided into three groups. The first group contains all the cases where there is a weed plant closer to the expected crop location than the nearest crop. These errors cannot be avoided, but the error rate can be estimated from NWP. Errors caused by missing crop plants, e.g. due to low upgrowth rates, belongs to the second group. If the row structure recognizer fails to locate the row pattern, the search for the nearest plant is unlikely to find a crop and the resulting error belongs to the third group. The performance differences observed from figure 4 to 5 can be explained by group three errors.

3.7. Assumptions and their validity

To derive the central equations in this paper a set of assumptions were used. During the analysis it was assumed that the weed density was uniform. Research by (Nørremark, 2009) shows that the weed pressure is lower close to sugar beet seedlings. This effect is only present within a few centimetres from the crop plant seedling and the effect on the obtained results should be neglegible. If the weed pressure near the crop plants is lower, the PPV of the context based classifiers will increase slightly.

Under real world conditions occlusion of leaf parts is often seen at high weed pressures. Occlusion of leafs can disturb estimation of the plant centres, but in the simulations it is assumed that the plant centres can be located under all conditions. The plant centre detection method determines how fragile the system will be to excessive occlusion. The method described in Midtiby et al. (2012) can predict plant centres of partial occluded plants.

4. Conclusion

When using position information to recognize crop plants, three types of errors can cause faulty classifications: (1) one or more weeds plants are closer to the expected crop location than the nearest crop, (2) no crop plant is at the expected crop location due to partial upgrowth or (3) the row structure is not located correctly and the classification algorithm will thus search at the wrong location for the next crop plant. The rate of the first error type can be estimated using the normalized weed pressure defined as $\lambda = 2\pi\sigma_x\sigma_y\rho$. The third error type depends on the used method for estimating location of the next crop plant.

An upper bound on PPV for a given normalized weed pressure can be determined using the relation PPV $= \frac{1}{1+\lambda}$. Classifier performance of context based crop recognizers described in the literature was compared with the estimated upper bound. The observed performance were similar to or lower than the predicted upper bounds. The predicted relation between normalized weed pressure and achievable PPV was supported by both simulations and reported classifier performance in the literature. The direct relation between λ and PPV indicates that for context based methods the precise placement of crop plants is vital for good performance.

Four different context based crop recognition methods was implemented and evaluated in a simulation environment. The methods based on position scores performed better when the number of examined neighbour crop positions were increased. When 20 neighbour positions were examined the method performed similarly to the path score method. All tested methods had PPV values below the theoretical upper bound. The performance of the two best methods could be predicted by the model PPV $= \frac{1}{1+2\cdot\lambda}$.

If positive predictive values above 95% is needed, classification based on plant position information alone will not be enough for typical conditions and additional information like plant morphology, spectral characteristics or similar will be needed.

Appendix A. Derivations

Appendix A.1. Definitions

$$p_{\sigma_c}(c) = \frac{1}{\sigma_c\sqrt{2\pi}} \exp\left(\frac{-c^2}{2\sigma_c^2}\right) \tag{A.1}$$

$$n_w(x,y) = \rho\pi\sigma_x\sigma_y\left(\frac{x^2}{\sigma_x^2} + \frac{y^2}{\sigma_y^2}\right) \tag{A.2}$$

Appendix A.2. The average number of weed plants closer to the grid location than the nearest crop plant

$$\lambda = \int_{-\infty}^{\infty}\int_{-\infty}^{\infty} p_{\sigma_x}(x)\cdot p_{\sigma_y}(y)\cdot n_w(x,y)\,dx\,dy \tag{A.3}$$

$$= \int_{-\infty}^{\infty}\int_{-\infty}^{\infty} \frac{1}{\sigma_x\sqrt{2\pi}}\exp\left(\frac{-x^2}{2\sigma_x^2}\right) \cdot \frac{1}{\sigma_y\sqrt{2\pi}}\exp\left(\frac{-y^2}{2\sigma_y^2}\right)\cdot \rho\pi\sigma_x\sigma_y\left(\frac{x^2}{\sigma_x^2}+\frac{y^2}{\sigma_y^2}\right)\,dx\,dy \tag{A.4}$$

Moving constants out of the double integral.

$$= \frac{\rho}{2}\int_{-\infty}^{\infty}\int_{-\infty}^{\infty}\exp\left(\frac{-x^2}{2\sigma_x^2}\right)\cdot\exp\left(\frac{-y^2}{2\sigma_y^2}\right)\cdot\left(\frac{x^2}{\sigma_x^2}+\frac{y^2}{\sigma_y^2}\right)\,dx\,dy \tag{A.5}$$

Changing integration variable to get rid of σ_x and σ_y inside the double integral. $[x' = x/\sigma_x \rightarrow dx = \sigma_x dx']$ and $[y' = y/\sigma_y \rightarrow dy = \sigma_y dy']$

$$= \frac{\rho}{2}\int_{-\infty}^{\infty}\int_{-\infty}^{\infty}\exp\left(\frac{-x'^2-y'^2}{2}\right)\cdot\left(x'^2+y'^2\right)\,\sigma_x\,dx'\,\sigma_y\,dy' \tag{A.6}$$

Taking constants out of the integral and changing to polar coordinates.

$$= \frac{\rho\sigma_x\sigma_y}{2}\int_0^{2\pi}\int_0^{\infty}\exp\left(\frac{-r^2}{2}\right)\cdot r^2\,r\,dr\,d\theta \tag{A.7}$$

Solve the θ integral and thereafter the r integral.

$$= \pi\rho\sigma_x\sigma_y\int_0^{\infty}\exp\left(\frac{-r^2}{2}\right)\cdot r^3\,dr = 2\pi\rho\sigma_x\sigma_y \tag{A.8}$$

Appendix A.3. Probability of not finding any weeds

Positive predictive value, given crop position uncertainty $\sigma_{x,y}$ and weed density ρ.

$$PPV = \int_{-\infty}^{\infty}\int_{-\infty}^{\infty} p_{\sigma_x}(x)\cdot p_{\sigma_y}(y)\cdot\exp\left(-n_w(x,y)\right)\,dx\,dy \tag{A.9}$$

$$= \int_{-\infty}^{\infty}\int_{-\infty}^{\infty}\frac{1}{\sigma_x\sqrt{2\pi}}\exp\left(\frac{-x^2}{2\sigma_x^2}\right)\cdot\frac{1}{\sigma_y\sqrt{2\pi}}\exp\left(\frac{-y^2}{2\sigma_y^2}\right) \cdot\exp\left(-\rho\pi\sigma_x\sigma_y\left[\frac{x^2}{\sigma_x^2}+\frac{y^2}{\sigma_y^2}\right]\right)\,dx\,dy \tag{A.10}$$

Separating the two integrals and collecting common factors.

$$= \frac{1}{2\pi\sigma_x\sigma_y} \int_{-\infty}^{\infty} \exp\left(-x^2 \cdot \left[\frac{1}{2\sigma_x^2} + \rho\pi\sigma_y/\sigma_x\right]\right) dx \cdot \int_{-\infty}^{\infty} \exp\left(-y^2 \cdot \left[\frac{1}{2\sigma_y^2} + \rho\pi\sigma_x/\sigma_y\right]\right) dy \quad \text{(A.11)}$$

Solve the integrals.

$$= \frac{1}{2\pi\sigma_x\sigma_y} \cdot \frac{\sqrt{\pi}}{\sqrt{\frac{1}{2\sigma_x^2} + \rho\pi\sigma_y/\sigma_x}} \cdot \frac{\sqrt{\pi}}{\sqrt{\frac{1}{2\sigma_y^2} + \rho\pi\sigma_x/\sigma_y}} \quad \text{(A.12)}$$

Simplifications

$$= \frac{1}{2} \cdot \frac{1}{\sqrt{\frac{1}{2} + \rho\pi\sigma_x\sigma_y}} \cdot \frac{1}{\sqrt{\frac{1}{2} + \rho\pi\sigma_x\sigma_y}} = \frac{1}{1 + 2\rho\pi\sigma_x\sigma_y} = \frac{1}{1+\lambda} \quad \text{(A.13)}$$

References

Åstrand, B., 2005. Vision based perception for Mechatronic weed control. Ph.D. thesis. Chalmers University of Technology.

Åstrand, B., Baerveldt, A., 2004. Plant recognition and localization using context information, in: Proc. of the IEEE Conference Mechatronics and Robotics, pp. 13–15.

Griepentrog, H.W., Nørremark, M., Nielsen, H., Blackmore, B.S., 2005. Seed mapping of sugar beet. Precision Agriculture 6, 157–165. 10.1007/s11119-005-1032-5.

Midtiby, H.S., Giselsson, T.M., Jørgensen, R.N., 2012. Estimating the plant stem emerging points (pseps) of sugar beets at early growth stages. Biosystems Engineering 111, 83–90.

Nørremark, M., 2009. Methods and instrumentation for automated physical weed control within crop rows. Ph.D. thesis. University of Copenhagen.

Nørremark, M., Søgaard, H., Griepentrog, H., Nielsen, H., 2007. Instrumentation and method for high accuracy geo-referencing of sugar beet plants. Computers and Electronics in Agriculture 56, 130–146.

Onyango, C.M., Marchant, J.A., 2003. Segmentation of row crop plants from weeds using colour and morphology. Computers and Electronics in Agriculture 39, 141–155.

Ross, T.D., 2003. Accurate confidence intervals for binomial proportion and poisson rate estimation. Computers in Biology and Medicine 33, 509–531.

Tillett, N.D., Hague, T., Miles, S.J., 2001. A field assessment of a potential method for weed and crop mapping on the basis of crop planting geometry. Computers and Electronics in Agriculture 32, 229–246.

Weis, M., Sökefeld, M., 2010. Detection and Identification of Weeds. Springer Netherlands.